Radiochemical measurements on nuclear reactions induced by fast neutrons

Davies, John Harris

"RADIOCHEMICAL MEASUREMENTS ON NUCLEAR REACTIONS INDUCED BY FAST NEUTRONS."

THESIS

presented in candidature for the degree of

DOCTOR OF PHILOSOPHY

in the

UNIVERSITY OF DURHAM

by

JOHN HARRIS DAVIES, B.Sc. (Dunelm)

MEMORANDUM

The work described in this Thesis was carried out in the Londonderry Laboratory for Radiochemistry, University of Durham, between September 1957 and September 1960, under the supervision of Mr. G.R. Martin, B.Sc., A.R.C.S., F.R.I.C., Reader in Radiochemistry.

This thesis contains the results of some original research by the author, and no part of the material offered has previously been submitted by the candidate for a degree in this or any other university. Where use has been made of the results and conclusions of other authors in relevant studies care has been taken to ensure that the source of information is always clearly indicated, unless it is of such general nature that indication is impracticable.

John H. Davies

ABSTRACT

Nuclear reactions induced by 14 MeV neutrons in a wide range of elements* have been investigated by activation techniques. The cross sections of (n,p), (n,pn), (n,α), (n,γ) and (n,2n) reactions have been measured and their values are discussed with reference to the theoretical predictions of different nuclear models.

The 14 MeV neutrons were produced by the $H^3(d,n)He^4$ reaction, the deuterons being accelerated to the optimum energy by a Cockroft-Walton accelerator.

A method for the accurate monitoring of fast neutron fluxes in conditions of poor geometry has been developed.

Counting equipment has been calibrated relative to a 4π counter. Greater accuracy in the determination of absolute disintegration rates, in conjunction with the separation of induced activities by radiochemical procedures, is considered the greatest improvement on the results of previous workers.

A recent report of (n,He^3) reactions, induced by 14 MeV neutrons with measurable cross sections, has been investigated, but the results could not be reproduced.

* Magnesium, aluminium, argon manganese, cobalt, arsenic, iodine, barium, gold, mercury, bismuth.

Irradiations of natural ytterbium and osmium have been performed in an attempt to observe new activities. 9.8 Minute rhenium, induced in osmium, has been re-assigned to Re^{192}.

CONTENTS

CHAPTER 1

INTRODUCTION

Neutrons are available over an extremely wide energy range from as low as 10^{-4} eV to an upper limit of 10^{10} eV and, because of their lack of charge, they are unique in their ability to interact with nuclei over the whole of this range. The premier importance of neutrons as a tool in nuclear research is a direct consequence of this property.

Corresponding to this wide energy range, there is a great variety in the types of interactions that are observed. The measure of the interaction of neutrons with matter is the neutron cross section and precise determination of cross sections can furnish a great deal of information about the nature of these interactions and hence about nuclear structure.

Nuclear cross-section data compiled from all types of interactions are invaluable for testing the predictions of nuclear models, which, although not sufficiently exact to predict cross sections accurately, nevertheless enable the nuclear theoretician to make intelligent "guesses" and provide him with a clearer insight into the true nature of the nucleus.

A nuclear model is valuable only insofar as it accounts adequately for observed phenomena and, as further experi-

mental data become available, the model has to be refined. For example, evidence, from cross-section measurements of a shell structure within the nucleus could not be accounted for on the basis of the simple liquid drop model of the nucleus, which, until then, had proved quite adequate. A new model was developed so that theory might correspond with experiment.

This is a continuous process, improved experimental techniques leading to more exact measurements and opening new fields of investigation. Ideally, it would be desirable to determine the neutron cross sections of each individual nuclide for every possible type of nuclear interaction over a large range of neutron energies. Investigations so far merely outline the fringes of the subject.

Much of the information about nuclear structure comes from examining the variation of cross sections with the energy of the incident neutrons. This variation is sometimes very irregular, especially for slow neutrons, where nuclear excitation levels are reflected in the fine structure of the excitation curves. Monoenergetic sources of neutrons of adjustable energy are required, if the fine structure is to be resolved.

The instrumental problem, at high as well as low energies, is then the production of neutrons of a precisely

defined and known energy and of sufficient intensity to make measurements. At low energies, up to about 1000 keV, this is achieved by one of two techniques, the time-of-flight neutron velocity selector and the crystal spectrometer velocity selector. These succeed in selecting neutrons of specific energy from a wide initial energy spectrum.

No device analogous to velocity selectors has yet been developed for the study of fast neutrons and recourse has to be made to a number of nuclear reactions which produce monoenergetic neutrons.

Early fast neutron cross sections were measured using neutrons obtained from Ra-α-Be sources, but these results are useless for comparison with theory, as these sources emit an extremely widespread and complicated neutron spectrum.

Photoneutron sources are more useful and monoenergetic neutrons, covering a range of energies from about 0.03 to 1 MeV, have been obtained in this way.

Monoenergetic neutrons have been obtained from the $H^2(d,n)He^3$ and $Li^7(p,n)Be^7$ reactions, but the latter has a negative Q-value and the incident protons must exceed a threshold energy of 1.88 MeV before the reaction occurs. Also the energy of the incident protons must be carefully controlled if the reaction is to produce neutrons

in a narrow energy range. The $H^2(d,n)He^3$ reaction has a positive Q-value (3.27 MeV) and produces a good yield of monoenergetic neutrons at comparatively low bombarding energies. Furthermore, since there are no accessible excited states of He^3, this reaction can be used to produce monoenergetic neutrons up to 7MeV, simply by increasing the energy of the incident deuterons.

Until recently it was difficult to obtain monoenergetic neutrons of energies greater than this. The reactions, $Li^7(d,n)Be^8$ and $Be^9(d,n)B^{10}$, give good yields of high energy neutrons, but both Be^8 and B^{10} have accessible excited states, and the high energy neutrons are contaminated by neutrons of lower energy corresponding to the various possible final states of the residual nucleus. Cross sections measured with these sources cannot be related to any particular neutron energy.

The availability in recent years of tritium has transformed this situation and the $H^3(d,n)He^4$ reaction is now commonly used to produce monoenergetic neutrons of energies between 13 and 20 MeV. Besides having a high positive Q-value (17.58 MeV), this reaction has a very high, broad resonance with a maximum for 109 keV deuterons. Consequently, large yields of high energy neutrons can be obtained using relatively low energy accelerating

machines. Further, due to the absence of excited states of He^4, these neutrons are essentially monoenergetic with an energy of about 14 MeV.

The use of 14 MeV neutrons from the $H^3(d,n)He^4$ reaction for cross-section measurements was pioneered by Paul and Clarke,[1] who, in a notable paper published in 1953, presented the values of activation cross sections measured for fifty-seven different elements.

Activation cross sections are a particular type of cross section, referring to those interactions measured by the radioactivity of the residual nucleus. These include (n,γ), (n,p), (n,α), (n,2n) and others.

Paul and Clarke observed thirty-eight (n,p), twenty-five (n,α) and thirty-four (n,2n) reactions. Theoretical values of the cross sections were calculated on the basis of the evaporation theory of the compound nucleus proposed by Blatt and Weiskopf.[2] These were compared with the experimentally determined values and, whereas the magnitude of (n,2n) cross sections was in agreement with the theoretical predictions, for (n,p) and (n,α) reactions, the theoretical cross sections were in general too small. This difference between measured and predicted cross sections increased with mass number and, for heavy nuclides, measured cross sections were as much as four orders of

magnitude higher than the theoretical predictions.

The evaporation theory supposes that the incoming neutron completely shares its energy with the nucleus, and this compound nucleus has a finite lifetime before sufficient of its excitation energy is concentrated on a particular nucleon to enable it to escape.

To account for the difference between the measured and predicted cross sections of reactions emitting charged particles, Paul and Clarke proposed a second mechanism by which these reactions might occur. Here the incoming neutron interacts strongly with only one proton or α - particle, which escapes before much energy sharing takes place. The "direct mechanism" for (n,p) reactions was put onto a theoretical basis in 1957 by Brown and Muirhead.[3]

Meanwhile in a series of papers published in 1955, 1956 and 1957, Blosser et al[4,5,6] reported values for some (n, α) cross sections for 14 MeV neutrons. These results differed substantially from the trend reported by Paul and Clarke and were in order-of-magnitude agreement with the predictions of the evaporation theory.

It was one of the purposes of the present work to try and resolve this discrepancy. It is worth noting that most of the measurements of both Paul and Clarke and Blosser et al were restricted to target nuclides with mass numbers

less than 100, and the really large discrepancies between measured and predicted cross sections were in the heavy nuclide region. Several cross-section measurements have been made in this region.

A number of activation cross sections for 14 MeV neutrons were published by Forbes[7] in 1952 and Yasumi[8] in 1957, but these are of little use for comparison with theory, as they are mostly (n,2n) cross sections or cross sections of light nuclides. Other workers have been concerned with investigating the cross sections of single nuclides. Martin[9] measured the cross section of the $O^{16}(n,p)N^{16}$ reaction and Battat and Ribe[10] studied reactions producing He^6. They presented values for the cross sections of the $Li^6(n,p)He^6$, $Li^7(n,d)He^6$ and $Be^9(n,\alpha)He^6$ reactions. Peck[11] used a nuclear emulsion technique to study the reaction $Au^{197}(n,p)Pt^{197}$.

Paul and Clarke's paper represented a major piece of work and its value in opening up the field cannot be overemphasised. The very enormity of the task they undertook, however, precluded very precise measurements. The authors themselves acknowledge that high accuracy in their counting techniques was not attempted. Further, the lack of any chemical separations led to the mis-assignment of several residual activities.

It was the purpose of the present work to improve the precision of activation cross-section measurements for 14 MeV neutrons by improved techniques for neutron flux determination and absolute β-assay. A method for the accurate determination of the neutron flux under bad geometrical conditions was developed (particularly useful in measuring the small cross sections of heavy nuclides) and a great deal of attention was paid to the standardisation of counting techniques. The chemical separation of residual activities was an important part of the work.

Besides measuring (n,p), (n,α) and (n,2n) cross sections, (n,γ) cross sections were also investigated and found to be much higher at this energy than would have been expected from theory. The only published data, concerning (n,γ) cross sections for fast neutrons, was the work of Hughes et al,[12,13,14] who had used unmoderated fission neutrons (effective energy 1 MeV) to measure the (n,γ) cross sections for a wide range of nuclides. Their results are in accord with the predictions of the compound nucleus treatment, but at higher energies other reactions, (n,2n), (n,p) and (n,α), would be expected to be greatly favoured at the expense of the (n,γ) reaction. Measured (n,γ) cross sections for 14 MeV neutrons are, in fact, several orders of magnitude higher

than expected. Here again the statistical treatment of Blatt and Weisskopf would appear to be inadequate.

One (n,pn) reaction has been studied and its cross section measured. This was the A^{40} (n,pn)Cl^{39} reaction, which presents one of the few cases where the (n,pn) cross section can be measured by activation techniques. Previously, a search for (n,pn) reactions by activation methods by Cohen, Hyder and White[15] showed, in no case, significant yields, although nuclear emulsion techniques gave strong evidence of their occurrence.[16]

The limits of some (n,He^3) reactions were also investigated.

Later work was concerned with an attempt to discover new nuclides in regions of the nuclide chart where obvious gaps occurred or assignment of activities was confused. To this end, several irradiations of osmium and ytterbium have been performed.

CHAPTER 2

OUTLINE OF TECHNIQUES FOR CROSS-SECTION MEASUREMENTS

The only type of neutron cross section that can be determined by a direct and simple method is the total cross section. The total cross section is the sum of the individual cross sections for every type of interaction, including scattering.

A disc of the sample material is inserted between a steady neutron source and a neutron detector and the transmission of the neutron beam through the disc is measured. The ratio, T, of the counting rates, observed with and without the intervening disc, is simply related to the total cross section, σ_T, by the expression

$$T = e^{-N \cdot \sigma_T \cdot t}$$

where, N = number of sample nuclei per $cm.^3$

and t = thickness of the disc.

To minimise the possibility of counting scattered neutrons, the neutron detector must subtend only a small solid angle at the source. Also, the neutron flux must remain steady over the course of the experiment. Absolute calibration of counting apparatus is, however, unnecessary, as only the ratio of the counting rates is required.

The measurement of individual reaction cross sections is a much more difficult operation, although there are examples where a particular reaction cross section is so large, as to constitute virtually the whole of the total cross section. An example of this is the $B^{10}(n,\alpha)Li^{7}$ cross section, which can be determined by the transmission technique.

These very large cross sections do not occur at high energies, however, and, if fast neutron cross sections for individual reactions are to be determined, a knowledge of the absolute neutron flux is required. Further, if the cross sections are being determined by an activation method, absolute disintegration rates must be known and the absolute calibration of counting apparatus is a prerequisite of the method.

The twin problems of absolute neutron flux and absolute disintegration rate determination impose a severe restriction on the accuracy with which activation cross sections can be measured. Errors of less than ten per cent are rarely claimed.

Determination of the absolute neutron flux

The impossibility of detecting neutrons directly, severely limits the methods by which neutron fluxes may be determined. The methods available are based, in general,

on the detection of secondary effects accompanying or induced by the neutrons. Of these, there are three main methods which are applicable to fast neutron studies - the recoil particle method, the associated particle method and the secondary standard method.

In the recoil particle method, the neutron beam impinges upon a thin layer of hydrogeneous material and the protons, recoiling from neutron collisions, are counted. For a quantitative measurement of the neutron flux, a knowledge of the n-p scattering cross section is required, but, since all n-p collisions are elastic, this can be accurately determined by the transmission technique, previously described. Having established this, the proton recoil detector can then be used to monitor irradiations.

During the irradiation the monitor (i.e. the proton radiator) and the sample subtend precisely determined solid angles at the neutron source. The flux through the sample is then simply related to that detected by the monitor. The calculation assumes that the neutrons are produced by a point source fixed in position and that the flux through the sample does not vary with thickness. Errors, arising from these assumptions and from errors in the measurement of the solid angles subtended by sample and monitor at the source, are minimised by irradiating

both the sample and the monitor under conditions of "good geometry". That is, well removed from the immediate target area.

In the associated particle technique, the charged particles, which are the secondary products of the neutron-producing reaction, are counted. For example, the neutron flux from the $H^3(d,n)He^4$ reaction is measured by counting the He^4 nuclei. This was the method employed by both Paul and Clarke[1] and Yasumi[8]. The α-particles, recoiling from the reaction into a carefully measured solid angle are detected (Paul and Clarke used a proportional counter and Yasumi an α-scintillation counter) and the number of these can be directly equated to the number of neutrons emitted into the corresponding solid angle, which, because of the motion of the centre of gravity of the system, does not lie in exactly the opposite direction. Since the neutron distribution with angle is known (and is, in fact, isotropic in the centre of mass system at these energies), the flux through the sample, which also subtends a precisely defined solid angle, can then be calculated.

Here again, the sample must be irradiated under conditions of good geometry to minimise errors due to the finite size of the neutron source and the finite thickness of the sample.

This condition is the limiting factor in the application of both the recoil particle and the associated particle techniques to the measurement of absolute neutron fluxes. Good geometry can only be attained at the expense of the neutron flux, which decreases with distance from the target in accordance with the inverse square law. A compromise has to be made between the geometry of the sample and the neutron flux through it, which must be sufficiently intense to induce a measurable activity. In fact, if very small cross sections are to be measured, good geometry simply cannot be afforded.

e.g. The strength of the 14 MeV neutron source in our laboratory is of the order of 10^9 neutrons/sec.

A calculation of the neutron flux required to make a typical cross section measurement shows very clearly that good geometry cannot be afforded.

At saturation

$$I = N.\sigma.\phi$$

where I is the activity produced in the reaction

N is the number of sample nuclei

σ is the cross section for the reaction

and ϕ is the neutron flux.

For an accurate measurement, the minimum value of I that can be tolerated is about 10 d.p.s.

Then $I = 10$ d.ps.

$N = 10^{21}$ (ca. 0.3 gm. of a heavy element)

$\sigma = 10^{-27} cm^2$ (i.e. 1 mb.)

$$\phi = \frac{10}{10^{21}.10^{-27}} = 10^7 \text{ neutrons/cm}^2\text{/sec.}$$

The usual length of an irradiation is about 2 hrs. (after which the source strength diminishes) and, if the half-life of the activity is 20 hrs, it can be assumed to have reached only one tenth saturation at the end of the irradiation. Then, the neutron flux required to produce an activity of 10 d.p.s. will be 10^8 neutrons/cm^2/sec. The total source strength is 10^9 neutrons/sec, so the sample must be irradiated within a centimetre or two of the target. This is not compatible with conditions of good geometry.

The third method of monitoring the neutron flux, the secondary standard method, is particularly adaptable to the measurement of small activation cross sections. The activity induced in the sample is compared with that induced in a reference element exposed to the same neutron flux. The unknown cross section can then be calculated in relation to the known cross section of the reference reaction. Obviously, the accuracy of all cross sections measured by the secondary standard method is

dependent upon the assumed value of the reference cross section, which must first be established by either the recoil particle or the associated particle techniques.

Experimental techniques are directed towards achieving the condition that the sample and reference are exposed to the same neutron flux.

In one method, which has been used,[4,5,6,7] a disc of the sample material is irradiated between two identically sized discs of the reference element, which is in the form of a thin metallic foil. The activities induced in each disc are measured and the mean of the two reference disc activities is a measure of the neutron flux through the sample. The error in this method is largely that of estimating the "true" reference disc activity (i.e. the activity which would have been induced in a reference disc occupying exactly the same position as the sample). The method is most successful when the sample is a thin foil and the "sandwich" is irradiated in good geometry. It is not suitable when the sample material is a powder, especially if it needs to be irradiated close up to the target.

An alternative method has been developed for the present work. In this method the sample material is irradiated in a homogeneous mechanical mixture with the

reference element. They are separated after the irradiation and their activities determined. This technique is particularly insensitive to fluctuations in the position of the neutron source and there is no objection to bulky samples. Consequently, the mixture can be placed right up against the target, making the best use of the neutron flux. The sample can also be irradiated in powder form, facilitating easy dissolution and speedy chemical separations after the irradiation. This is a great advantage. No precise geometrical measurements need to be made the the only inherent error of the method lies in the possibility that the mixture may not be homogeneous. This possibility was thoroughly investigated and errors arising from inhomogenity of the mixture were shown to be less than five per cent.

The criteria governing the choice of a secondary standard or reference reaction are

i) It should have a fairly high cross section, which has been reliably determined by an absolute method.

ii) The reference element should be easily attainable in a high state of chemical purity.

iii) The resultant activity should have a convenient

half-life (allowing it to be left for a short time while attention is being paid to the sample) and it should be uncontaminated by other activities induced in the reference element by other reactions.

iv) It should have a fairly high threshold energy to discriminate against scattered and degraded neutrons.

Another criterion applies only to the homogeneous mixture technique.

v) The reference element should be easily separable from mechanical mixtures.

Reactions which have been employed as secondary standards are:

$$Al^{27}(n,\alpha)Na^{24}$$
$$Fe^{56}(n,p)Mn^{56}$$
$$Cu^{63}(n,2n)Cu^{62}$$

Of these, only the $Fe^{56}(n,p)Mn^{56}$ reaction satisfies the fifth criterion, iron granules being easily separable from mechanical mixtures magnetically. This was chosen as the reference reaction in the present work.

Several tolerably concordant values for the $Fe^{56}(n,p)Mn^{56}$ cross section exist in the literature and the value assumed in this work, 124 millibarns, is an average of these. At the same time, an experiment is being conducted in conjunction with this work to determine the $Fe^{56}(n,p)Mn^{56}$ cross section absolutely, and all results will be re-adjusted to fit this value when it becomes available.

The method used is a variation of the associated particle technique. The He^4 nuclei are collected in an aluminium foil. This is dissolved releasing the helium, which is measured using an apparatus specially designed for the separation, purification and measurement of small volumes of helium (of the order of 10^{-7} c.c.).[17] The Mn^{56} activity induced in an iron foil, irradiated in the same geometry as the aluminium, is measured absolutely and, with a knowledge of the absolute cross section of the $Fe^{56}(n,p)Mn^{56}$ reaction can be calculated. The experimental set-up is depicted in Fig. 1.

In Fig. 1:-

A is a very thin Al foil (1.5 mgm./cm^2) to stop He^3 particles produced by the $H^2(d,n)He^3$ reaction.

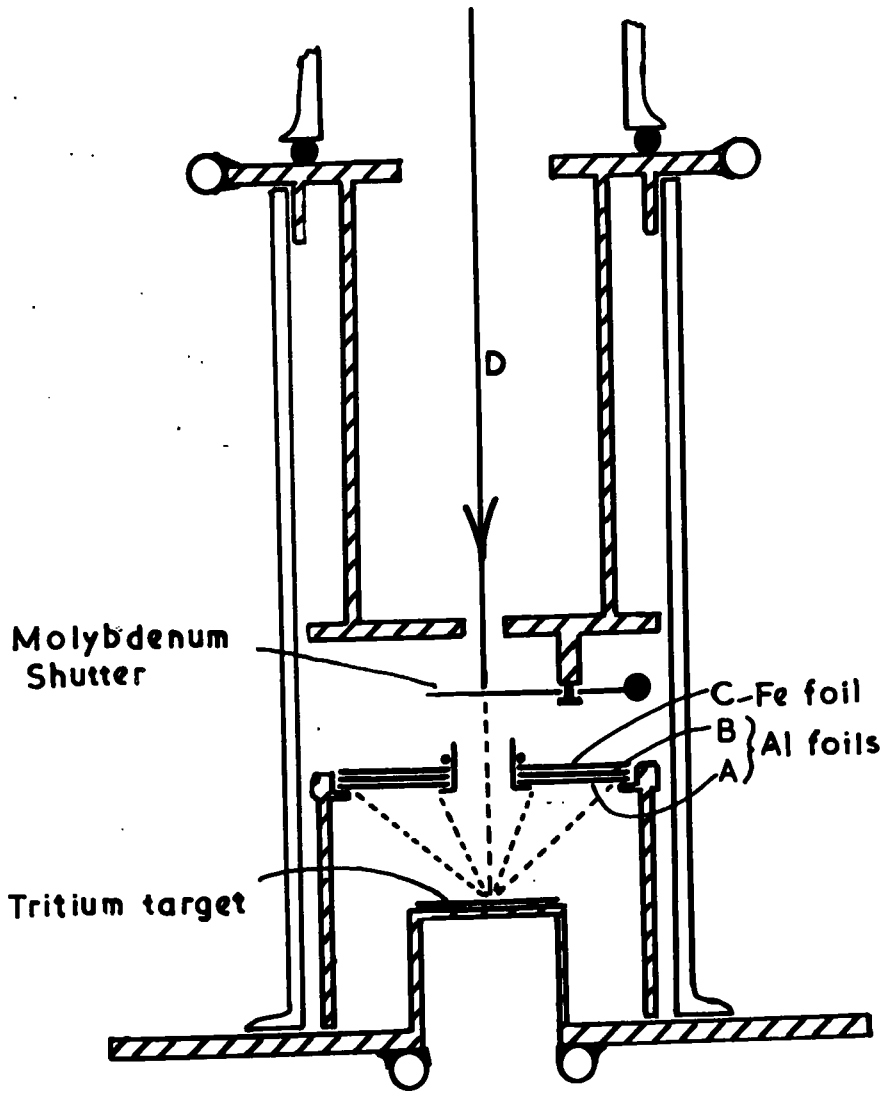

FIG.1 ABSOLUTE DETERMINATION OF THE $Fe^{56}(n,p)Mn^{56}$ CROSS SECTION.

B is a thicker Al foil (6.0 mgm./cm^2) to collect all He^4 nuclei recoiling from the reaction into the solid angle depicted.

C is an iron foil (120 mgm./cm^2) activated by neutrons emitted into the same solid angle as the He^4 nuclei.

Corrections must be made for the centre of mass motion of the system and for the small spread in particle energies, arising from the finite thickness of the tritium target. The excitation function of the $Fe^{56}(n,p)Mn^{56}$ reaction must also be known to calculate its cross section for neutrons emitted in the forward direction, which are more energetic than those in the backward direction. The excitation function of the $Fe^{56}(n,p)Mn^{56}$ reaction has been plotted by Terrel and Holm.[18]

Determination of absolute disintegration rates

Several methods of determining absolute disintegration rates are available and, in choosing one, a compromise must be made between the accuracy of the technique and its simplicity.

Very accurate assays of absolute β-disintegration rates can be made by 4π counting techniques, but good 4π sources require considerable skill and attention to prepare. They also require time and this method is not applicable to the measurement of activities with short

half-lives. Then, if self-absorption effects are to be negligible, chemical separations must be performed with very small amounts of carriers and the difficulty of estimating chemical yields must be taken into account. 4π Counting does not commend itself for routine measurements.

At the other extreme, no chemistry is performed and activities are measured directly in the activated material. After irradiation, the sample and reference element are counted with the same low geometry under an end window Geiger counter. Counting corrections are made with reference to empirical data like that compiled by Gleason, Taylor and Tabern[19] (window absorption), Burt[20] (saturation back-scattering) and Nervik and Stevenson[21] and Cunninghame, Sizeland and Willis[22] (self-absorption and self-scattering). Although this method facilitates quick and easy counting, without time wasted by chemical procedures and source preparation, the determination of absolute disintegration rates cannot be accurate, especially where decay schemes are complex.

This was essentially the technique employed by Forbes[7] and by Blosser et al,[4,5,6] although the latter did chemically separate, resultant activities.

Paul and Clarke[1] preceded their cross-section measurements by an examination of their counter efficiencies as a function of maximum β-particle energy, but accurate calibrations were not attempted. No chemical separations were performed.

Yasumi[8] calibrated his counting apparatus against a 4π counter, but he also did not make any chemical separations.

In the present work, the determination of absolute disintegration rates has been given close attention. The 4π counting technique, developed by Pate and Yaffe[23] and Hawkings et al,[24] has been thoroughly investigated and used to standardise an end window proportional counter and a halogen-quenched liquid counter.

The direct use of the 4π counter for absolute β-counting was rejected for the reasons outlined above, namely, the time consumed by the process of source preparation and their introduction into the sensitive volume of the counter, and the difficulty of performing chemical separations with the very small amounts of carriers which must be used. The time-consuming necessity of introducing sources into the sensitive volume of the counter was also an objection to the use of a 2π counter and, at the sacrifice of some of the counting efficiency, an end window counter was preferred.

Scintillation counting does not easily lend itself to absolute β-counting, the absence of a counting plateau making reproducibility difficult, and an end window gas-flow proportional counter was preferred to a Geiger counter, mainly because of its better reproducibility and thinner window. The latter facilitates the assay of less energetic β-activities.

The activities induced in the various elements irradiated were counted either under the proportional counter or in the liquid counter, depending upon which was the most efficient or reproducible for a particular activity. Usually, those activities produced by (n,p) and (n,α) reactions were chemically separated from the irradiated material and mounted as solid sources (ca. 10 mgs./cm^2) for counting under the end window counter. Activities induced by (n,γ) and (n,2n) reactions were more efficiently measured in the liquid counter, since they were inevitably mixed with the isotopic target material.

Both the end window counter and the liquid counter were calibrated for various radioactive nuclides, standardised by the 4π counter. Curves of counting efficiency as a function of maximum β-particle energy were constructed for each. Then, when it was not possible to calibrate the counters for the particular

nuclide under investigation, for example, when the nuclide had a short half-life or was for some other reason unobtainable with a high specific activity, the counter efficiencies could be accurately interpolated from the curves. This was particularly true of the end window counter, the efficiency of which was not very sensitive to changes in β-energy.

CHAPTER 3

EXPERIMENTAL PROCEDURES

Part 1 The neutron generator

A high flux of essentially monoenergetic neutrons ($E_n \sim$ 14MeV) was produced by the $H^3(d,n)He^4$ reaction ($Q = +17.58$ MeV). This reaction had a high broad resonance with a maximum for 109 keV deuterons, and a deuteron beam of suitable energy was produced by the Cockroft-Walton type accelerator, built in this laboratory by G.R. and E.B.M. Martin.[25] A photograph of the accelerator is included.

The Cockroft-Walton voltage quadrupling circuit is depicted in Fig. 2. The mains voltage ($\sim$ 240 volts and 50 cycles/sec.) is supplied via a Variac to the primary of a big transformer, capable of 100 kV peak output voltage. This is fed to the quadrupling circuit via a limiting resistance, and the high D.C. voltage built up is shared equally across the two gaps in the accelerating tube, depicted in Fig. 3.

To prevent electrical breakdown, the accelerating tube must be maintained at a pressure of about 10^{-5} mm. Hg, and, as deuterium gas is continuously being fed into the ion source, this requires high speed pumping. The deuterium is fed into the ion source through a heated

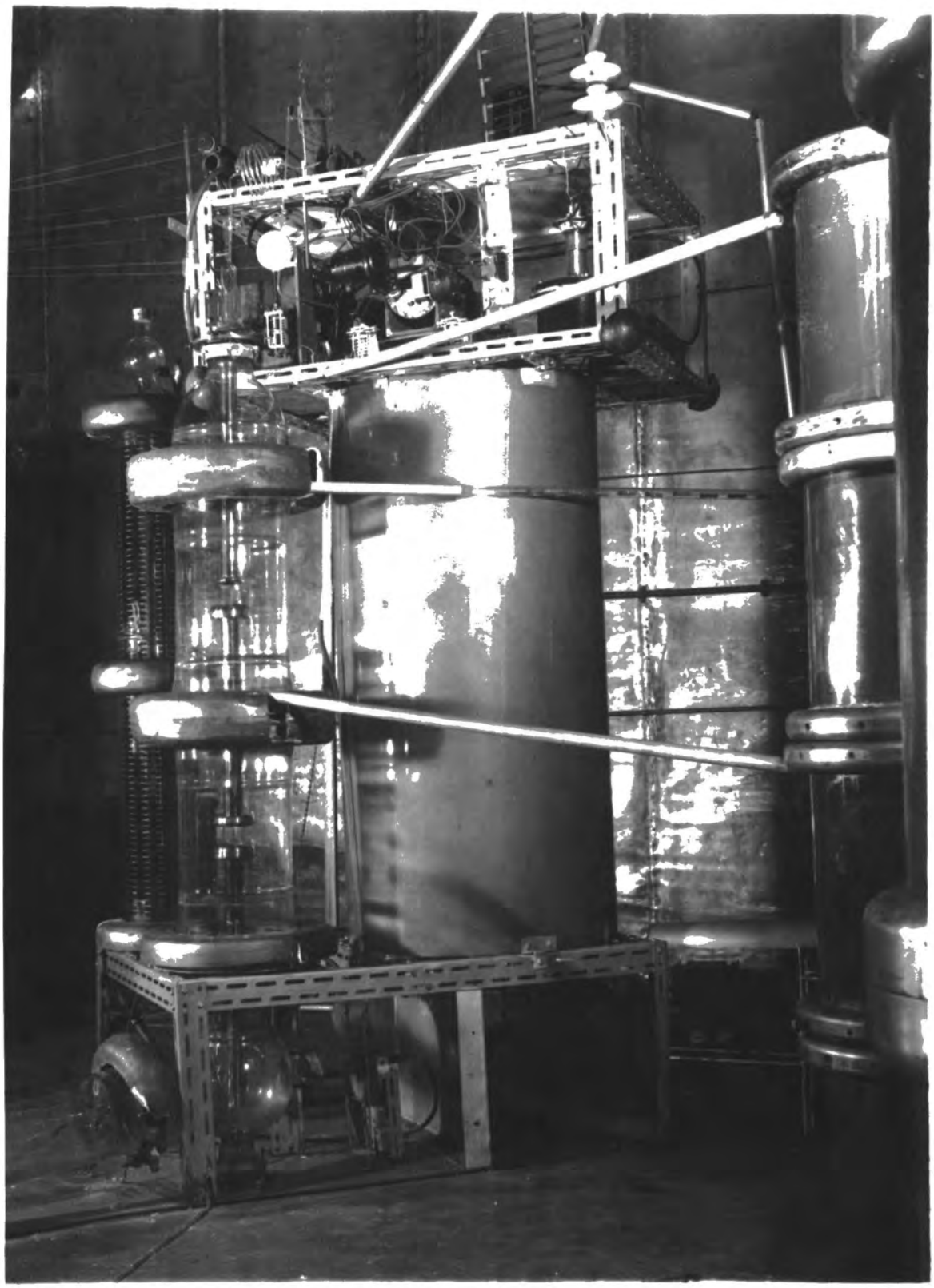

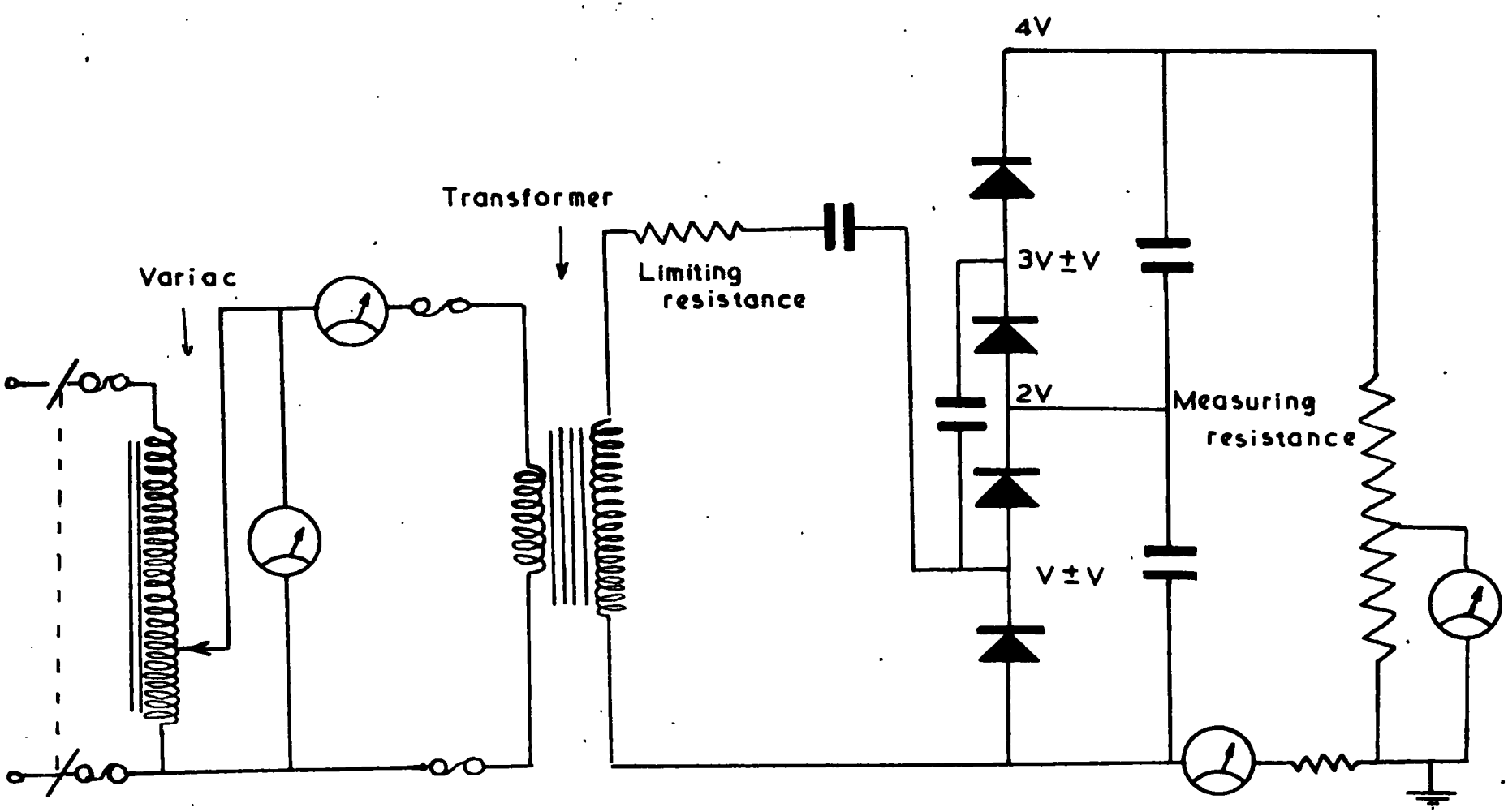

FIG. 2 VOLTAGE-QUADRUPLING CIRCUIT.

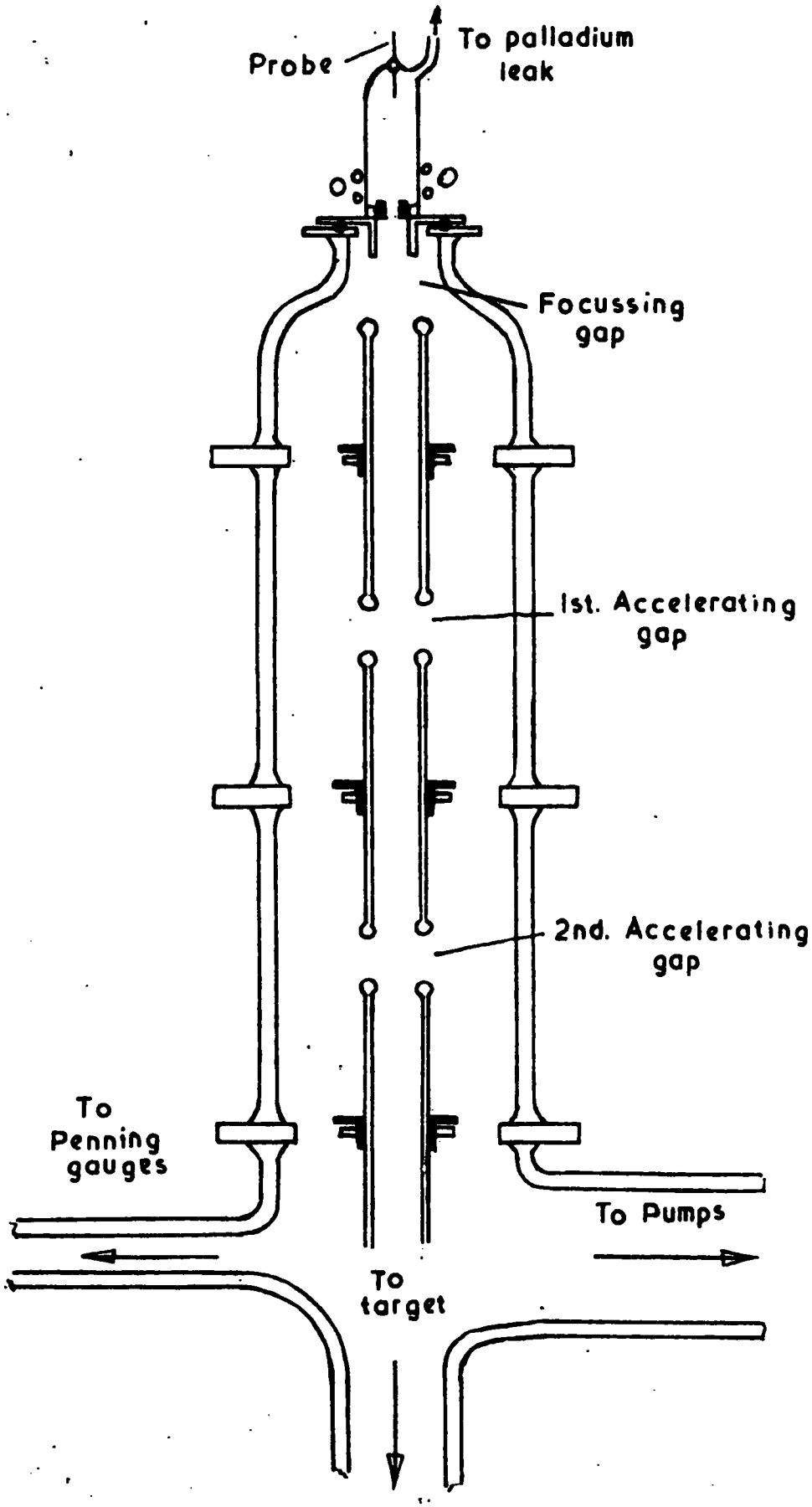

FIG. 3 ACCELERATING TUBE.

palladium tube and ionised by a high frequency electrodeless discharge. This is maintained by an R.F. oscillator, the ion source being encircled by a copper tube, which forms part of a circuit tuned to resonance with the oscillator. Ions are extracted from the discharge through a narrow canal, by applying a voltage of a few kV between the canal and a tungsten probe at the top of the source. The extracted deuterons are focussed into a beam and accelerated by a voltage of about 40 kV applied across the carefully adjusted gap between the canal and the top of accelerating tube. The beam is further accelerated to its maximum energy by the high D.C. potential shared across the two gaps in the tube.

The deuteron beam impinges on a tritium target, the tritium being absorbed in a thin film of zirconium or titanium metal supported on a copper backing. Each target disc (diameter 2.5 cms.) contains about one curie of tritium (0.3 ml. at S.T.P) absorbed in 2 mgs. of titanium. This is equivalent to an atomic ratio of $_3H^3$ to 4Ti, although higher ratios can be obtained.

The targets, prepared by the method developed by Graves et al,[26] were bought from A.E.R.E. Harwell, and, for convenience, each disc was divided into four segments, which were bombarded separately.

The target segments were soldered on to the brass

target block of the accelerator and samples were irradiated close up to the bottom of the block. The target assembly is depicted in Fig. 4. It is centrally situated in the target chamber, well removed from the floor, walls and objects that might increase the flux of scattered, degraded neutrons in the area of the sample. A movable molybdenum disc protects the target from bombardment until the neutron flux is required.

The energy of the incident deuterons was slowly increased by means of the Variac to about 130 keV and the beam current was usually of the order of 200 μ amps. This corresponded to the dissipation in the target block of about 30 watts and, during an irradiation, the block was water-cooled.

A rough estimate of the neutron yield has been made by measuring the Cu^{62} activities induced in copper discs, irradiated with known geometry - the secondary standard method. About 10^9 neutrons/sec. are obtained from a fresh target.

As stated, the energy of the incident deuterons was 130 keV, but, as they penetrate the titanium-tritium layer, the deuterons are degraded. Deuterons, ranging in energy from 130 keV down to zero, react with tritium nuclei to produce neutrons, but it can be seen,

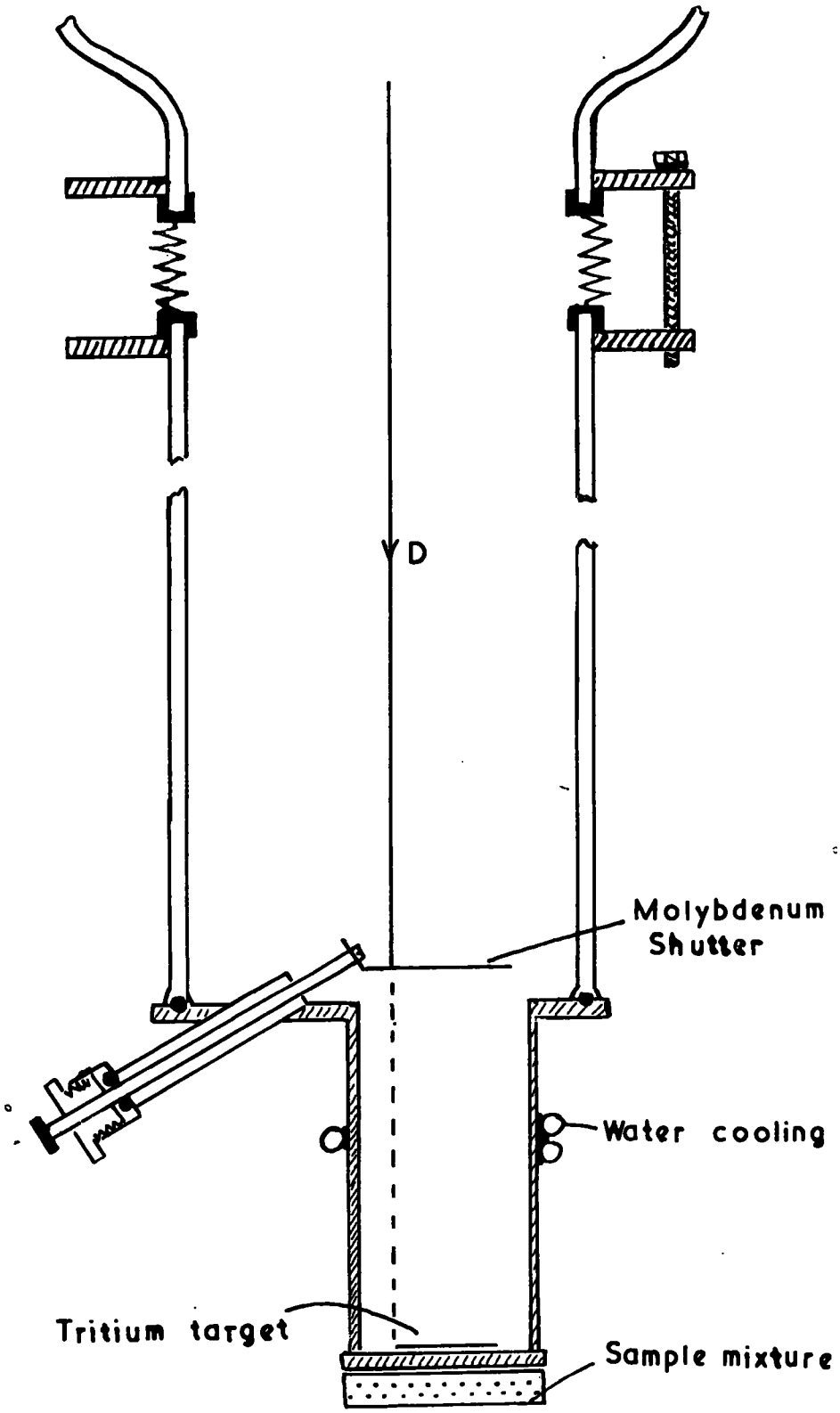

FIG. 4 THE TARGET ASSEMBLY.

on examining the graph of the cross section of the $H^3(d,n)He^4$ reaction as a function of deuteron energy,[27] that over eighty per cent of the neutron flux is produced by deuterons with energies between 80 keV and 130 keV. The resonance peak of the reaction is for 109 keV deuterons. Neutron energies as a function of angle of emission have been plotted for these three deuteron energies (Fig. 5) and it can be seen that in the angular spread of neutrons utilised, energies range from 14.5 MeV to 14.9 MeV, with the average energy of the neutron flux at 14.7 MeV. Thus, although the neutrons are not truly monoenergetic, they are defined in a narrow energy range.

Irradiations were usually started by removing the molybdenum shutter from the path of the deuteron beam and they could be instantaneously stopped by running down the probe voltage on the ion source. This was convenient as it did not necessitate entering the target chamber, which presented a considerable health hazard while the set was running.

Fluctuations in the neutron yield were monitored by a proton-recoil scintillation counter, which operated with a high bias voltage to discriminate against neutrons of lower energy. Knowledge of the variation of the neutron flux during the course of an irradiation was

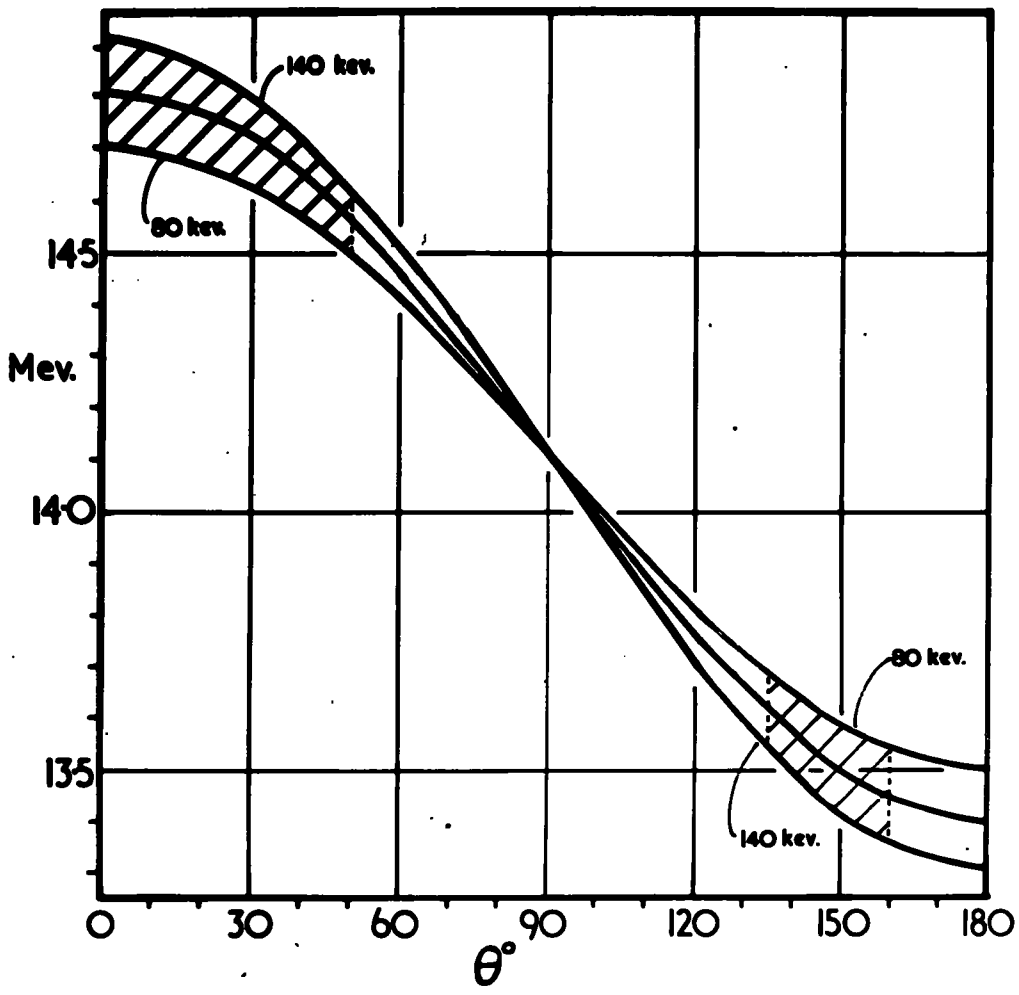

FIG. 5 NEUTRON ENERGY AS A FUNCTION OF ANGLE OF EMISSION.

essential, as the corrections, which had to be applied to different induced activities, varied considerably with their half-lives. The neutron monitor count was recorded at intervals which were short compared to the shortest half-life under investigation.

Besides the fluctuations in the neutron yield, which were probably due to small fluctuations in the position of the deuteron beam, there was a steady fall in the yield, probably due to loss of tritium from the heated area of the target. A device for moving the target assembly about with respect to deuteron beam was operated by remote control from the control room. This ensured that the whole area of the target segment was exposed to deuteron bombardment, but the life of one segment was, in general, limited to about five hours bombardment, by which time the neutron yield had dropped to about ten per cent of its initial value.

At this stage, the contribution to the total neutron flux of neutrons of lower energy becomes appreciable. During the course of an irradiation, deuterium accumulates in the target from the deuteron beam and 2.5 MeV neutrons are produced by the $H^2(d,n)He^4$ reaction. Most of the reactions studied had thresholds above 2.5 MeV and these D+D neutrons did not represent a problem, but (n,γ) cross sections increase with decreasing energy, and the

contribution of neutrons of lower energy to measured (n, γ) cross sections had to be ascertained. The experiment is described in relation to the measurement of the $I^{127}(n, \gamma)I^{128}$ cross section, but the build-up of deuterium in the tritium target is depicted in Fig. 6. The flux of D+D neutrons can be seen to rise to a saturation level after about 500 μamp. hrs. bombardment.

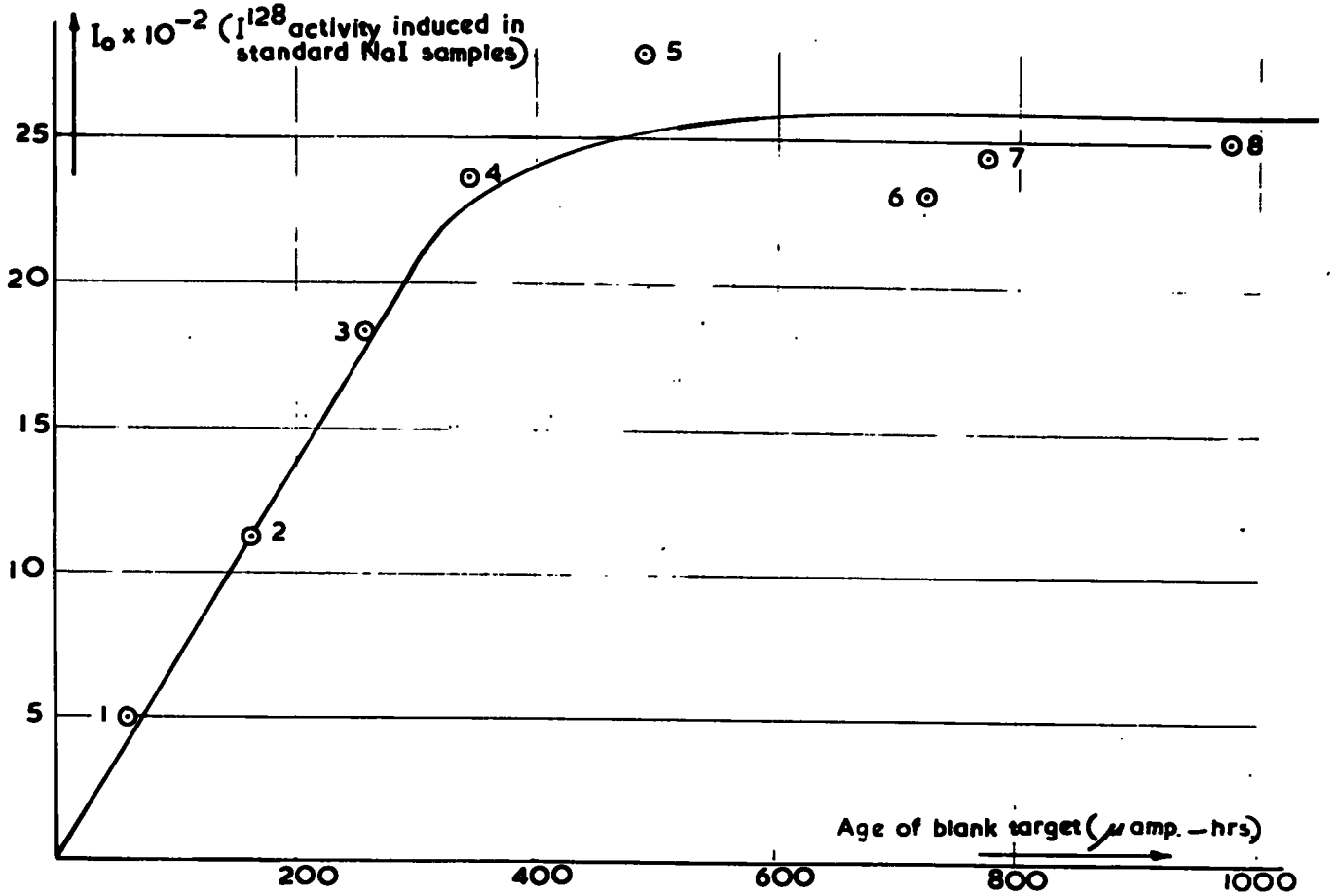

FIG. 6 FLUX OF D+D NEUTRONS AS A FUNCTION OF AGE OF TARGET.

Part 2 Counting Equipment

As stated in Chapter 2, the activities induced in the irradiated materials were measured by either an end window proportional counter or a halogen-quenched liquid counter and these were calibrated for absolute counting by comparison with a 4π technique.

a) The 4π counter

The 4π counter is depicted in Fig. 7. It is a gas-flow proportional counter, consisting of two cylindrical chambers hinged together so that, when in operation, the source support lies in the equatorial plane. The chambers have separate anode wires, lying parallel above and below the source support and connected externally to the E.H.T. supply.

The gas, a standard mixture of 90% argon and 10% methane, was freed of oxygen and water vapour by passage through tubes containing heated platinum gauze and "Anhydrone", and passed through the counter at a pressure just slightly above atmospheric. The flow rate was determined by a needle valve at the inlet. It was shown that counting rates were virtually independent of the gas flow rate above a certain minimum, which was about 0.5 ml./sec. The counter was operated with a gas flow rate of about 0.75 ml./sec.

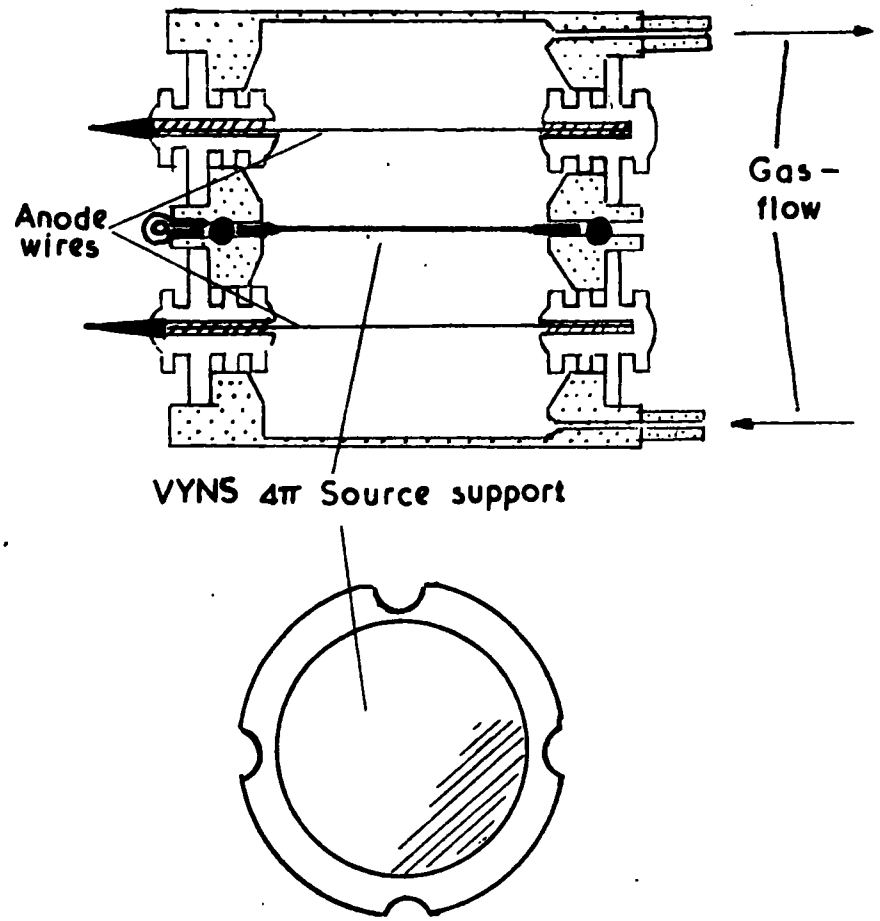

FIG. 7 4π COUNTER.

The electronic apparatus and the gas-flow system, associated with the counter, were identical to those associated with the end window counter, which are depicted in Fig. 11. In fact, the 4π and end window counters were completely interchangeable.

The 4π counter normally gave a plateau more than 300 volts long. The optimum counting voltage for the standard RaE source was about 1.5 kV, but this was found to vary considerably with β-energy, and it was the usual practice to draw a fresh plateau for each activity. The counter was operated with the scaler paralysis time set at 50 μsecs. It was completely enclosed in a standard lead castle, which reduced the background count to about 35 c.p.m. for the twin counters.

As can be seen from Fig. 7, the active sources are placed inside the sensitive volume of the counter, which has to be opened whenever it is desired to change a source. After every such operation, the counter was slow to regain its sensitivity. Although this process could be speeded up by flushing the air out of the counter with an increased gas flow rate, there was, of necessity, an interval of about seven minutes associated with the changing of sources.

b) Preparation of 4π sources

The source supports were very thin (ca. 20 μ gms./cm^2) VYNS plastic films, supported on aluminium rings (internal diameter - 2.6 cms.) and gold coated on one side to give them conducting properties. The manufacture and properties of these 4π source supports are described by Pate and Yaffe.[23]

A one-third saturated solution of VYNS resin in cyclohexanone (a saturated solution contains 1 volume of resin in 2 volumes of solvent) was allowed to spread evenly over the surface of a trough of water. The cyclohexanone solvent dissolved, leaving a VYNS plastic film on the surface. A rough guide to the thicknesses of different sections of the film is provided by the interference colours in reflected light. The thinnest sections were generally too fragile to be useful, but slightly thicker sections (20 μ gms/cm^2) were lifted from the surface on a wire frame and placed on the aluminium rings while still tacky. The exact thickness of the films could, if needed, be determined spectrophotometrically with reference to the calibration curves constructed by Pate and Yaffe.[23]

The source supports were rendered conducting by evaporating a thin layer of gold on to one side of the films. The thickness of the gold layer need be no more

than 5 μgms/cm.^{2}, when the films appear a pale blue-green by transmitted light and purple in reflected light. The exact thickness of the gold layer could be measured, again by using a spectrophotometer.

These film source supports were, understandably, not very robust and some broke, apparently unaccountably, at different stages during the process of source preparation. But, with practice and care, ninety per cent success was attained.

Before preparing a source, the uncoated side of the film was treated with a very dilute insulin solution to facilitate the uniform spreading of the activity. About 1 mg. of insulin was dissolved in 10 mls. of distilled water with 1 drop of conc. HCl. By means of a finely adjustable dropper arrangement (Fig. 8), a little of this solution was placed on the film and allowed to wet the surface around the centre. Excess insulin solution was drawn off and the remainder evaporated under a heat lamp. Later, when a drop of the active solution was evaporated on the film, the activity was distributed evenly over the area wetted by the insulin solution. In the absence of a spreading agent, the active solute retreated to the centre of the film with the diminishing globule of solvent and crystallised from the last drop.

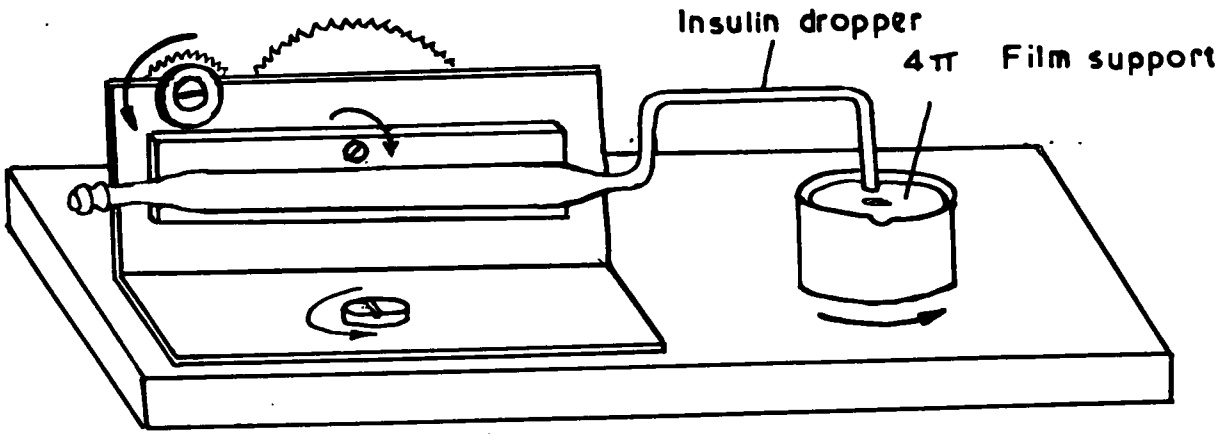

FIG. 8 INSULIN SPREADING DEVICE.

As the solutions used were never truly "carrier-free", counting losses due to self-absorbtion would have become significant, and not easily calculable in the absence of the insulin spreading agent.

Aliquot parts of the active solutions were weighed onto the films and evaporated under a heat lamp. Replicate sources for each activity were prepared and counted.

c) The performance of the 4π counter

The reproducibility of the 4π counting technique was firmly established, and its 100% efficiency confirmed by comparison with several other methods of absolute β-counting.

Whenever standardisations were performed, replicate 4π sources were prepared from different weights of active solution. The specific activities of these sources were always in close agreement, demonstrating that with the relatively carrier-free solutions used, counting losses from self-absorption were negligible. Sources were also occasionally counted in two or three different 4π counters, using different electronic equipment, and results varied by less than half a per cent. A typical group of results is presented in Table 1.

It was also shown that the 4π efficiency was independent

TABLE 1. MEASURED SPECIFIC ACTIVITY OF A Au^{198} SOLUTION

	4π counter(59)			4π counter (60)	4π counter (61)
Source No.	Weight of active solution mgs.	Specific activity d.p.m./mg.	Mean	Mean specific activity d.p.m./mg.	Mean specific activity d.p.m./mg.
1	67.6	187.2			
2	85.8	187.7			
3	59.4	188.0	187.6	187.0	188.0
4	78.0	187.0			
5	82.9	187.9			

of β-particle energy, at least, within the normally encountered range of energies. In connection with the calibration of the end window counter for Sr^{90} ($E\beta max$ = 0.54 MeV), 4π sources of cleanly separated Sr^{90} were prepared and quickly counted. The growth of Y^{90} ($E\beta max$ = 2.26 MeV), the 64 hr. daughter of Sr^{90}, was traced to secular equilibrium, when the total activity was exactly twice the initial activity of the Sr^{90}, as it should be if the Sr^{90} and Y^{90} β-particles were being counted with the same efficiency. The growth curve is reproduced in Fig. 9.

In another experiment, a small movable S^{35} source was

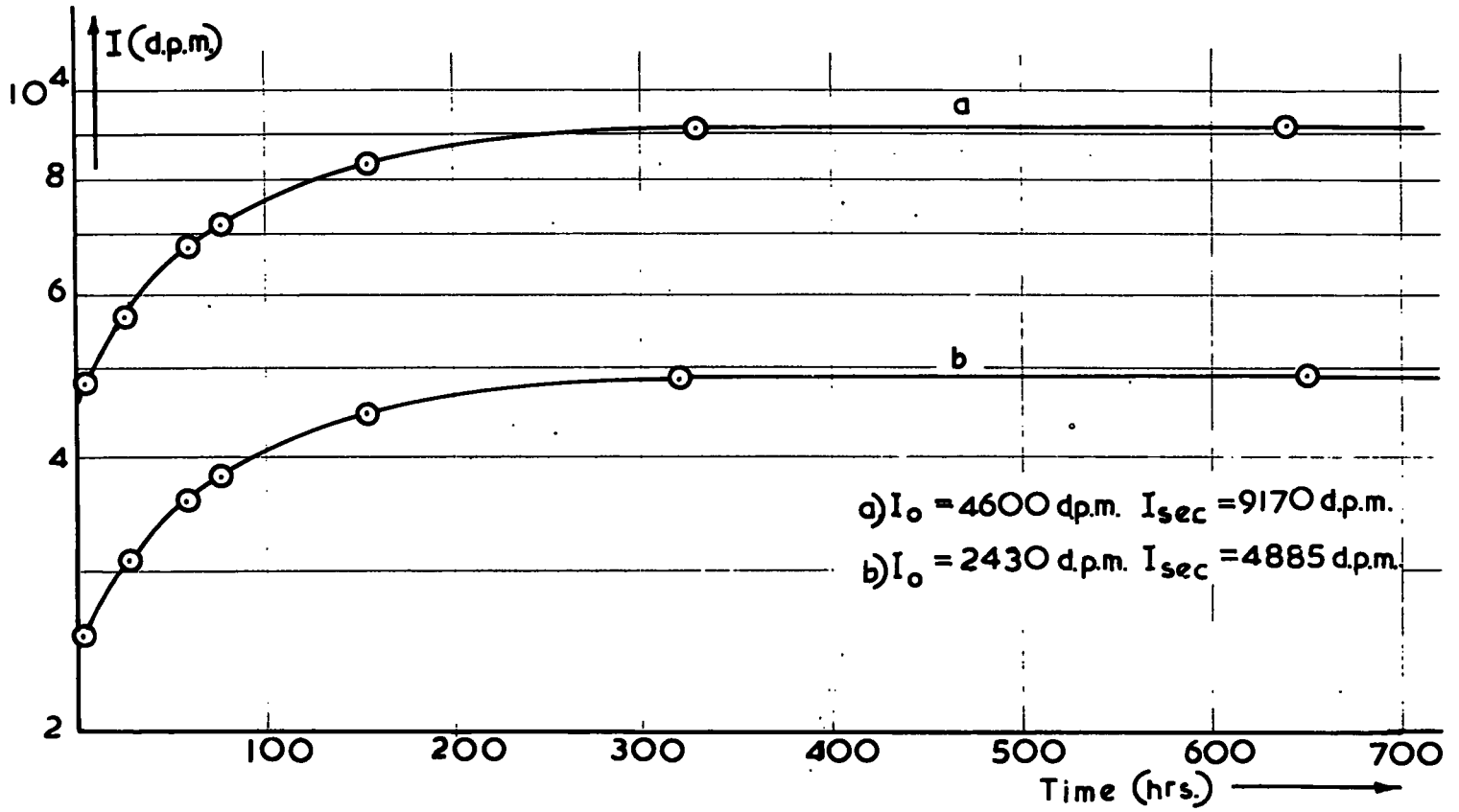

FIG. 9 Sr^{90}-Y^{90} GROWTH CURVES.

counted in different positions in the plane normally occupied by a 4π source. The measured decreases in the counting efficiency at different distances from the centre of this plane are tabulated below (Table 2). It can be seen that counting losses from edge effects can be

TABLE 2. VARIATION OF COUNTING EFFICIENCY WITH DISTANCE FROM THE CENTRE OF THE 4π COUNTER

Distance from centre of counter mms.	% Loss of efficiency perpendicular to anode wire	parallel to anode wire
1	0+	0+
5	0.6	0.2
9	0.6	0.3
13	0.5	2.0

+ The counter is assumed 100% efficient at the centre. The diameter of the counter is 26 mms.

neglected so long as the source is confined to a small area (diameter $\sim$ 1.5 cms.) at the centre of the source support.

The absolute specific activities of standardised solutions of Au^{198} and P^{32}, distributed by the National Physical Laboratory, were measured by the 4π technique and agreed with the N.P.L. values to within their quoted

errors. The absolute disintegration rate of the Au^{198} solution was determined separately by $\beta - \gamma$ coincidence counting. A value of 24.43 μc./gm. was obtained compared to the value of 24.80 μc./gm. obtained by 4π counting.

The absolute specific activity of a S^{35} solution was determined by several groups of workers. Their results are presented in Table 3. It can be seen that the result obtained here compares favourably with the others.

TABLE 3. RESULTS OF THE STANDARDISATION OF A S^{35} SOLUTION BY DIFFERENT ESTABLISHMENTS

Where the standardisation was performed	Technique used	Mean value of specific activity μc./gm.
N.P.L.	4π proportional counting	192.3
A.E.R.E. Harwell	4π Geiger counting	191.7
R.C.C. Amersham	4π proportional counting	205.0
Here	4π proportional counting	195.8

The 4π counting technique used here has been thoroughly investigated. The calibration of other counters with respect to the 4π counter could be confidently assumed accurate to within a per cent or two.

d) The end window gas-flow β-proportional counter

The counter is depicted in Fig. 10 and the associated electronic equipment and gas-flow system are shown schematically in Fig. 11. As stated, these were identical to those of the 4π counter, and the gas-flow system is described in Section (a). The gas flowed through the counter at a rate of about 0.75 ml./sec. As in the case of the 4π counter, the flow rate was found to be not very critical above a certain minimum, in this case about 0.4 ml./sec.

The end window of the counter (diameter - 2.6 cms.) was a very thin VYNS plastic film (80 μ gms./cm.^{2}), prepared in the same way as the 4π source supports, but with several layers of film. The film was gold-coated on one side to give it conducting properties. With this very fragile window, care had to be taken to ensure that the gas did not build up a pressure, especially when removing and replacing the gas leads.

The anode loop, kinkless and $\frac{3}{8}$ inch in diameter, was of constantan (0.001 inch in diameter). It was soldered into a fine nickel tube and suspended $\frac{5}{8}$ inch from the counter window. The nickel tube was insulated from the counter walls by suspension from a teflon plug. With the sensitive volume of the counter thus defined, a plateau of about 250 volts was obtained. The optimum

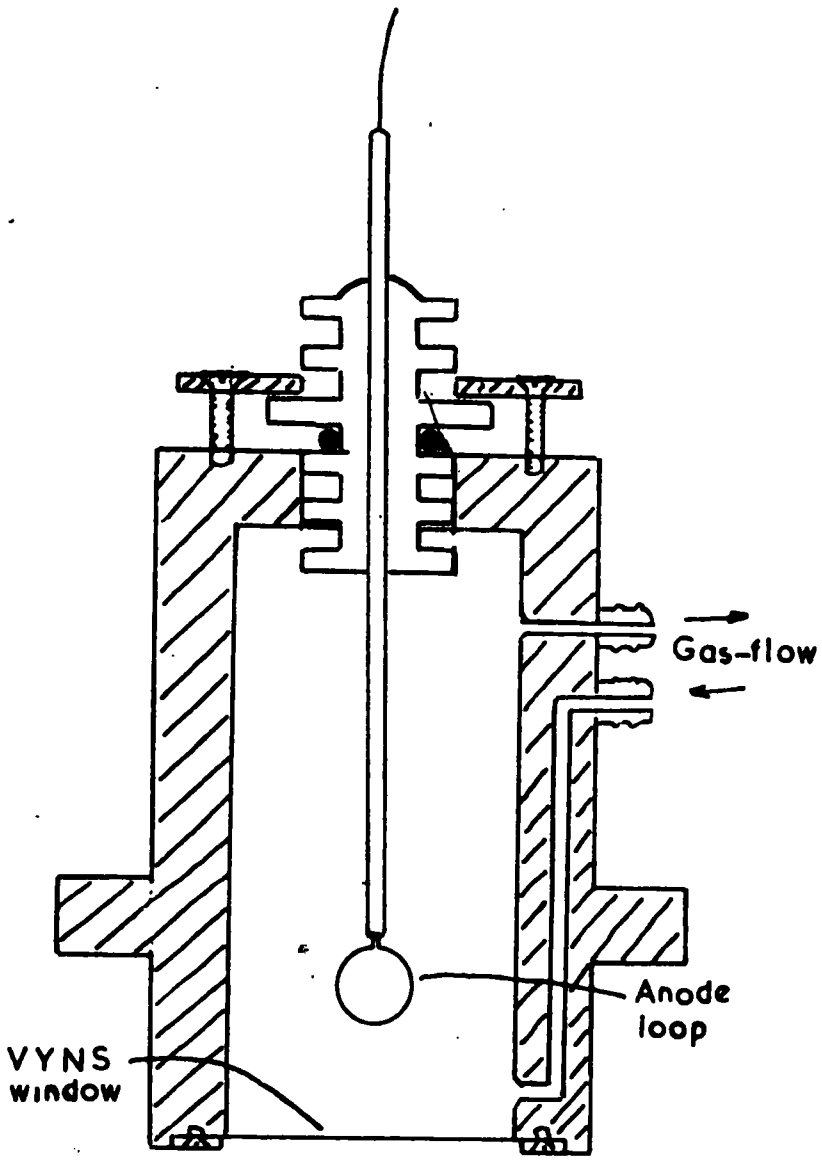

FIG. 10 END WINDOW COUNTER.

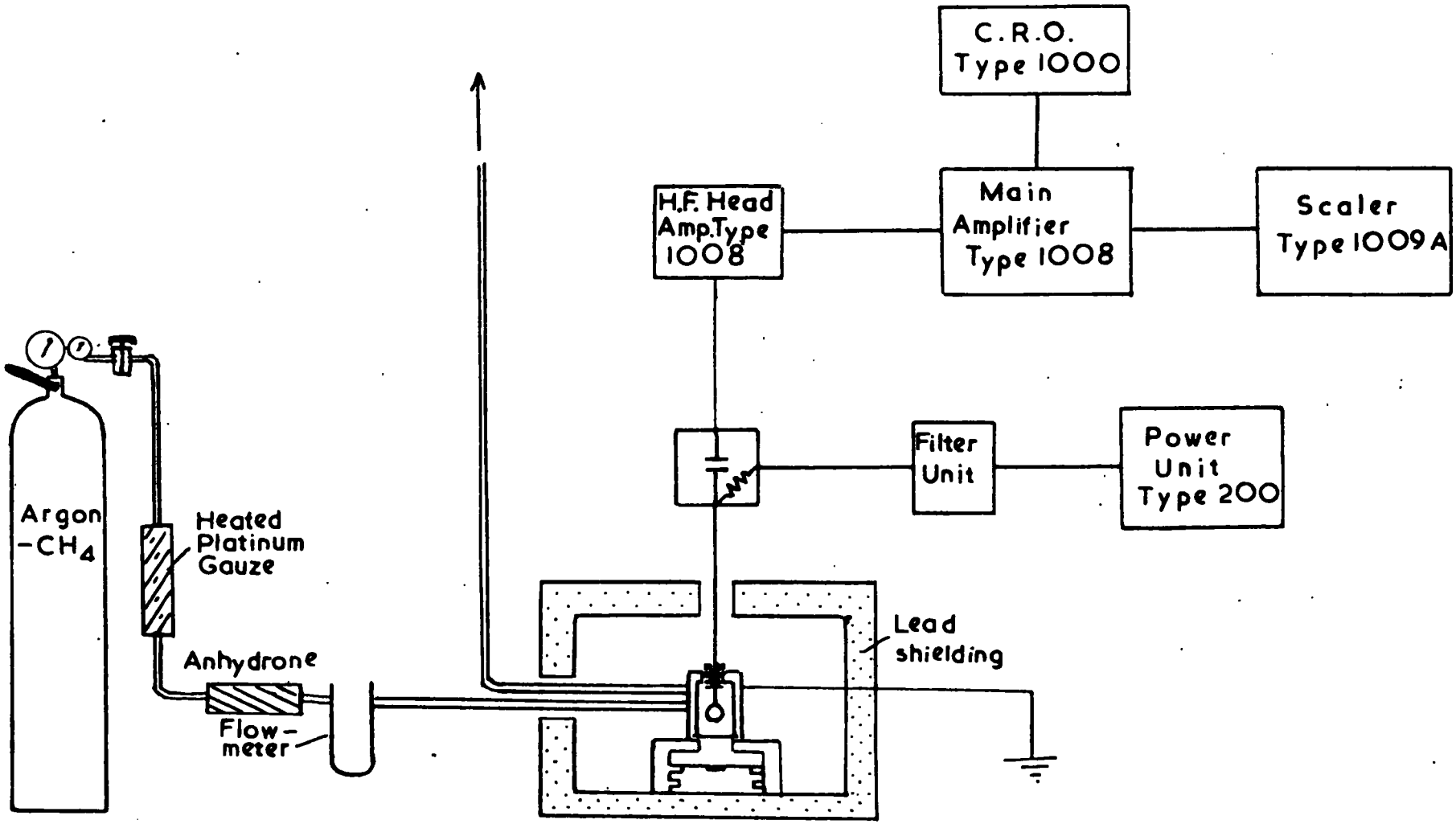

FIG. 11 GAS-FLOW SYSTEM & ELECTRONICS FOR THE END WINDOW COUNTER.

counting voltage was of the order of 1.7 kV, but varied slightly with β-energy. Like the 4 π counter, the end window counter was operated with the scaler paralysis time set at 50 μsecs.

The counter was enclosed in a lead castle, which reduced the background count to about 14 c.p.m.

Pulses from the proportional counters, 4 π as well as end window, were amplified externally by a factor of 10^6. Care had to be taken to prevent spurious pulses, passed along the mains, from recording. Sources of spurious pulses were traced and eliminated.

In humid weather there was a tendency for the counter insulation to break down across the surface. This was cured by wiping the insulation with methanol and drying it with a hot-air drier.

e) Preparation of solid sources for the end window counter

To facilitate the accurate calibration of the end window counter, all solid sources were prepared by a standardised technique.

In the final stage of a chemical procedure, the activity with its inactive carrier was precipitated in a suitable gravimetric form. The precipitate would normally weigh about 10-20 mgs., depending upon the chemical yield of the procedure. The sources were prepared by uniformly

collecting the active precipitates on glass-fibre filter discs (Whatman GF/A 2.1 cms.) supported on sintered polythene in a demountable filter funnel (Fig. 12). The internal diameter of the filter funnels was standardised at $\frac{5}{8}$ inch. The sources were supported on standard aluminium trays and counted with reproducible geometry with respect to the sensitive volume of the counter.

Chemical yields were determined by direct weighing. Herein lay the great advantage of using glass-fibre filter discs as opposed to filter-paper discs, which were used initially. A considerable error was introduced in the use of the latter by their hydrophilic property. It was necessary to tare the discs and weigh the sources under very carefully regulated conditions, if the weights of the discs were to be assumed constant. This was most unsatisfactory. The glass-fibre filter discs absorbed negligible amounts of water vapour and could be weighed on an open tray with little or no variation.

A Stanton semi-micro balance (Model MC1A) was used and the discs were weighed to the nearest 0.01 mg. These weights were accurately known to within $\pm$ 0.05 mg., so that chemical yields, determined in this fashion, were accurate to within $\pm$ 0.5%.

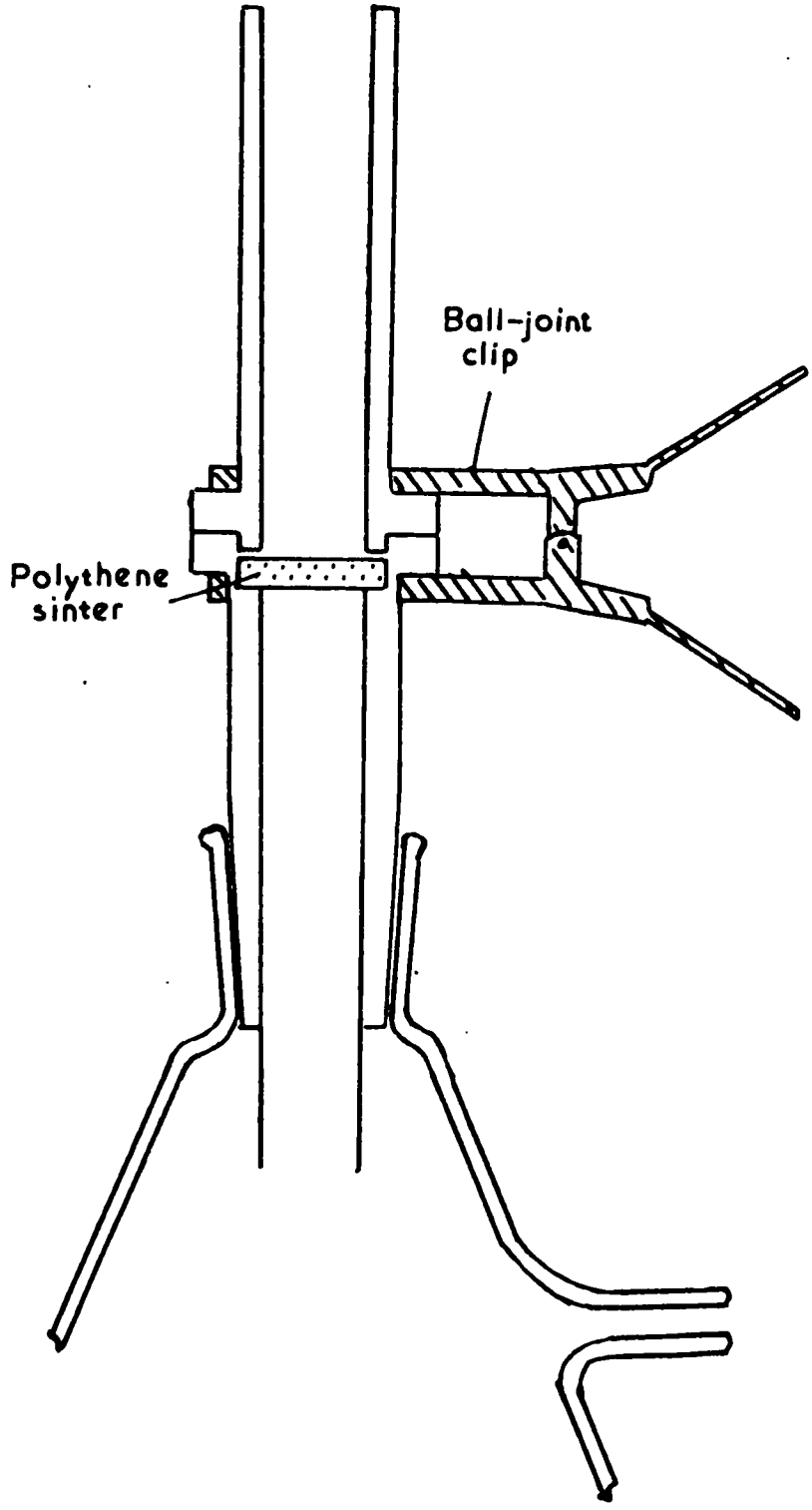

FIG. 12 DEMOUNTABLE FILTER-FUNNEL.

f) Calibration of the end window counter

The absolute disintegration rates of carrier-free solutions of several β-active nuclides were determined by the 4π counting technique.

Aliquot parts of these standardised solutions were added to solutions of the respective inactive carriers and precipitated by a recommended gravimetric procedure. Sources of varying thickness were prepared by the standard filter-funnel technique and counted with reproducible geometry.

The efficiency of the counter $\left(\frac{\text{observed counting rate}}{\text{absolute disintegration rate}}\right)$ was calculated for each individual source and plotted against the weight of the source. These self-absorption curves were plotted for sources ranging from about 5 mgs. to 50 mgs. and, except for the nuclides emitting low energy β-particles, counter efficiency varied little with source thickness over this range. Typical curves are reproduced in Fig. 13.

The β-active nuclides, for which self-absorption curves have been constructed, are shown in Table 4.

The counting efficiencies for 20 mg. sources were interpolated from the curves and plotted against the β-particle end point energies of the different nuclides. This curve is reproduced in Fig. 14. It can be seen that, above about 0.6 MeV, there is little or no

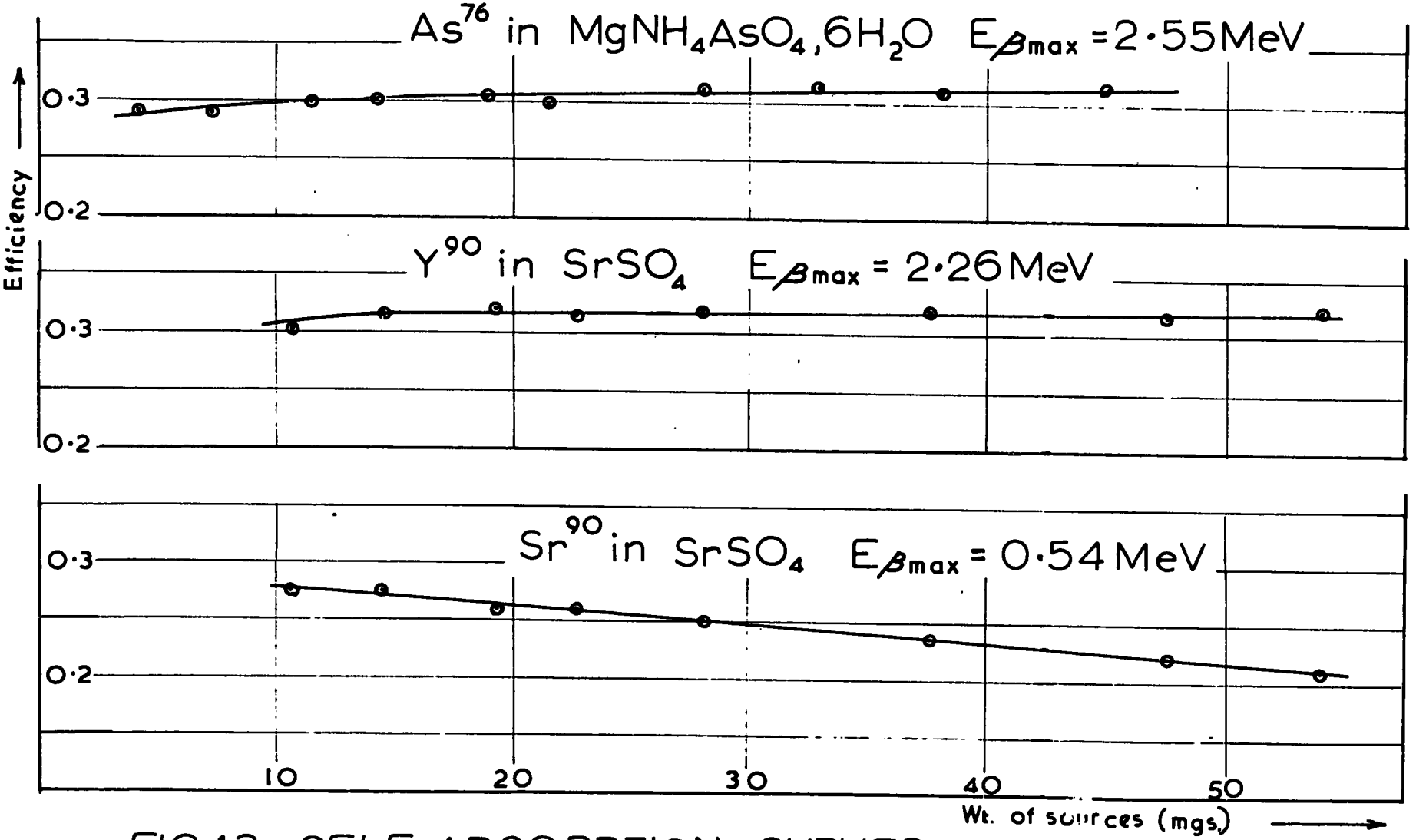

FIG.13 SELF-ABSORPTION CURVES.

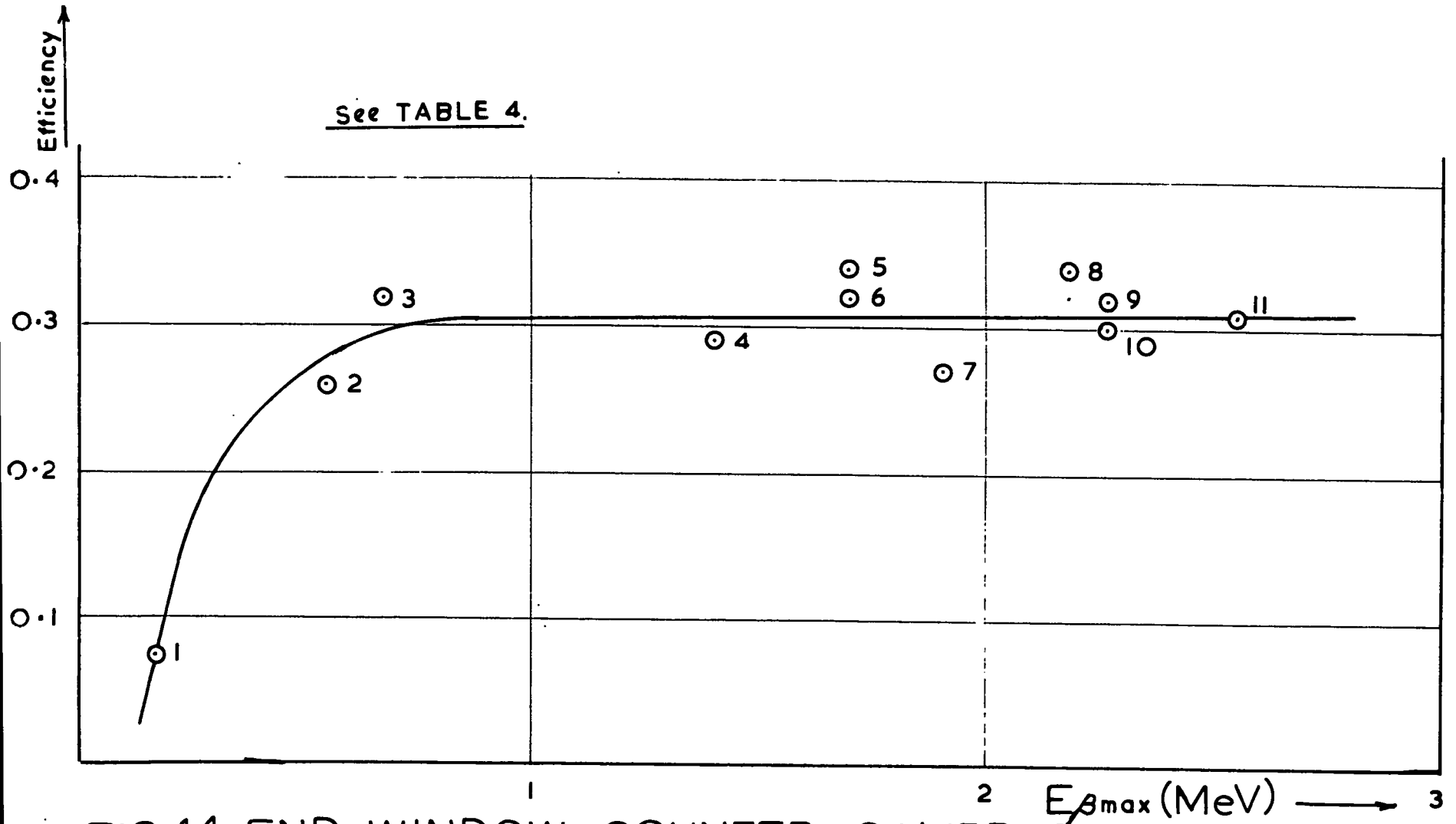

FIG.14 END WINDOW COUNTER CALIBRATION CURVE.

variation in counter efficiency with increasing β^--energy This made it possible to interpolate accurately the counting efficiencies of activities, for which it was not possible to perform separate calibrations. Precise knowledge of β-energies was not required, but merely assurance that they were greater than 0.6 MeV.

TABLE 4. CALIBRATION OF END WINDOW COUNTER

	Active nuclide	Carrier precipitate	$E\beta_{max}$(MeV) (weighted mean)	Counter efficiency for a 20mg source
1	S^{35}	$BaSO_4$	0.167	0.076
2	Sr^{90}	$SrSO_4$	0.54	0.26
3	Pt^{197}	elemental Pt	0.67	0.32
4	Na^{24}	NaCl	1.40	0.29
5	P^{32}	$BiPO_4$	1.70	0.34
6	P^{32}	$MgNH_4PO_4,6H_2O$		0.32
7	Mn^{56}	$MnNH_4PO_4,H_2O$	1.90	0.27
8	Ir^{194}	elemental Ir	2.18	0.34
9	Y^{90}	$SrSO_4$	2.26	0.32
10	Y^{90}	$Y_2(C_2O_4)_3,7H_2O$		0.30
11	As^{76}	$MgNH_4AsO_4,6H_2O$	2.55	0.31

Counting efficiencies are, to some extent, dependent on the electron density of the precipitate and this had to be regarded when interpolating.

g) The liquid counter

A halogen-quenched liquid counter (Model M6H) with a capacity of 10 mls. was calibrated and used to assay the absolute β^--disintegration rates of those activities for which it was not convenient to prepare solid sources.

The counter characteristics were very good. The threshold voltage for counting was at about 340 volts. Above this voltage the counter plateau stretched for several hundred volts. The optimum counting voltage was 410 volts. The paralysis time on the external quenching unit (Probe Unit Type 110A) was set at 500 μsecs. This limited counting rates to about 10^4 c.p.m. and made "dead-time" corrections important.

The counter was supported in a lead castle, in which the background count rarely exceeded 14 c.p.m.

The counter efficiency was checked periodically with a standard Co^{60} solution.

h) Calibration of the liquid counter

10 ml. aliquot parts of solutions of different β-active nuclides, standardised by the 4 π counting technique, were counted in the liquid counter. The efficiency, with which they were counted, was calculated and plotted against β-particle end point energy.

The points, all except one, fit onto a smooth curve (Fig. 15) over an energy range of from 0.765 MeV (Tl^{204}) to 2.55 MeV (As^{76}). The anomalous point is Bi^{210}, for which the counting efficiency appears much too low for its β end point energy. This is accounted for by the shape of the Bi^{210} β-spectrum, which is for a "forbidden" transition. In this case, the end point energy does not bear the same relation to the mean energy of the emitted β-particles as it does in the normal "allowed" transition.

The calibration curve, not including Bi^{210}, appeared to be essentially linear between 1 MeV and 3MeV and, provided β-energies and decay schemes were well established, interpolation on this curve was accurate. This was very useful for, although it was still preferred to calibrate counters for the particular activity to be measured, it was not always possible.

Much below 1 MeV, the liquid counter became so inefficient as to be impractical.

The β-active nuclides used for the calibration are presented in Table 5. It can be seen that the electron density of the solution affects the counting efficiency somewhat.

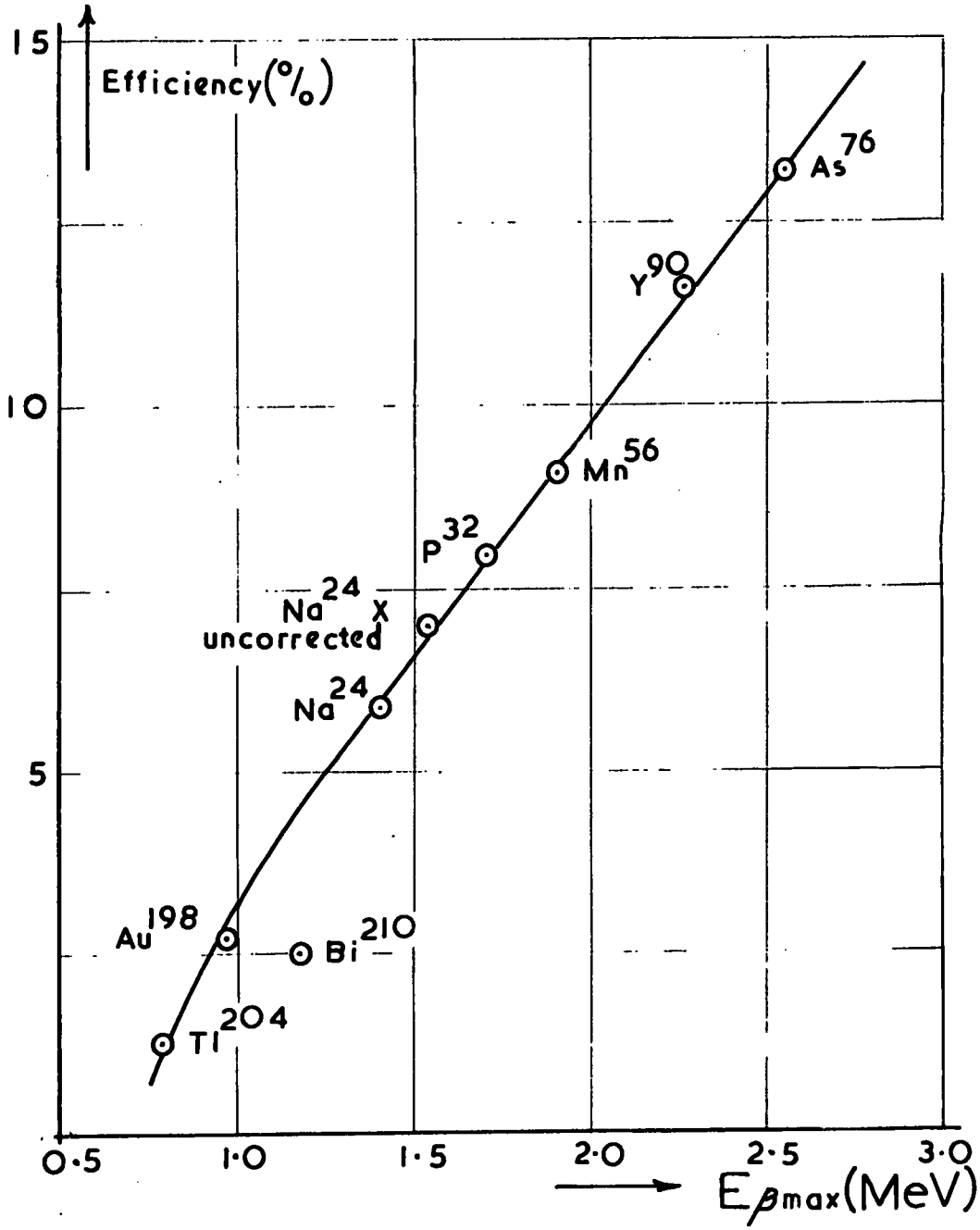

FIG. 15 LIQUID COUNTER CALIBRATION CURVE.

TABLE 5. CALIBRATION OF LIQUID COUNTER

Active Nuclide	$E_{\beta max.}$ (MeV) (Weighted mean)	Counter efficiency (%)
Tl^{204}	0.78	1.24
Au^{198}	0.97	2.70
Bi^{210} (in dilute acid)	1.17	2.52
Bi^{210} (in conc. soln. of $Bi(NO_3)_3$)		1.95
Na^{24}	1.40	6.97
Ni^{65}	1.53	7.00
P^{32}	1.70	7.93
Mn^{56} (in dilute acid)	1.90	9.05
Mn^{56} (in standard acid mixture with 0.5 gm. of Fe)		8.93
Y^{90}	2.26	11.63
As^{76}	2.55	13.32

i) Accessories to counting equipment

In general, no activities with half-lives shorter than a few minutes were measured, but there were occasions when it was desired to investigate an activity with a half-life of the order of seconds. In these cases, of course, no chemistry was performed and it was necessary

to transfer samples from the target chamber to the counting room in a very short time. This was accomplished by means of a vacuum tube. The sample, attached to the "rabbit", was released from beneath the target by a mechanism operated from the counting room and dropped into the tube, which transferred it to the counting room in about two and a half seconds.

The counting of these very short-lived activities was facilitated by an electronic timing device, which stopped the scaler at predetermined intervals for a small fixed period, during which the scaler could be read. The timer also operated a camera which could be used to record the scaler readings.

The camera was also useful for tracing the decay of activities with long half-lives (of the order of several days). The camera was focussed on the scaler panel and the timing mechanism was set to take exposures at predetermined intervals over a long period of time.

Part 3 Chemical separations associated with the calibration of counters

a) Separation of Ni^{65} from Co^{58m}

The liquid counter was calibrated for 2.56 hr. Ni^{65} ($E_{\beta max}$ = 1.53 MeV).

A high specific activity of Ni^{65} was obtained by irradiating about 20 mgs. of nickel wire in the BEPO pile at A.E.R.E. Harwell, but it was contaminated by some 9.2 hr. Co^{58m}, formed by the $Ni^{58}(n,p)Co^{58m}$ reaction.

The Co^{58m} was removed by the ion-exchange technique described by Kraus and Nelson.[28]

The nickel wire was dissolved in a minimum of conc. HNO_3 and a few mgs. of cobalt carrier were added. The solution was evaporated to dryness several times with the addition of conc. HCl. The nickel and cobalt chlorides were finally taken up in 1 ml. of 9N HCl. Under these conditions, cobalt forms complex cobaltichloride ions, which are strongly retained on an anion-exchange resin.

The resin bed (Dowex 2; medium porosity; mesh-200 to 400) was prepared in a column 5 cms. long and 0.25 cms. in diameter. The active solution was placed on the column and eluted with 9N HCl at a rate of 0.2 ml./min.

A clean separation was effected, the nickel being eluted and the cobalt remaining tightly bound in a blue band at the top of the column. If it had been required, the cobalt could have been stripped from the column by elution with dilute HCl or water.

b) Separation of Sr^{90} from its daughter, Y^{90}.

It was required to calibrate the end window counter for solid sources of Sr^{90}, precipitated as $SrSO_4$, because of the similarity of its β-energy to that of Pb^{209}. The counter efficiency for Pb^{209} was required in connection with the measurement of the $Bi^{209}(n,p)Pb^{209}$ cross section.

20 yr. Sr^{90}, in secular equilibrium with 64 hr. Y^{90}, was obtained from the Radiochemical Centre, Amersham and the Sr^{90} was freed from its daughter by the ion-exchange technique summarised by Dalton and Welch.[29] A neutral solution of the Sr^{90}-Y^{90} mixture, containing added strontium carrier, was passed through a column of an anion-exchange resin in the hydroxide form. Yttrium, which forms an insoluble hydroxide, was precipitated by the resin and did not appear in the eluate. No yttrium carrier was added, as macroscopic amounts of yttrium form a gelatinous precipitate with the resin, impeding further elution.

Dowex 2 anion-exchange resin (medium porosity, 200-400 mesh) was activated by repeated washing with baryta, which gradually replaced the chloride ions on the resin by hydroxides. Baryta was preferred to ammonia for this purpose, as it contains no free carbonate ions from contact with the atmosphere ($BaCO_3$ is precipitated). Carbonate ions would compete favourably with hydroxide ions for places on the resin and, on elution, the resin would retain strontium as well as yttrium and a clean separation would not be effected

A bed of the activated resin was prepared in a column, 12 cms. long and 0.4 cms. in diameter, and washed with CO_2-free water.

0.25 ml. of a neutral solution, containing about 6 μc. of Sr^{90} with 1 mg. of strontium carrier added, was placed on the column and eluted with CO_2-free water at a rate of 0.2 ml./min. An estimated 95% of the Sr^{90} appeared in the first three column volumes of eluate (3 mls). The first six column volumes were collected and made upto 10 mls. Aliquot parts of this solution were diluted for the preparation of Sr^{90} 4 π sources and solid sources.

Residual traces of strontium were washed from the column by the passage of several more column volumes of water, then the yttrium, which had not appeared in the eluate, was stripped from the column by eluting with 2N HCl. 1 mg. of yttrium carrier was added to this solution, which was also made up to 10 mls. Y^{90} 4 π sources were prepared, and both the end window and liquid counters were calibrated.

The growth of Y^{90} into the Sr^{90} 4 π sources was traced and the growth curve is reproduced in Fig. 9. It is proof of the efficiency of the separation, the activity at secular equilibrium being just twice the activity at t_o, the effective time of the separation. The decay of Y^{90} 4 π sources was traced and they decayed almost to background. Also, the separation was quantitative. The absolute specific activity of the Sr^{90} solution was 1.428×10^3 d.p.m./mg. and that of the Y^{90} solution was 1.43×10^3 d.p.m./mg. at t_o.

c) Separation of RaE from an equilibrium mixture of RaD-E-F

It was required to calibrate the liquid counter for RaE(Bi^{210}) in connection with the measurement of the $Bi^{209}(n, \gamma)Bi^{210}$ cross section.

The RaE was separated from RaD(Pb^{210}) and RaF(Po^{210}) electrochemically, under the conditions described by Haissinsky[30] and by Bagnall.[31] The electropositivity of the RaD-E-F chain increases with atomic number, and RaF and RaE can be removed in turn from solution by spontaneous deposition on silver and nickel foils respectively. The process is facilitated by raised temperatures.

A solution containing about 0.1 μc./ml. of Bi^{210} was available. 2 mls. of this solution were made 0.5 N with respect to HCl and warmed to about 80°C over a water bath. A piece of silver gauze was rotated in the solution for 45 mins. and, after removal and washing, this was shown to have collected a high α-activity (Po^{210}). The Bi^{210} was then deposited on a nickel foil under the same conditions. The nickel foil was removed from the solution after an hour. It was thoroughly cleaned to remove all traces of solution, which still contained the Pb^{210} parent of the chain, and the nickel surface with the deposited Bi^{210} was dissolved in conc. HNO_3. This solution was evaporated to dryness several times with conc. HCl, to remove all traces of nitrous fumes, and diluted for the preparation of the 4 π sources.

The decay of the Bi^{210} was traced in both the 4π counter and the liquid counter. The solution in the latter decayed to near background with the reported half-life of 5 days, giving proof of a clean separation from Pb^{210}. A certain amount of α-activity from Po^{210} was detected in the 4π sources. This amounted to about 0.5% of the total activity at t_o and was corrected for.

Part 4 Examination of the homogeneous mixture technique for monitoring the neutron flux

The iron used as a reference element was supplied by the Bureau of Analysed Samples, Ltd. in the form of granules (~ 0.5 mm. diameter). The granules were guaranteed 99.8% pure and the limits of different impurities were specified. The shape and size of the granules were chosen in preference to others, because they appeared to have better mixing properties. The 2.58 hr. Mn^{56} activity should be free from contaminating activities after a few minutes. This was checked by tracing the decay of Mn^{56}, induced in a sample of the iron, for several half-lives. A specimen decay curve is reproduced in Fig. 16.

The iron granules were used to monitor irradiations by the homogeneous mixture technique. Intimate mechanical mixtures of iron granules and sample materials were irradiated close up to the target. After irradiation, the iron was separated from the sample, using an electromagnet. A clean separation could be effected in less than a minute and chemical procedures on the sample started immediately.

After separation from the sample mixture, the iron

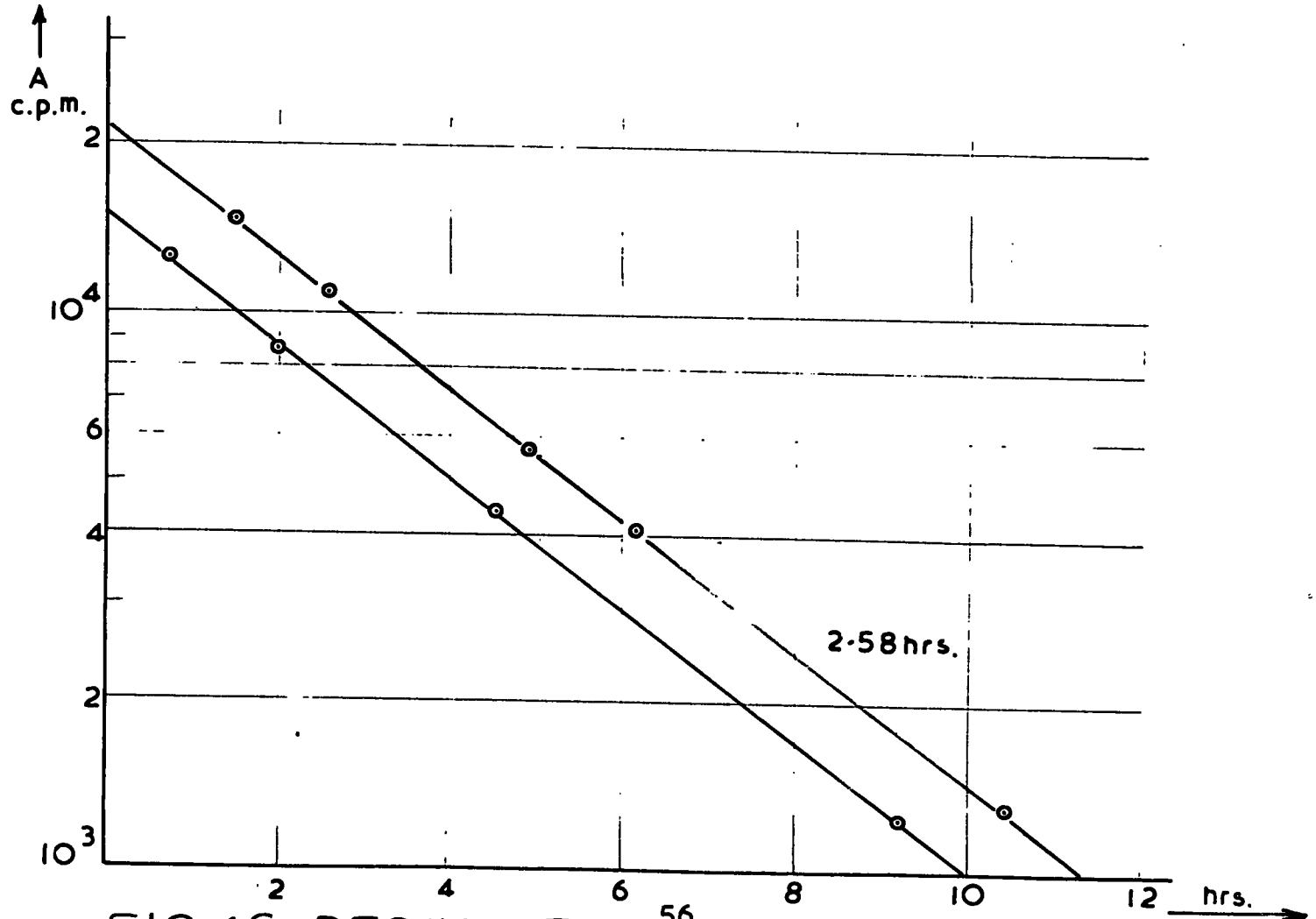

FIG. 16 DECAY OF Mn^{56} INDUCED IN THE IRON MONITOR.

(ca. 0.5 gm.) was dissolved in 10 mls. of a standard acid mixture (50% 5N HNO_3 and 50% 5N H_2SO_4), containing a little manganese carrier. The solution was made up to 12 mls. in a graduated flask and 10 mls. were withdrawn and counted in the liquid counter. The liquid counter was accurately calibrated for Mn^{56}.

Before applying the homogeneous mixture technique to the measurement of unknown cross sections, it was necessary to establish that it was valid in practice, i.e. to establish that the iron granules and sample powder could be mechanically mixed so as to satisfy the assumption of the technique, that, during an irradiation, the sample and monitor are exposed to the same neutron flux.

To test the efficiency of mixing, several mixtures of iron granules and finely divided cobalt carbonate were irradiated. Both cobalt and iron give 2.58 hr. Mn^{56}, and it is possible to determine the $Co^{59}(n,\alpha)Mn^{56}$ cross section relative to the $Fe^{56}(n,p)Mn^{56}$ cross section without the necessity of correcting measured activities for counting efficiency and fluctuations in the neutron flux during the course of the irradiation. The reproducibility of values obtained for the $Co^{59}(n,\alpha)Mn^{56}$ cross section is a measure of the homogenity of the mixture.

The values obtained for the cross section of the $Co^{59}(n,\alpha)Mn^{56}$ reaction, from four repetitions of this experiment, differed by less than four per cent.

In another experiment triple mixtures of iron, magnesium oxide and aluminium granules were irradiated and the cross sections of two other possible monitor reactions, $Al^{27}(n,\alpha)Na^{24}$ and $Mg^{24}(n,p)Na^{24}$ were measured relative to the $Fe^{56}(n,p)Mn^{56}$ cross section.

Four of these mixtures were irradiated and the values obtained for the $Al^{27}(n,\alpha)Na^{24}$ and $Mg^{24}(n,p)Na^{24}$ reactions were reproducible to within five per cent.

The values obtained for these cross sections were also consistent with those obtained by other workers (see Chapter 4, Sections (a) and (b)), demonstrating that the principle of this monitoring technique was quite sound in practice.

The possibility was not overlooked that Mn^{56} nuclei, recoiling from nuclear interaction, might lodge in the sample material and interfere with the measurement of the activities indueced in the latter, in spite of subsequent chemical separations. In the course of similar work, Mrs. E.B.M. Martin irradiated homogeneous mixtures of iron granules and glucose and, after removal of the iron, the glucose was dissolved and

counted in a liquid counter. The presence of Mn^{56} nuclei was detected to the extent of less than 0.1% of the total. This amount was so small as to be negligible, except in cases where the activity induced in the sample decayed with a comparable half-life, was formed with a low cross section and was counted without prior chemical separation. One such case was the measurement of the $Mn^{55}(n, \gamma)Mn^{56}$ cross section. This irradiation was monitored by the $Al^{27}(n, \alpha)Na^{24}$ reaction.

Part 5. Methods of Calculation.

All the cross sections reported have been measured relative to that of a reference reaction, usually $Fe^{56}(n,p)Mn^{56}$, on the assumption that both the sample and reference element have been exposed to the same neutron flux. But, as the radioactive products, induced in the sample and reference substance, decay at different rates, it is necessary to make corrections for the decay of products during the course of the irradiation.

As mentioned in Chapter 3, the 14 MeV neutron generator does not produce a steady neutron flux and allowance must be made for this.

Consider an irradiation of duration T. Resultant activities are plotted and the activities at time t_o, the end of the irradiation, are determined by extrapolation.

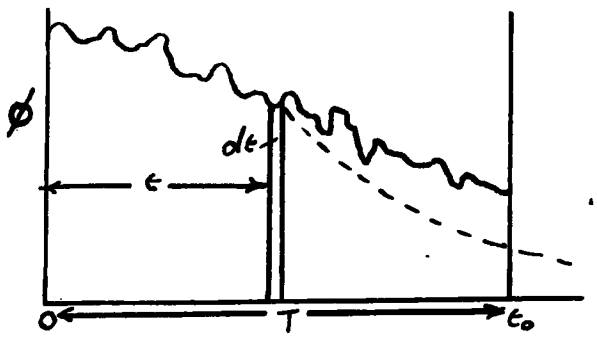

Variation of neutron flux with time during the course of an irradiation.

a) A stable nuclide, 1, is activated during the irradiation, producing a radioactive nuclide, 2. The radio-

active nuclide, 2, subsequently decays to a stable nuclide at a rate determined by its disintegration constant, λ.

i.e. $1 \xrightarrow{(n,x)} 2 \xrightarrow[\lambda]{\beta} \text{stable}$

The nuclide, 2, is produced throughout the irradiation at an irregular rate given by the expression

$$\frac{dN_2}{dt} = N_1 . \sigma_{12} . \phi(t)$$

where, $\frac{dN_2}{dt}$ is the rate of production of 2.

N_1 is the number of nuclei of 1 exposed to the neutron flux.

σ_{12} is the cross section for the reaction $1 \xrightarrow{(n,x)} 2$.

$\phi(t)$ is the neutron flux as a function of time.

During the short interval, dt, the number of nuclei of 2 which are produced is

$$dN_2 = N_1 . \sigma_{12} . \phi(t).dt.$$

and these decay exponentially so that at the end of the irradiation, time t_o, the number remaining is

$$dN_2(t_o) = N_1 . \sigma_{12} . \phi(t).e^{-\lambda(T-t)}.dt.$$

The value of $\phi(t)$ at any instant is not known

absolutely, but its variation is proportional to the variation in the counting rate of the proton-recoil monitor, I(t).

i.e. $$\phi(t) = I(t)/\zeta$$

where, ζ is the factor relating flux at the sample position to the counting rate of the neutron monitor.

Thus:

$$N_2(t_o) = \frac{N_1 \cdot \sigma_{12}}{\zeta} \int_{t=o}^{t=t_o} I(t).e^{-\lambda(T-t)}.dt$$

The integral is conveniently replaced by the summation

$$\sum (I.e^{-\lambda(T-t)}).\delta t \quad \text{(abbreviated to } S_2)$$

so long as δt is small compared to the half-life of nuclide 2. Then:

$$N_2(t_o) = \frac{N_1 \cdot \sigma_{12} \cdot S_2}{\zeta}$$

A similar expression applies to every nuclear reaction occurring during the irradiation and, if

$$1r \longrightarrow 2r \xrightarrow[\lambda_r]{\beta} \text{stable}$$

represents the reference reaction,

$$\frac{N_2(t_o)}{N_{2r}(t_o)} = \frac{N_1 \cdot \sigma_{12} \cdot S_2}{N_{1r} \cdot \sigma_{12r} \cdot S_{2r}}$$

the unknown factor, $\mathcal{J}$, cancelling between the two expressions, provided both sample and reference substance are exposed to the same flux.

As stated, the activities of resultant nuclides at time t_o, the end of the irradiation, are determined by extrapolation of their decay curves. Then, since $A_o = c. \lambda . N_o$,

$$\frac{A_o(2)}{A_o(2r)} = \frac{C_2 \cdot \lambda . N_1 \cdot \sigma_{12} \cdot S_2}{C_{2r} \cdot \lambda_r \cdot N_{1r} \cdot \sigma_{12r} \cdot S_{2r}} \quad \text{equation (1)}$$

where, C_2 and C_{2r} are the detection coefficients for the respective nuclides.

b) In some cases, it was required to measure the relative cross sections for the independent production of a pair of nuclear isomers.

A stable nuclide, 1, is activated during an irradiation, producing both the metastable and ground states of a radioactive nuclide, 2. Allowance must be made for the formation of ground state nuclei via the metastable state during the course of the irradiation. The process can be represented:

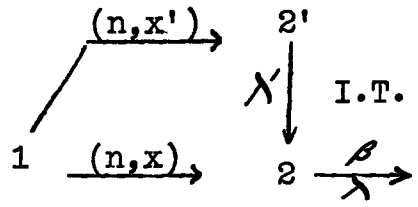

The decay curve of the resultant activities is plotted and the number of nuclei of 2 and 2' at time t_o, the end of the irradiation is calculated by solving two simultaneous equations of the type

$$I = cN_2' \cdot \lambda' \cdot \left[1 + \frac{\lambda}{\lambda - \lambda'}\right] \cdot e^{-\lambda' t} + c \cdot \lambda \cdot \left[N_2 - \frac{\lambda'}{\lambda - \lambda'} \cdot N_2'\right] \cdot e^{-\lambda t}$$

where, I is the observed activity at time t.

N_2 and N_2' are the number of nuclei of the respective nuclides at the end of the irradiation, time t_o.

c, the detection coefficient, is assumed to be the same for both isomers. (This is justified in the case in point See Table 22).

The total number of nuclei of 2' present at the end of the irradiation is given by

$$N_2'(t_o) = \frac{N_1 \cdot \sigma_{12'}}{\beta} \cdot \sum (I.e^{-\lambda'(T-t)}) \cdot \delta t.$$

$$= \frac{N_1 \cdot \sigma_{12'} \cdot S_2'}{\beta}$$

The total number of nuclei of 2 present at the end of the irradiation is given by

$$N_2(t_o) = \frac{N_1 \cdot \sigma_{12}}{\beta} \sum (I.e^{-\lambda(T-t)}) \delta t + N$$

$$= \frac{N_1 \cdot \sigma_{12} \cdot S_2}{\beta} + N$$

where, N is the number of nuclei of 2 formed via the metastable state 2', during the course of the irradiation.

The rate of formation of 2 via 2' is given by

$$\frac{dN}{dt} = N_2' \lambda' - N \lambda$$

Then:

$$N = \frac{N_1 \sigma_{12'}}{\beta} \cdot \frac{\lambda'}{\lambda - \lambda'} \cdot \sum I(e^{-\lambda'(T-t)} - e^{-\lambda(T-t)}) \cdot \delta t$$

$$= \frac{N_1 \sigma_{12'}}{\beta} \cdot \frac{\lambda'}{\lambda - \lambda'} \quad (S_2' - S_2)$$

and the total number of nuclei of 2 present at the end of the irradiation is

$$\frac{N_1}{\beta} \cdot \left[\sigma_{12'} \cdot \frac{\lambda'}{\lambda - \lambda'} (S_2' - S_2) + \sigma_{12} S_2 \right]$$

$$\frac{N_2'}{N_2} = \frac{\sigma_{12'} S_2'}{\sigma_{12'} \cdot \frac{\lambda'}{\lambda - \lambda'} (S_2' - S_2) + \sigma_{12} S_2} \quad \text{... equation (2)}$$

CHAPTER 4

THE DETAILED APPLICATION OF GENERAL PROCEDURES TO INDIVIDUAL ELEMENTS AND THE RESULTS OF IRRADIATIONS

a) IRRADIATION OF COBALT

Homogeneous mixtures of basic cobalt carbonate and iron granules were irradiated.

The reaction observed in the cobalt was:-

$$Co^{59}(n,\alpha)Mn^{56}(t_{\frac{1}{2}} = 2.58 \text{ hrs.})$$

The Mn^{56} activities induced in both the iron and the cobalt were traced for several half-lives.

EXPERIMENTAL DETAILS

Treatment of cobalt carbonate.

Mixtures usually consisted of about 0.5 gm. of iron and 1 gm. of cobalt carbonate. After removal of the iron, the cobalt carbonate was weighed and carefully dissolved in about 10 mls. of the standard acid mixture used to dissolve the iron (50% 5N HNO_3 and 50% 5N H_2SO_4 with a little manganese carrier). The dissolution of the carbonate is facilitated by the addition of a few drops of a 6% solution of $NH_2OH.HCl$, which reduces any cobaltic salts present.

The active solution was made up to 12 mls. and a 10 ml. aliquot was counted in the same liquid counter as the solution of the iron monitor.

Estimation of the cobalt content of the carbonate.

The cobalt content of the basic cobalt carbonate was determined volumetrically, titrating an approx. 0.01M solution of the cobalt directly against a standard EDTA solution with muxexide as indicator. The procedure is described by Schwarzenbach.[32]

RESULTS AND DISCUSSION

Four mixtures were irradiated and the results are presented in Table 6.

The primary purpose of this irradiation, as described in Chapter 3, Part 4, was to test the validity of the homogeneous mixture technique of monitoring the neutron flux. The reproducibility of the values obtained for the $Co^{59}(n, \alpha)Mn^{56}$ cross section is a measure of the success of the method.

The mean value, 34.8 mbs. $\pm$ 1.3, is relative to an assumed value of 124 mbs. for the $Fe^{56}(n,p)Mn^{56}$ cross section. This compares very well with the values reported by Paul and Clarke[1] (39.1 mbs. $\pm$ 8) and

Blosser et al[6] (35.0 mbs. ± 3).*

* All Blosser's cross sections were measured, by the sandwich technique, relative to an assumed value of 110 mbs. for the $Fe^{56}(n,p)Mn^{56}$ monitor cross section. The cross section quoted above has been adjusted relative to the value, assumed in the present work, of 124 mbs. for the monitor cross section.

TABLE 6 RESULTS FOR THE $Co^{59}(n, \alpha)Mn^{56}$ REACTION.

IRRADIATION NO.	SAMPLE REACTION		REFERENCE REACTION		MEASURED CROSS SECTION (mbs.)	MEAN
	No. of target nuclei x N^{-1}	A_o c.p.m.	No. of target nuclei x N^{-1}	A_o c.p.m.		
1	6.14×10^{-3}	3.40×10^{3}	9.15×10^{-3}	1.89×10^{4}	33.2	34.8 mbs. $\pm$ 1.3
2	7.50×10^{-3}	2.12×10^{3}	1.40×10^{-2}	1.42×10^{4}	34.6	
3	6.02×10^{-3}	3.36×10^{3}	7.39×10^{-3}	1.40×10^{4}	36.5	
4	6.17×10^{-3}	3.92×10^{3}	9.58×10^{-3}	2.15×10^{4}	35.0	

N is the Avogadro Number .

$\sigma_{Fe^{56}(n,p)Mn^{56}} = 124$ mbs.

b) IRRADIATION OF ALUMINIUM AND MAGNESIUM

Triple mixtures of iron granules, aluminium granules and finely divided magnesium oxide were irradiated.

The following reactions were observed and their cross sections determined:-

$$\left.\begin{array}{l} Al^{27}(n,\alpha)Na^{24} \\ Mg^{24}(n,p)Na^{24} \end{array}\right\} \quad (t_{\frac{1}{2}} = 15.0 \text{ hrs. } \pm 0.1)$$

The Na^{24} activities were traced for about three half-lives.

Later, a piece of aluminium foil was irradiated and the cross section of the reaction:-

$$Al^{27}(n,p)Mg^{27} \qquad (t_{\frac{1}{2}} = 9.5 \text{ mins})$$

was measured relative to the predetermined value of the $Al^{27}(n,\alpha)Na^{24}$ cross section.

EXPERIMENTAL DETAILS.

Treatment of the mixture.

The iron was separated using an electromagnet and the aluminium granules were efficiently separated from the magnesium oxide by a seiving technique followed by agitation in ether.

After separation the aluminium and magnesium oxide were dissolved in 5N HCl with a little sodium carrier. The active solutions were made up to standard volumes

and 10 ml. aliquot parts of each were counted in the liquid counter. This had previously been calibrated for Na^{24}.

Treatment of the aluminium foil.

The aluminium foil, irradiated to observe the $Al^{27}(n,p)Mg^{27}$ reaction, was dissolved in 5N HCl with a little magnesium, as well as sodium, carrier added. The solution was counted in the liquid counter.

RESULTS AND DISCUSSION.

The results are presented in Tables 7, 8 and 9 for four irradiations of iron, aluminium, magnesium oxide mixtures and one irradiation of aluminium foil. The good agreement of these was further proof of the success of the homogeneous mixture technique.

It can be seen from Table 10, that the values obtained in the present work are in close agreement with other reported values, especially for the often-measured $Al^{27}(n,\alpha)Na^{24}$ cross section.

IRRADIATION NO.	SAMPLE REACTION				REFERENCE REACTION				MEASURED CROSS SECTION (mbs.)	MEAN
	No. of target nuclei x N^{-1}	A_o observed c.p.m.	A_o correct d.p.m.	S	No of target nuclei x N^{-1}	A_o observed c.p.m.	A_o correct d.p.m.	S		
TABLE 7	**RESULTS FOR THE $Al^{27}(n,\alpha)Na^{24}$ REACTION.**									
5	2.38×10^{-2}	1.15×10^{4}	1.65×10^{5}	4.68	6.01×10^{-3}	1.51×10^{4}	1.70×10^{5}	3.22	119	
6	2.63×10^{-2}	1.12×10^{4}	1.61×10^{5}	4.68	9.66×10^{-3}	2.14×10^{4}	2.39×10^{5}	3.22	122	117mbs. ± 5
7	2.07×10^{-2}	8.25×10^{3}	1.18×10^{5}	9.71	8.32×10^{-3}	2.16×10^{4}	2.42×10^{5}	7.68	111	
8	2.60×10^{-2}	1.31×10^{4}	1.88×10^{5}	9.71	7.08×10^{-3}	2.25×10^{4}	2.52×10^{5}	7.68	114	
TABLE 8	**RESULTS FOR THE $Mg^{24}(n,p)Na^{24}$ REACTION.**									
5	1.71×10^{-2}	1.19×10^{4}	1.70×10^{5}	4.68	"	"	"	"	167	
6	1.76×10^{-2}	1.21×10^{4}	1.74×10^{5}	4.68					196	178mbs. ± 12
7	1.43×10^{-2}	8.86×10^{3}	1.27×10^{5}	9.71					173	
8	1.48×10^{-2}	1.14×10^{4}	1.63×10^{5}	9.71					176	
TABLE 9	**RESULTS FOR THE $Al^{27}(n,p)Mg^{27}$ REACTION.**									
9	-	2.20×10^{4}	2.86×10^{5}	1.93	-	4.80×10^{2}	7.88×10^{3}	2.77	73.5	73.5 mbs.

N is the Avogadro Number

$\sigma_{Fe^{56}(n,p)Mn^{56}} = 124$ mbs.

$t_{\frac{1}{2}}\ Na^{24} = 15.0$ hours.

$t_{\frac{1}{2}}\ Mg^{27} = 9.5$ mins.

$c_{Na^{24}} = 0.0697$

$c_{Mg^{27}} = 0.077$

$c_{Mn^{56}} = 0.0893$

TABLE 10 — COMPARISON OF VALUES OBTAINED FOR $Al^{27}(n,p)$ AND (n,α) AND $Mg^{24}(n,p)$ CROSS SECTIONS WITH WITH LITERATURE VALUES.

Reaction	Measured cross section (mbs.) Present Work	Literature
$Al^{27}(n,\alpha)Na^{24}$	117 ± 5	78.9 ± 16[1] 135 ± 9[7] 120 ± 15[8] 116 ± 8[33] 114 ± 7[34] 111 ± 9[35]
$Al^{27}(n,p)Mg^{27}$	73.5	52.4 ± 10[1] 79 ± 5[7] 79 ± 15[36] 87 ± 7[8] 115 ± 10[35] 53 ± 5[34]
$Mg^{24}(n,p)Na^{24}$	178 ± 12	191 ± 37[1] 190 ± 25[33]

c) IRRADIATION OF IODINE

Either ammonium or sodium iodide was irradiated in homogeneous mixtures with iron granules. The reactions observed in the iodine were:-

$I^{127}(n, \gamma)I^{128}$ ($t_{\frac{1}{2}}$ = 25.0 mins. ± 0.1)

$I^{127}(n,2n)I^{126}$ ($t_{\frac{1}{2}}$ = 13.0 days)

$I^{127}(n,p)Te^{127}$ ($t_{\frac{1}{2}}$ = 9.2 hrs. ± 0.1)

The product nuclides were chemically separated. I^{128} and I^{126} decay rates were measured in the liquid counter and tellurium solid sources were prepared and counted under the end window counter.

The I^{128} and Te^{127} activities were, in every case, traced for several half-lives. The value obtained for the Te^{127} was slightly lower than the accepted value of 9.4 hrs. The decay of the longer lived I^{126} activity was traced on one occasion for three half-lives, and was consistent with a half-life of 13 days.

No evidence of either a 1.3 min. or a 21 min. antimony activity, corresponding to the reported meta-stable states of Sb^{124}, was obtained, using the counting techniques described. The apparent absence of the 60 day ground state of Sb^{124} is explained by its long

half life. For the same reason, no sign of the 115 day metastable state of Te^{127} was observed.

EXPERIMENTAL DETAILS.

Preparation and standardisation of carrier solutions.

A suitable Te(IV) carrier solution was prepared by dissolving sodium tellurite, Na_2TeO_3, in water and a Te(VI) carrier solution by dissolving telluric acid, $H_2TeO_4.2H_2O$. Both solutions were standardised by the recommended gravimetric procedure, weighing as elemental tellurium. Both solutions contained about 10 mgs./ml. of tellurium.

An Sb(V) carrier solution containing about 10 mgs./ml. of antimony was prepared by oxidising a solution of $SbCl_3$ in 2N HCl with chlorine. This solution was not standardised.

Separation of iodine and tellurium activities.

After separation from the iron granules, the irradiated iodide was dissolved in 1N NaOH. 2mls. of the Te(IV) carrier solution were added and a redox cycle was performed to secure exchange between active and inactive species.

Step 1. The solution, containing about 1 gm. of iodide was diluted to 40 mls. and warmed with the

addition of a 5% NaOCl solution until insoluble $NaIO_4$ began to crystallise.

Step 2. The solution was acidified by the addition of conc. HCl and excess chlorine was extracted into carbon tetrachloride.

Step 3. The solution was placed in a 500 ml. separating funnel and a 10% solution of $NH_2OH.HCl$ was added, reducing IO_4^- to I_2. This was extracted into carbon tetrachloride, leaving the tellurium fraction in the aqueous phase.

Iodine fraction:-

Step 4. The I_2 was back-extracted into a sodium sulphite solution. An aliquot part of this active solution was counted in the standardised liquid counter.

Tellurium fraction:-

Step 5. The aqueous phase of the extraction, containing the tellurium fraction, was evaporated in an open dish until sodium chloride began to crystallise. This was redissolved and the solution was made 3N with respect to HCl.

Step 6. Sulphur dioxide was passed into the solution, precipitating elemental tellurium. The Te

ppt. was coagulated by boiling for one minute and centrifuged.

Step 7. The Te ppt. was purified by dissolving it in 5N HNO_3 and, after removal of nitrate by repeated evaporation with HCl, it was re-precipitated from 3N HCl by reduction with SO_2.

Step 8. The Te ppt. was mounted on a glass fibre filter disc, dried at 110°C., weighed and counted under the end window counter.

In general, the I^{128} activity was counted after twenty minutes and the Te^{127} within one hour of the end of the irradiation.

Estimation of iodide.

The number of iodine nuclei irradiated was estimated volumetrically by the standard method described by Vogel.[37] This method employs the reaction:-

$$KIO_3 + 6HCl + 2KI = 3KCl + 3ICl + 3H_2O$$

The end point is indicated by the disappearance of the purple iodine colour in a layer of carbon tetrachloride in the titration vessel and, with practice, it can be precisely determined.

In cases where the residual iodine activity only

had been measured, it was sufficient to estimate the iodine content of the solution counted in the liquid counter, but, where the Te^{127} activity had been measured, an aliquot of the active iodide solution, before addition of the tellurium carrier, had also to be removed and estimated.

Confirmation of complete exchange between active and carrier tellurium.

Preliminary measurements of the $I^{127}(n,p)Te^{127}$ cross section, although in close agreement with each other, were nearly two orders of magnitude smaller than the then only reported value. There was, then, some doubt as to whether complete exchange between carrier and active tellurium had been effected.

To verify this, mixtures of potassium iodate with iron were irradiated and the tellurium carrier was added to the active iodate solution in the Te(VI) state. Tellurium solid sources were prepared by the following procedure.

Step 1. The solution was made 3N in HCl and SO_2 was passed through it, reducing IO_3^- to I^-.

Step 2. On warming, the iodide in acid solution reduced Te(VI) to Te(IV).

Step 3. In the presence of SO_2, the Te(IV) was

further reduced to elemental tellurium.

Step 4. The Te ppt. was coagulated by boiling and centrifuged. It was purified, as described in Step 7, above, and mounted for counting.

The values obtained for the $I^{127}(n,p)Te^{127}$ cross section by this procedure were in close accord with those obtained from the iodide irradiations. Then any possibility of incomplete exchange between the active and carrier species of tellurium was most unlikely.

A second experiment, confirming this conclusion, was performed.

Some irradiated iodide was dissolved in 1N NaOH and 2 mls. of Te(IV) carrier were added. The solution was then divided into two equal parts. From the first part a Te solid source was prepared, employing the procedure already described. The chemical yield of the procedure was determined. The second part of the active solution was counted directly in the standardised liquid counter.

The Te^{127} β-particles are very inefficiently counted in the liquid counter and it was difficult to determine its absolute decay rate in the presence of a high background of 13 day I^{126}. This was done, however, and it was closely comparable with that obtained from the Te solid source.

This experiment furnished conclusive proof that the exchange between Te^{127} and carrier tellurium was complete in the chemical procedures described.

Procedure for isolating antimony activities.

Attempts to isolate a 21 min. activity, attributable to Sb^{124m_2}, were unsuccessful. An antimony solid source was prepared from irradiated iodide as follows.

Step 1. Irradiated ammonium iodide was dissolved in 2N HCl and 2 mls. of Sb(V) carrier solution (ca. 10 mg./ml.) were added. The Sb(V) was reduced to Sb(III) by the iodide, iodine being liberated.

Step 2. The bulk of the iodide was oxidised to free iodine by the addition of a saturated solution of sodium nitrite. The iodine was extracted into carbon tetrachloride and discarded.

Step 3. The aqueous phase was made 3N with respect to HCl and a little Te(IV) carrier was added.

Step 4. Elemental tellurium was precipitated by reduction with sulphur dioxide and the precipitate was discarded.

Step 5. After removal of excess SO_2 by boiling, H_2S was passed into the solution, precipitating Sb_2S_3.

Step 6. The antimony fraction could be further purified by preparing and mounting antimony pyrogallate, but this proved unnecessary. The Sb_2S_3 ppt. was dissolved in conc. HCl and reprecipitated from 3N HCl by passing more H_2S.

Step 7. This procedure took about twenty-five minutes. The Sb_2S_3 ppt. was mounted and counted under the end window counter, but it proved to be totally inactive.

In another experiment, samples of ammonium iodide were irradiated for two minutes and the resultant activities were counted without chemical separation, both in the liquid counter and under the end window counter. There was no sign of any activity that could be assigned to 1.3 min. Sb^{124m}.

The contribution of thermal and epithermal neutrons to the $I^{127}(n, \gamma)I^{128}$ cross section.

It was realised, before measuring any (n, γ) cross-sections for 14 MeV neutrons, that the contribution to these from lower energy neutrons might be considerable.

Then, when values for the $I^{127}(n, \gamma)I^{128}$ cross section had been obtained from several irradiations, it was noticed that the variance of these values was much greater than the variance of the values obtained

for the $I^{127}(n,2n)I^{126}$ cross section, measured at the same time. As there was no possibility of there being any random error introduced into the relative values of these two cross sections, the larger variance of the (n, γ) cross section values could only be due to variations in the flux of lower energy neutrons, i.e. neutrons with energies lower than the threshold energy of the (n,2n) reaction (9.4 MeV).

These thermal and epithermal neutrons arise from the scattering of 14 MeV neutrons from the floor and walls of the target chamber and from the $H^2(d,n)He^3$ reaction. The latter reaction is a source of 2.5 MeV neutrons and becomes more favoured, the older the target, as deuterium from the deuteron beam builds up in the tritiated titanium layer (See Fig. 6).

Both these sources of lower energy neutrons were studied and their contributions to the measured values of the $I^{127}(n, \gamma)I^{128}$ cross section were estimated. Suitable corrections were made to the cross sections.

The contribution of the scattered, degraded neutrons to the (n, γ) cross section was estimated by irradiating two mixtures of ammonium iodide and iron, one close up to the target and one at a distance of 8 cms. from it. The flux of scattered neutrons could be taken as being

the same in both positions, but the 14 MeV neutron flux decreased, according to the inverse square law. After the irradiation, the amounts of I^{128} and Mn^{56} induced in both mixtures were measured. The ratio of the specific activities of Mn^{56} induced in the near and removed mixtures was found to be four times greater than the corresponding ratio of I^{128}. As the decrease in the specific activity of the Mn^{56} with distance was indicative of the decrease in the 14 MeV neutron flux, three-quarters of the I^{128} activity in the lower mixture must have been induced by thermal and epithermal neutrons with energies less than the threshold energy of the $Fe^{56}(n,p)Mn^{56}$ reaction. But, assuming that the flux of degraded neutrons was the same in both positions, its contribution to the $I^{127}(n, \gamma)I^{128}$ reaction in the mixture close up to the target was only three per cent of that of the much higher flux of 14 MeV neutrons.

The contribution of neutrons from the $H^2(d,n)He^3$ reaction to the $I^{127}(n, \gamma)I^{128}$ cross section was more important. The proportion of the total neutron flux, of these 2.5 MeV neutrons, increases with the age of the tritium target. Deuterium from the deuteron beam is absorbed into the titanium or zirconium film and accumulates during an irradiation. At the same time,

the flux of 14 MeV neutrons is falling as the tritium is exhausted.

To measure the contribution of D+D neutrons, typical samples of ammonium iodide were irradiated with neutrons produced by the bombardment of "blank", or tritium-free, target backings. Plotting the specific activity of I^{128}, induced in these iodide samples, against the microampere-hours of bombardment (Fig. 6) the flux of D+D neutrons is seen to rise to a saturation level after 500 μamp. hrs.

RESULTS AND DISCUSSION.

Values obtained for the $I^{127}(n, \gamma)I^{128}$, $I^{127}(n,2n)I^{126}$ and $I^{127}(n,p)Te^{127}$ cross sections are presented in Tables 11, 12 and 13 respectively.

The mean value obtained for the (n, γ) cross section, 6.5 mbs. $\pm$ 0.8, is somewhat larger than the only other reported value, 2.5 mbs. $\pm$ 0.5,[38] but, in general, (n, γ) cross-section values do not compare so well. This is probably due to the added uncertainty in monitoring the neutron flux, although both these values have been corrected for the effect of lower energy neutrons.

The present value for the (n,2n) cross section

(1600 mbs. ± 100) is in agreement with Paul and Clarke's value of 1120 mbs. ± 400.[1]

Paul and Clarke[1] reported a value of 231 mbs. ± 140 and Coleman et al[39] a value of 11.7 mbs. ± 1.7 for the (n,p) cross section. No light is thrown on the wide disparity of these results by the present work, in which a value of 3.17 mbs. ± 027 has been obtained. Paul and Clarke's value is almost two orders of magnitude larger than this and it is felt that it is simply wrong. In reporting a value of 11.7 mbs., Coleman et al have not indicated whether this includes the cross section for the formation of 115 day Te^{127m}. If it does, this would explain the difference between it and the present value, which is a lower limit, since only the Te^{127} ground state was observed.

Paul and Clarke[1] reported the reaction, $I^{127}(n, \alpha)Sb^{124m_2}$, occurring with a cross section of 18.4 mbs. Sb^{124m_2} has a half-life of 21 mins and decays by the emission of a highly converted γ-ray and, perhaps, a β. But they did not make any chemical separations and have probably mistaken the 25 min. I^{128} activity, which they did not report, for 21 min. Sb^{124m_2}.

As described, no sign of either 21 min. Sb^{124m_2} or

1.3 min. Sb^{124m_1} was detected from an $I^{127}(n, \alpha)$ reaction. Besides contradicting Paul and Clarke's results, this deficiency throws some doubt on to the existence of these metastable states of Sb^{124} or, at least, their reported β-particles.

TABLE 11. RESULTS FOR THE $I^{127}(n,\gamma)I^{128}$ REACTION.

IRRADIATION NO.	SAMPLE REACTION: No. of target nuclei x N^{-1}	Low energy neutron factor (%)	A_o observed c.p.m.	A_o correct d.p.m.	REFERENCE REACTION: S	No. of target nuclei x N^{-1}	A_o observed c.p.m.	A_o correct d.p.m.	S	MEASURED CROSS SECTION (mbs.)	MEAN
10	3.96×10^{-3}	20	2.29×10^{3}	1.99×10^{4}	1.71	6.87×10^{-3}	1.56×10^{4}	1.75×10^{5}	3.04	7.0	
11	4.33×10^{-3}	20	3.00×10^{3}	2.61×10^{4}	0.86	7.65×10^{-3}	2.23×10^{4}	2.50×10^{5}	1.60	6.9	
12	4.96×10^{-3}	20	2.10×10^{3}	1.82×10^{4}	0.96	7.98×10^{-3}	1.47×10^{4}	1.65×10^{5}	1.55	5.7	6.5mbs. ±
13	8.60×10^{-3}	20	1.90×10^{3}	1.65×10^{4}	0.56	5.84×10^{-3}	4.56×10^{3}	5.10×10^{4}	0.98	7.7	0.8
14	3.98×10^{-3}	4	2.38×10^{3}	2.48×10^{4}	1.42	6.90×10^{-3}	2.08×10^{4}	2.32×10^{5}	2.23	5.8	
15	1.112×10^{-2}	12	8.60×10^{3}	8.23×10^{4}	1.39	9.10×10^{-3}	2.45×10^{4}	2.77×10^{5}	1.75	6.1	

TABLE 12. RESULTS FOR THE $I^{127}(n,2n)I^{126}$ REACTION.

10	3.96×10^{-3}	-	1.40×10^{2}	1.19×10^{4}	3.44	"	"	"	"	1560	
11	4.33×10^{-3}	-	2.06×10^{2}	1.75×10^{4}	1.82					1630	
12	4.96×10^{-3}	-	1.44×10^{2}	1.22×10^{4}	1.71					1610	1600mbs. ±
13	8.60×10^{-3}	-	1.10×10^{2}	9.34×10^{3}	1.10					1660	60
14	3.98×10^{-3}	-	1.90×10^{2}	1.61×10^{4}	2.46					1640	
15	1.112×10^{-2}	-	4.17×10^{2}	3.54×10^{4}	1.83					1500	

N is the Avogadro Number. $t_{\frac{1}{2}}$ I^{128} = 25 mins.

$\sigma_{Fe^{56}(n,p)Mn^{56}}$ = 124 mbs. $t_{\frac{1}{2}}$ I^{126} = 13 days.

C_{I128} = 0.092 and C_{I126} = 0.0118.

TABLE 13 RESULTS FOR THE $I^{127}(n,p)Te^{127}$ REACTION.

IRRADIATION NO.	SAMPLE REACTION: No. of target nuclei x N^{-1}	Chemical yield (%)	Self-absorption factor	A_o observed c.p.m.	A_o correct d.p.m.	S	REFERENCE REACTION: No. of target nuclei x N^{-1}	A_o observed c.p.m.	A_o correct d.p.m.	S	MEASURED CROSS SECTION (mbs.)	MEAN
10	1.14×10^{-2}	57.1	0.31	4.48×10^{2}	2.53×10^{3}	3.58						
11	1.46×10^{-2}	89.5	0.30	1.18×10^{3}	4.40×10^{3}	1.89					3.42	
16	1.25×10^{-2}	46.3	0.31	4.70×10^{2}	3.28×10^{3}	2.18	4.65×10^{-3}	1.45×10^{4}	1.63×10^{5}	2.00	3.48 3.07	3.17mb. ± 0.27
17	1.44×10^{-2}	19.1	0.31	2.50×10^{2}	4.22×10^{3}	2.18	5.04×10^{-3}	1.80×10^{4}	2.02×10^{5}	2.00	3.00	
18	5.17×10^{-3}	95.0	0.30	3.10×10^{2}	1.09×10^{3}	0.74	2.63×10^{-3}	7.20×10^{3}	8.06×10^{4}	0.72	2.86	

N is the Avogadro Number. $t_{\frac{1}{2}}$ Te^{127} = 9.2 hours.

$\sigma_{Fe^{56}(n,p)Mn^{56}}$ = 124 mbs. $t_{\frac{1}{2}}$ Mn^{56} = 2.58 hours.

$C_{Mn^{56}}$ = 0.0893.

d) IRRADIATION OF BISMUTH

Homogeneous mixtures of iron and basic bismuth carbonate (later metallic bismuth) were irradiated.

The reactions observed in the bismuth were:-

$Bi^{209}(n, \gamma)\ Bi^{210}$ ($t_{\frac{1}{2}}$ = 5 days)

$Bi^{209}(n,p)\ Pb^{209}$ ($t_{\frac{1}{2}}$ = 3.17 hrs. $\pm$ 0.04)

$Bi^{209}(n, \alpha)\ Tl^{206}$ ($t_{\frac{1}{2}}$ = 3.18 mins. $\pm$ 0.02)

The resultant β-activities of the Bi^{210}, Pb^{209} and Tl^{206} were easily resolved graphically, but, in order to assay the absolute β-decay rates accurately, it was preferred to separate the product nuclides and count them by the standardised techniques.

The decay of the Bi^{210} was traced in the liquid counter, independently calibrated for that nuclide which has the β-spectrum shape of a "forbidden" transition.

The lead and thallium fractions were chemically separated, mounted on glass fibre filter discs and counted under the end window counter.

All three activities were traced for several half-lives. The measured half-lives of the Pb^{209} and Tl^{206}, with standard deviations, are reported above.

The yield of Bi^{210} was not great enough to claim more than that its decay was consistent with a 5 day half-life.

EXPERIMENT DETAILS.

Preparation and standardisation of carrier solutions.

Suitable carrier solutions, containing about 15 mg./ml. of the respective elements, were prepared by dissolving thallous and lead carbonates in 2N HNO_3. Both solutions were standardised gravimetrically, weighing the thallium as chromate and the lead as sulphate.

Isolation of Tl^{206}.

After short irradiations (5-10 mins.), the iron was removed from the mixture and the bismuth carbonate (ca. 1 gm.) was dissolved with warming in the minimum amount of conc. HNO_3 (ca. 1 ml.). 1 ml. of the Tl(I) carrier solution was added and the solution was further treated.

Step 1. The solution was diluted until it was 2N in HNO_3.

Step 2. TlCl was precipitated by the addition of a few drops of conc. HCl and scratching the tube with a glass rod.

Step 3. The crystalline TlCl ppt. was washed with 2N HNO_3 and then water and collected on a glass fibre filter disc. This source was then washed with alcohol and ether and dried in a vacuum dessicator. (The source was weighed after counting).

This process could be completed in seven minutes from the end of the irradiation to the start of the first count.

The Pb^{209}, formed during the short period of the irradiation, which co-precipitated with the thallous chloride, was resolved graphically from the Tl^{206}.

Isolation of Pb^{209}.

Longer irradiations, not less than an hour, were necessary for the formation of appreciable quantities of Pb^{209}.

The bismuth carbonate was dissolved, as before, and 1 ml. of lead carrier solution was added.

Step 1. The solution was diluted until it was 2N with respect to HNO_3.

Step 2. $PbSO_4$ was precipitated by the addition of a few drops of 2N H_2SO_4.

Step 3. The $PbSO_4$ ppt. was washed with 2N HNO_3 then water. It was collected on a glass fibre

filter disc and dried by washing with alcohol and ether and placing in a vacuum dessicator.

Step 4. The chemical yield of the precedure was determined by weighing the lead as $PbSO_4$. The accuracy of this method was confirmed in some cases by dissolving the $PbSO_4$ source in a 0.1 M solution of the Mg-EDTA complex, as described by Schwarzenbach.[32] The yield of Mg^{++} ions liberated was then determined by titrating against EDTA at pH = 10. with Erio T as indicator.

Measurement of Bi^{210} activity.

The activity of Bi^{210} from the $Bi^{209}(n, \gamma)Bi^{210}$ reaction was low, amounting to only a few c.p.m. above background. This was due to the combination of a low cross section, a low counting efficiency and a long half-life.

In order to get the maximum possible yield, metallic bismuth was irradiated instead of bismuth carbonate, which is much bulkier.

After irradiation and the complete removal of the iron monitor, the bismuth (ca. 2.5 gm.) was weighed and dissolved in 6 mls. of conc. HNO_3. The solution was diluted to 12 mls. and a 10 ml. aliquot part was counted in the standardised liquid counter.

The β^--decay rate of the Bi^{210}, after the disappearance of all the 3.2 hr. Pb^{209}, was traced by camera for fifteen days. A continuous record of the background throughout this period was obtained by alternating the active solution with an identical solution of inactive bismuth.

The decay rate of the active bismuth solution was consistent with a half-life of 5 days.

Determination of the bismuth content of the carbonate.

The bismuth content of the basic bismuth carbonate was determined volumetrically, titrating against a standard EDTA solution using potassium iodide as indicator. The conditions for the titration were investigated by Cheng.[40]

The bismuth carbonate was dissolved in nitrite-free nitric acid. An aliquot part of this solution was diluted, so as to contain not more than 1 mg./ml. of Bi^{+++}, and its pH was adjusted to between 1.5 and 2.0 with dilute ammonia. The solution was directly titrated with a standard 0.01 M solution of EDTA after addition of 1 ml. 0.5% KI solution as indicator. Another 9 mls. of the KI indicator were added just before the end point, which was from yellow to colourless.

The end point for this titration was very clear, and good, reproducible titres were obtained. But care had to be taken not to add excess KI until just before the end point, as the bismuth iodide complex was not easily soluble in EDTA.

RESULTS AND DISCUSSION.

Values obtained for the $Bi^{209}(n,\alpha)Tl^{206}$, $Bi^{209}(n,p)Pb^{209}$ and $Bi^{209}(n,\gamma)Bi^{210}$ cross sections are presented in Tables 14, 15 and 16 respectively.

The value obtained in the present work for the (n,α) cross section, 0.46 mb. $\pm$ 0.06, is within the estimated error of Paul and Clarke's value of 1.2 mbs. $\pm$ 1.0[1] and confirms the recent value reported by Coleman et al[39] of 0.52 mb. $\pm$ 0.08 . The value reported by Fink and Poularikas,[34] 1.1 mbs. $\pm$ 0.3, seems too high, but they did not pay much attention to the calibration of their counters.

The present value for the (n,p) cross section, 0.97 mb. $\pm$ 0.08, is in close accord with the recently reported values of 1.33 mbs. $\pm$ 0.26[39] and 0.83 mb. $\pm$ 0.4.[34]

The present value, 0.67 mb. $\pm$ 0.04, for the (n,γ) cross section is less than half the value reported by

Perkin et al[38] (1.45 mbs. ± 0.17). Neither values have been corrected for the effect of lower energy neutrons, in the present work, because it was not possible to estimate this effect. In the absence of this correction, a lower value for the (n, γ) cross section might simply indicate a smaller contribution from thermal and epithermal neutrons. Then the lower value is more likely to be accurate.

IRRADIATION NO.	SAMPLE REACTION				A_o correct d.p.m.	S	REFERENCE REACTION				MEASURED CROSS SECTION (mbs.)	MEAN
	No. of target nuclei x N^{-1}	Chemical yield %	Self-absorption factor	A_o observed c.p.m.			No. of target nuclei x N-1	A_o observed c.p.m.	A_o correct d.p.m.	S		
TABLE 14	RESULTS FOR THE $Bi^{209}(n, \alpha)Tl^{206}$ REACTION.											
19	3.62×10^{-3}	52.0	0.30	2.10×10^{3}	1.34×10^{4}	0.74	8.09×10^{-3}	5.12×10^{4}	5.74×10^{5}	1.74	0.42	0.46 mbs. ± 0.06.
20	7.30×10^{-3}	60.4	0.30	3.28×10^{3}	1.82×10^{4}	3.57	7.75×10^{-3}	2.49×10^{4}	2.79×10^{5}	7.48	0.48	
21	9.55×10^{-3}	49.2	0.30	3.48×10^{3}	2.36×10^{4}	2.00	7.67×10^{-3}	2.20×10^{4}	2.46×10^{5}	4.33	0.56	
22	7.18×10^{-3}	95.5	0.26	3.54×10^{3}	1.42×10^{4}	1.76	6.64×10^{-3}	3.01×10^{4}	3.37×10^{5}	5.38	0.40	
23	8.46×10^{-3}	47.7	0.30	3.20×10^{3}	2.24×10^{4}	2.62	6.78×10^{-3}	2.85×10^{4}	3.20×10^{5}	5.65	0.41	
24	8.52×10^{-3}	58.4	0.30	3.38×10^{3}	1.92×10^{4}	0.69	7.35×10^{-3}	1.82×10^{4}	2.04×10^{5}	1.25	0.49	
$t_{\frac{1}{2}}$ Tl^{206} = 4.18 mins.												
TABLE 15	RESULTS FOR THE $Bi^{209}(n,p)Pb^{209}$ REACTION.											
25	2.78×10^{-3}	79.5	0.24	3.40×10^{2}	1.78×10^{3}	2.44	6.73×10^{-3}	5.13×10^{4}	5.74×10^{5}	2.31	1.10	0.97 mbs. ± 0.08.
26	8.13×10^{-3}	87.4	0.225	3.56×10^{2}	1.81×10^{3}	1.26	8.76×10^{-3}	2.62×10^{4}	2.93×10^{5}	1.17	0.95	
27	1.02×10^{-2}	71.0	0.24	5.60×10^{2}	3.28×10^{3}	2.20	7.77×10^{-3}	3.60×10^{4}	4.03×10^{5}	2.07	0.90	
28	9.72×10^{-3}	61.4	0.245	6.35×10^{2}	4.22×10^{3}	2.20	7.27×10^{-3}	4.53×10^{4}	5.07×10^{5}	2.07	0.90	
29	5.51×10^{-3}	85.0	0.23	7.69×10^{2}	4.46×10^{3}	2.62	7.59×10^{-3}	6.89×10^{4}	7.71×10^{5}	2.45	1.01	
$t_{\frac{1}{2}}$ Pb^{209} = 3.17 hours.												

N is the Avogadro Number

$t_{\frac{1}{2}}$ Mn^{56} = 2.58 hours

$\sigma_{Fe^{56}(n,p)Mn^{56}}$ = 124 mbs.

$C_{Mn^{56}}$ = 0.0893

TABLE 16. RESULTS FOR THE $Bi^{209}(n, \gamma)Bi^{210}$ REACTION.

IRRADIATION NO.	SAMPLE REACTION				REFERENCE REACTION				MEASURED CROSS SECTION (mbs.)	MEAN
	No. of target nuclei x N-1	A_o observed c.p.m.	A_o correct d.p.m.	S	No. of target nuclei x N^{-1}	A_o observed c.p.m.	A_o correct d.p.m.	S		
30	1.082×10^{-2}	15.6	8.00×10^{2}	15.40	4.84×10^{-3}	1.45×10^{5}	1.62×10^{6}	8.66	0.71	
31	1.040×10^{-2}	8.4	4.30×10^{2}	15.40	8.75×10^{-3}	1.66×10^{5}	1.86×10^{6}	8.66	0.63	0.67mbs.
32	1.220×10^{-2}	10.8	5.54×10^{2}	8.24	9.20×10^{-3}	1.65×10^{5}	1.85×10^{6}	4.26	0.67	$\pm$ 0.04.

N is the Avogadro Number.

$\sigma_{Fe^{56}(n,p)Mn^{56}}$ = 124 mbs.

$t_{\frac{1}{2}}$ Bi^{210} = 5 days.

$t_{\frac{1}{2}}$ Mn^{56} = 2.58 hours.

$C_{Bi^{210}}$ = 0.0195

$C_{Mn^{56}}$ = 0.0893

e) IRRADIATION OF MANGANESE

Homogeneous mixtures of manganese carbonate and aluminium granules were irradiated.

The reaction observed in the manganese was:-

$Mn^{55}(n, \gamma)Mn^{56}$ ($t_{\frac{1}{2}}$ = 2.58 hrs.)

The Mn^{56} activity was traced to background.

The irradiation was monitored by the $Al^{27}(n, \alpha)Na^{24}$ reaction, because of the possibility of Mn^{56} nuclei, recoiling from the $Fe^{56}(n,p)Mn^{56}$, lodging in the manganese carbonate. The cross section of the latter reaction is considerably larger than the $Mn^{55}(n, \gamma)Mn^{56}$ cross section and the contribution of recoiled Mn^{56} nuclei to the total Mn^{56} activity would not be negligible.

A 3.5 min. activity was observed. This would be a combination of 3.76 min. V^{52} and 3.52 min. Cr^{55}, but no method of chemically separating these activities in the time available presented itself.

EXPERIMENTAL DETAILS.

Treatment of the mixture.

The aluminium granules were separated from the mixture by a simple sieving process. The aluminium was treated as in Section (b).

The manganese carbonate (ca. 1 gm.) was dissolved in 10 mls. of 5N HCl with the passage of sulphur dioxide to dissolve residual traces of manganese dioxide. The solution, was diluted to 12 mls. and 10 mls. were counted in the liquid counter.

Determination of the manganese content of the carbonate.

The manganese content of the manganese carbonate was determined gravimetrically by a procedure recommended by Vogel.[37] The manganese was weighed as $MnNH_4PO_4$, H_2O.

The contribution of lower energy neutrons to the $Mn^{55}(n,\gamma)Mn^{56}$ cross section.

A sample of manganese carbonate was irradiated for two hours close up to a "blank" target, i.e. a tritium-free target. The bias on the proton-recoil neutron monitor was reduced and neutrons produced by the $H^2(d,n)He^3$ reaction were recorded.

After the irradiation, the manganese carbonate was dissolved and counted in the liquid counter. The solution was inactive. It was concluded that the flux of D+D neutrons during an irradiation was, in this case, too small to interfere with the measurement of the (n,γ) cross section for 14 MeV neutrons.

RESULTS AND DISCUSSION.

The results are presented in Table 17.

The value obtained in the present work for the $Mn^{55}(n, \gamma)Mn^{56}$ cross section, 1.29 mbs. $\pm$ 0.23, is in rough agreement with the only other reported value of 0.76 mb. $\pm$ 0.08,[38] allowing for the uncertainty in (n, γ) cross section measurements at this energy.

IRRADN. NO.	SAMPLE REACTION: No. of target nuclei x N^{-1}	A_o observed c.p.m.	A_o correct d.p.m.	S	REFERENCE REACTION: No. of target nuclei x N-1	A_o observed c.p.m.	A_o correct d.p.m.	S	MEASURED CROSS SECTION (mbs.)	MEAN
TABLE 17. RESULTS FOR THE $Mn^{55}(n, \gamma)Mn^{56}$ REACTION.										
33	5.40×10^{-3}	2.36×10^{2}	2.65×10^{3}	1.54	7.86×10^{-3}	5.17×10^{3}	7.41×10^{4}	1.73	1.25	
34	5.28×10^{-3}	1.68×10^{2}	1.88×10^{3}	1.61	8.03×10^{-3}	2.80×10^{3}	4.02×10^{4}	1.76	1.66	
35	6.05×10^{-3}	1.99×10^{2}	2.23×10^{3}	0.80	1.31×10^{-2}	8.56×10^{3}	1.23×10^{5}	0.96	1.01	1.29 mbs. $\pm$ 0.23.
36	1.10×10^{-2}	1.53×10^{3}	1.71×10^{4}	5.42	1.68×10^{-2}	4.71×10^{4}	6.75×10^{5}	8.33	1.27	
37	1.00×10^{-2}	1.31×10^{3}	1.47×10^{4}	5.42	1.28×10^{-2}	3.48×10^{4}	5.00×10^{5}	8.33	1.24	

N is the Avogadro Number. $c_{Mn^{56}} = 0.0893$.

$\sigma_{Al^{27}(n,\alpha)Na^{24}} = 117$ mbs. $c_{Na^{24}} = 0.0697$.

$t_{\frac{1}{2}}$ Mn^{56} = 2.58 hours. $t_{\frac{1}{2}}$ Na^{24} = 15.0 hours.

f) IRRADIATION OF BARIUM

Homogeneous mixtures of iron and barium carbonate were irradiated. The cross sections of the following reactions were measured:-

$Ba^{138}(n, \gamma)Ba^{139}$ ($t_{\frac{1}{2}}$ = 84.0 mins. ± 2)

$Ba^{138}(n,p)Cs^{138}$ ($t_{\frac{1}{2}}$ = 33.1 mins. ± 0.6)

The Ba^{139} and Cs^{138} activities were, in every case, traced for several half-lives after separation. The measured half-lives are reported above. Counting statistics were not good enough to make accurate measurements.

EXPERIMENTAL DETAILS.

Separation of cesium and barium fractions.

After removal of the iron, the barium carbonate (ca. 1 gm.) was dissolved in the minimum amount of 3N HCl, containing a little cesium carrier. This solution was neutralised by the addition of a saturated solution of Na_2CO_3, reprecipitating the barium as $BaCO_3$. The $BaCO_3$ was filtered and washed with water. The filtrate and washings containing the Cs^{138} activity were retained. The $BaCO_3$ was redissolved and the process was repeated. The two filtrates were combined and made up to 25 mls.

A 10 ml. aliquot part of this solution was counted in the standardised liquid counter.

The $BaCO_3$ ppt. was redissolved and an aliquot part of this solution was counted in another standardised liquid counter.

The whole procedure took about 25 mins.

The separation of the cesium fraction was quantitative. The concentration of the barium solution was confirmed gravimetrically, weighing the barium as $BaSO_4$.

The contribution of lower energy neutrons to the $Ba^{138}(n, \gamma)Ba^{139}$ cross section.

No activity was induced in a barium carbonate sample irradiated close up to a "blank" target. Then the contribution to the measured cross section of D+D neutrons, from deuterium which accumulates on the target, could be neglected.

The flux of scattered, degraded neutrons in the target area was also neglected on the basis of the experiments performed on the $I^{127}(n, \gamma)I^{128}$ reaction (see Section (c)).

RESULTS AND DISCUSSION.

All results are presented in Tables 18 and 19.

Values of 1.70 mbs. ± 0.15 and 1.56 mbs. ± 0.26 have been obtained for the $Ba^{138}(n, \gamma)Ba^{139}$ and $Ba^{138}(n,p)Cs^{138}$ cross sections. Perkin et al[38] have reported a value of 1.30 mbs. ± 0.40 for the (n, γ) cross section. This is in good agreement with the present value, particularly in view of the added uncertainty in measuring (n, γ) cross sections.

The value, reported by Coleman et al,[39] for the (n,p) cross section (2.20 mbs. ± 0.33) is slightly higher than the present value. It is possible that in the present work the counting efficiency of the liquid counter for Cs^{138} has been over estimated. Several different values of the Cs^{138} β end point energy have been reported and the highest of these was used for interpolating the liquid counter efficiency from the calibration curve (Fig. 15), as it appeared the most reliable. The variation of the liquid counter efficiency with β end point energy is quite sharp and any error in the latter is reflected in the interpolated value of the efficiency. Paul and Clarke[1] report a value of 6.3 mbs. ± 2 and more recently G. Wille[41] gives 2.5 ± 1.0 mb.

The (n,p) cross section is unexpectedly small for this region of the Periodic Table. This can probably be

attributed to some effect of the closed neutron shell, N = 82. Weight was lent to this theory by the publication of the cross-section measurements of Coleman et al.[39] They also reported a value for the Ba^{136} (n,p)Cs^{136} cross section of 38.3 mbs $\pm$ 3.8. Here the Neutron Number is two less than the closed shell. The only other (n,p) cross section in this region comparable to the low Ba^{138}(n,p)Cs^{138} cross section is the equally low La^{139}(n,p)Ba^{139} cross section (2.33 mbs. $\pm$ 0.35) where N is again equal to 82.

IRRADN. NO.	SAMPLE REACTION: No. of target nuclei x N^{-1}	A_o observed c.p.m.	A_o correct d.p.m.	S	No. of target nuclei x N-1	REFERENCE REACTION: A_o observed c.p.m.	A_o correct d.p.m.	S	MEASURED CROSS SECTION mbs.	MEAN

TABLE 18. RESULTS FOR THE $Ba^{138}(n, \gamma)Ba^{139}$ REACTION.

38	1.385×10^{-3}	1.43×10^{2}	1.51×10^{3}	1.35	6.15×10^{-3}	2.96×10^{4}	3.32×10^{5}	1.51	1.53	
39	1.385×10^{-3}	9.80×10^{2}	1.03×10^{3}	0.84	4.28×10^{-3}	1.27×10^{4}	1.42×10^{5}	0.92	1.66	1.70 mbs. ± 0.15.
40	1.345×10^{-3}	2.30×10^{2}	2.42×10^{3}	1.37	3.19×10^{-3}	2.08×10^{4}	2.33×10^{5}	1.54	1.88	
41	6.380×10^{-3}	8.20×10^{2}	8.65×10^{3}	2.93	1.07×10^{-2}	5.57×10^{4}	6.24×10^{5}	3.21	1.73	

$c_{Ba^{139}} = 0.095$ $\quad t_{\frac{1}{2}} Ba^{139} = 84$ mins.

TABLE 19. RESULTS FOR THE $Ba^{138}(n,p)Cs^{138}$ REACTION.

38	6.14×10^{-3}	1.80×10^{3}	1.08×10^{4}	0.96	"	"	"	"	1.34	
39	5.52×10^{-3}	9.90×10^{2}	5.95×10^{3}	0.63					1.25	
40	3.58×10^{-3}	1.90×10^{3}	1.14×10^{4}	0.94					1.88	1.56 mbs. ± 0.26.
41	6.38×10^{-3}	2.72×10^{3}	1.64×10^{4}	2.18					1.69	
42	8.60×10^{-3}	8.62×10^{2}	5.13×10^{3}	0.54	5.66×10^{-3}	6.26×10^{3}	7.01×10^{4}	0.68	1.61	

N is the Avogadro Number. $\quad t_{\frac{1}{2}} Cs^{138} = 33.1$ mins.

$\sigma_{Fe^{56}(n,p)Mn^{56}} = 124$ mbs. $\quad c_{Cs^{138}} = 0.168.$

$t_{\frac{1}{2}} Mn^{56} = 2.58$ hours.

$c_{Mn^{56}} = 0.0893.$

g) IRRADIATION OF GOLD

Homogeneous mixtures of finely divided gold and iron granules were irradiated for periods of from one to two hours.

The reactions observed in the gold were:-

$Au^{197}(n,2n)Au^{196m}$ ($t_{\frac{1}{2}}$ = 9.5 hrs. ± 0.1)

$Au^{197}(n,2n)Au^{196}$ ($t_{\frac{1}{2}}$ = 5.6 days ± 0.1)

$Au^{197}(n,p)Pt^{197}$ ($t_{\frac{1}{2}}$ = 19.7 hrs. ± 0.4)

$Au^{197}(n,p)Pt^{197m}$ ($t_{\frac{1}{2}}$ = 88 mins. ± 2)

$Au^{197}(n,\alpha)Ir^{194}$ ($t_{\frac{1}{2}}$ = 19.4 hrs. ± 0.6)

The resulting species were chemically separated. Solid sources were prepared and counted under the end window counter.

The decay rates of all activities were traced for several half-lives. The measured half-lives are reported above with standard deviations. The greater accuracy in the measurement of the Au^{196} and Au^{196m} half-lives is accounted for by better counting statistics.

The value of 9.5 hrs. for the Au^{196m} half-life, previously reported as 13 hrs. and 14 hrs., has since been confirmed by the thorough investigation of Van Lieshout et al.,[42] who report a half-life of 10.0 hrs. ± 0.5. The decay curve of a Au^{196} source is reproduced

in Fig. 17.

Similarly, the value of 19.7 hrs. for the Pt^{197} half-life, which is somewhat higher than those previously reported, has been confirmed by a recent value of 20.00 hrs. $\pm$ 0.12.[43]

Previously reported values of the Pt^{197m} half-life are 78 mins, 88 mins. and 87 mins. On the basis of this work, the former is quite clearly wrong. The decay curve of a typical Pt^{197} source is reproduced in Fig. 18.

Any sign of the 2.69 day activity of Au^{198}, produced by the $Au^{197}(n, \gamma)Au^{198}$ reaction, was obscured by the high activity of the 5.6 day Au^{196}.

The 9.5 hr. Au activity has been assigned to a metastable state of Au^{196}. This is the most likely possibility, but it could not be confirmed either here or by Van Lieshout and his co-workers,[42] who suggest that a second metastable state of Au^{197} may be another possibility.

Attempts were made to confirm the assignment of the 9.5 hr. activity to a metastable state of Au^{196} by separating carrier-free Au^{196} nuclei by a recoil method.

EXPERIMENTAL DETAILS.

Preparation of carrier solutions.

A platinum carrier solution (ca. 10 mgs./ml.) was

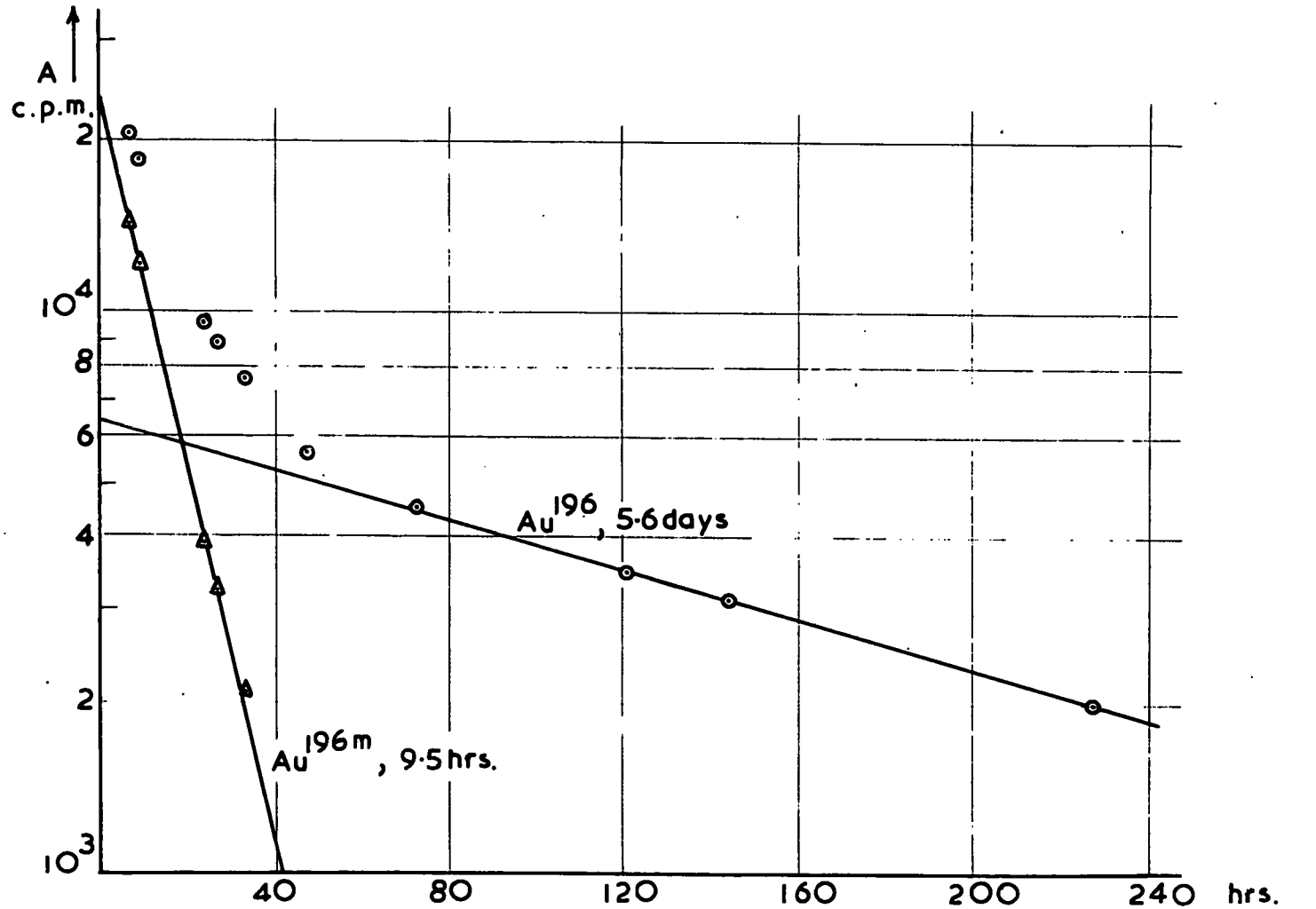

FIG. 17 Au ACTIVITIES INDUCED IN GOLD.

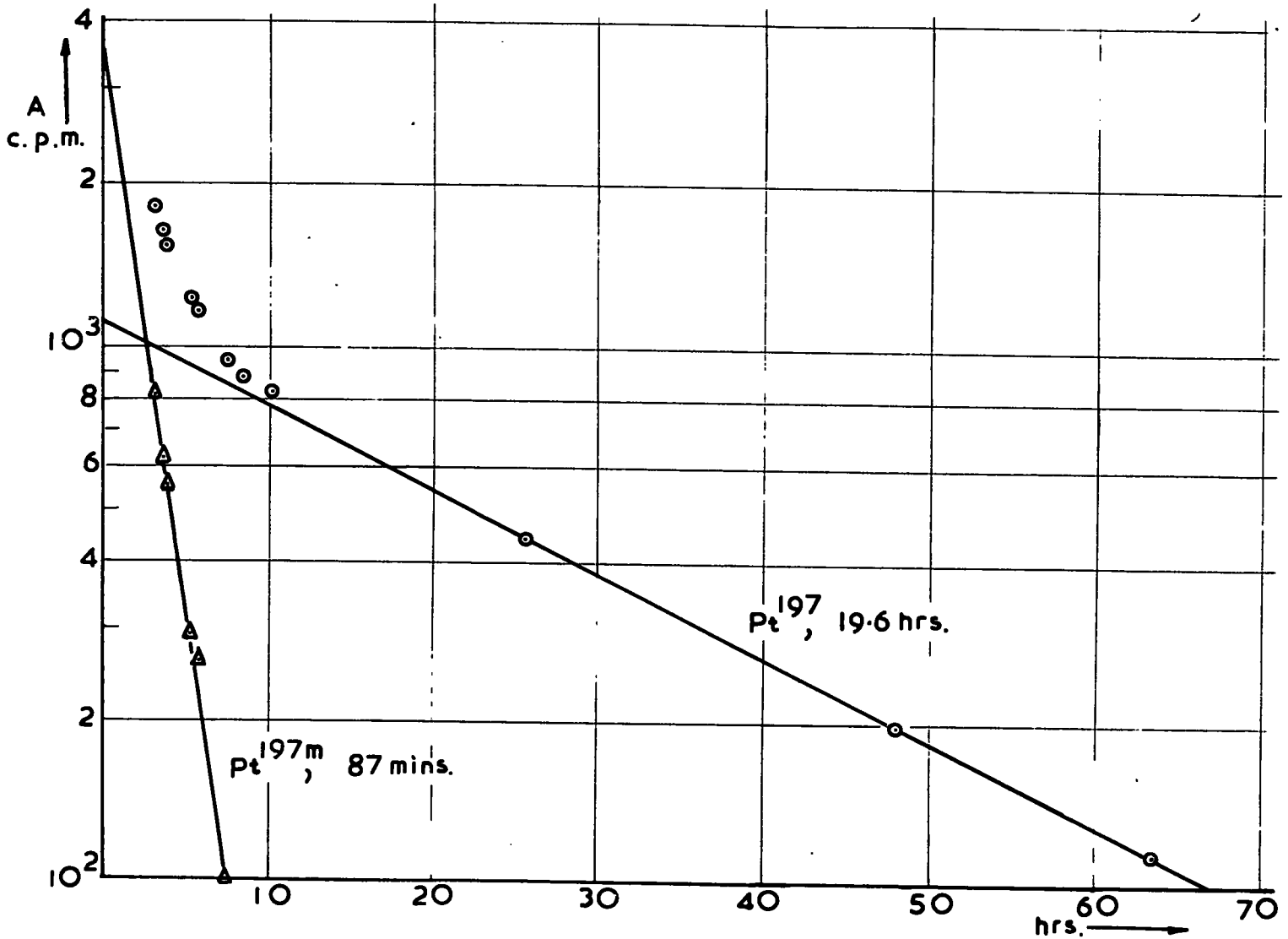

FIG. 18 . Pt ACTIVITY INDUCED IN GOLD

prepared by dissolving a weighed amount of platinum wire in aqua regia and an iridium carrier (ca. 10 mgs./ml.) by dissolving ammonium chloro-iridate. Both these solutions were freed from nitrate, by evaporating several times to near dryness with the addition of conc. HCl, before diluting to volume.

Separation of milligramme quantities of platinum and iridium.

Both Pt^{197} and Ir^{194}, the (n,p) and (n, α) products of the irradiation of gold, have half-lives of the order of 19 hrs. In order to assay the activity of each, a good clean separation of platinum from iridium was required.

At the outset, two procedures were considered. Both employed ion-exchange techniques.

The first procedure, reported by Stevenson et al,[44] had been used to effect a clean separation of a mixture of all four of the platinum group metals. A solution of platinum group metal chlorides is evaporated to near dryness with $HClO_4$. The resultant solution of perchlorates is placed on a cation-exchange column (Dowex 50) and eluted with water. Iridium, rhodium and palladium are retained on the column to a greater or lesser degree and only platinum is eluted. The other metals can be

stripped off the column in turn by eluting with increasingly concentrated solutions of HCl. Iridium is the most recalcitant and requires 6N HCl to elute it.

It followed that a very clean separation of platinum from iridium could be effected by this method. One disadvantage was that the iridium was reported to come off the column only very slowly.

The second procedure, reported by Busch et al,[45] employed an anion-exchange technique, specifically designed for the separation of irridium and platinum fractions. A mixture of chloroplatinate and chloroiridate is reduced with NH_2OH and placed on a Dowex 1 anion-exchange column. The iridium fraction is eluted with 9N HCl at 80°C., but contains a little platinum impurity (ca. 3%). The remainder of the platinum is eluted with a 50% $HClO_4$ solution at the same temperature and has a purity of greater than 99%.

The former procedure had the advantages over the latter that it was simpler and that the platinum fraction was the first to come off the column. This was an important consideration, because Pt^{197} has a metastable state with an 88 min. half-life, and the quick separation of the platinum fraction facilitated the study of this activity. The slowness of the iridium fraction to

elute was not a great disadvantage for, with a 19 hr. half-life, there was some time to spare.

Also, the 3% platinum impurity in the iridium fraction raises a serious objection to the second method, because the Pt^{197} activity from irradiated gold is several times higher than the Ir^{194} activity.

Preliminary experiments on the cation-exchange method were successful, and it was used in all cases for the separation of platinum and iridium fractions.

Tracer experiment to test the efficiency of the cation-exchange method of separating platinum and iridium.

Dowex 50 cation-exchange resin (cross linking ~ 12 DVB, mesh - 50 to 100) was placed into a column (length - 6 cms., diameter - 1.4 cms.) and freed from all traces of chloride by washing with distilled water.

4 day Pt^{195m} plus Pt^{193m} and 74.5 day Ir^{192} tracers were added to a mixture of 2 mls. each of the platinum and iridium carrier solutions. The mixture was treated as follows.

Step 1. The solution was evaporated very carefully to dryness. The residue was taken up in 2 mls. of 70% $HClO_4$ and warmed until the $HClO_4$ began to fume copiously. (It had been found previously that, if the

solution was evaporated beyond this stage, turbidity and precipitation of the Pt ensued). At this stage the red-brown colouration of the chloroiridate was replaced by the mauve colour of the iridium perchlorate complex.

Step 2. The mauve solution was diluted to 20 mls. and placed on the column. The Pt fraction, which was a deep yellow, appeared to come straight off the column and was eluted at a rate of 0.5 ml./min. The mauve iridium fraction was very tightly adsorbed on the first centimetre of the column, forming a sharply defined mauve band.

Step 3. The column was eluted with distilled water and the first ten column volumes (40 mls.) of elutriant, containing the platinum fraction, were collected. The column was washed with a further fifteen column volumes of water, which were discarded. This treatment removed the last traces of Pt.

Step 4. The column was eluted with 6N HCl.

About 20% of the Ir was stripped off in the first column volume or so of HCl, but the remainder stayed tightly bound to the resin and could not, at this stage, be eluted.

Step 5. After remaining for about four hours under a head of 6N HCl, the mauve band had turned a deep blue colour. In this state, the Ir was much more readily eluted, although it seemed that there was always a little that could not be stripped under any circumstances.

(It was difficult to understand what the chemical changes, involved in this process, were. The blue Ir complex may be the higher valence Ir(VI) chloro-complex or a chloro-perchlorate intermediate complex. The change from mauve to blue can be accelerated by warming. On boiling the blue solution, it rapidly assumes the familiar red-brown chloroiridate colour).

Step 6. The Pt fraction from Step 3 was evaporated down to half its volume, i.e. 20 mls., and made 3N in HCl. The Ir fraction, which was contained in about 40 mls. of 6N HCl, was evaporated down to about a third of this volume and then made 3N in HCl. Elemental Pt and Ir were precipitated from these solutions by reduction with Grignard magnesium.

Step 7. The Pt and Ir ppts. were collected on glass fibre filter discs, washed with water, dried at 110°C., weighed and mounted for counting.

The decay rates of the two sources were traced for

several weeks until all the 4 day Pt activity had decayed. Inspection of the decay curves indicated a slight contamination of the Pt source by Ir^{192}, but the Ir source was free from any contamination from the Pt^{193m}-Pt^{195m} tracer.

From the results of this experiment it was clear that:-

(i) virtually 100% of the Pt was collected in the Pt fraction. The last traces of Pt were washed off the column by the passage of copious volumes of distilled water.

(ii) ca. 3% of the Ir was collected in the Pt fraction. This was doubtless due to failure to remove last traces of Cl^{-} from the solution of perchlorate complexes, but, as mentioned earlier, a limitation was imposed here by the tendency of the Pt to come out of solution at this stage.

(iii) ca. 50% of the Ir was stripped off the column by eluting with 6N HCl. Although about a third of this was collected almost immediately, it was a slow process to strip the remainder from the resin, taking about four hours at room temperature. The Ir fraction was uncontaminated by the Pt^{193m}-Pt^{195m} tracer.

(iv) The remainder of the Ir stayed tightly bound to the resin and could not be removed at this stage.

The contamination of the Pt source by 3% of the Ir activity was the only objection to this procedure. Forunately, this was not a serious objection in practice, because the Pt^{197} activity induced in gold by 14 MeV neutrons was about five times higher than the Ir^{194} activity. Then the contribution of Ir^{194} activity to the total activity of a Pt source, prepared from irradiated gold, was less than 1%. On the other hand, the preparation of an Ir source, uncontaminated by Pt^{197}, was a great advantage of this procedure.

Treatment of irradiated gold.

After removal of the iron monitor, the gold (ca. 1 gm.) was weighed and dissolved in about 20 mls. of aqua regia. 2 mls. each of Pt and Ir carrier were added, the solution was evaporated down to about 10 mls. and then diluted to 20 mls. with water. The Pt plus Ir fraction was separated from the gold by solvent extraction.

Step 1. The solution was placed in a 100 ml. separating funnel and shaken with an equal volume of ethyl acetate. Au was extracted leaving Pt and Ir in the aqueous phase.

Step 2. This extraction process was performed five times with the addition of a little Au carrier (ca. 10 mgs.) for the fourth extraction. Both phases were retained.

Step 3. The aqueous phase contained the Pt and Ir fractions. These were separated by means of the ion-exchange procedure already described.

Step 4. The ethyl acetate phase, containing the gold, was evaporated to near dryness and the gold was taken up in 2N HCl.

Step 5. The Au was precipitated by reduction with SO_2 and washed with water.

Step 6. A Au source was prepared by drying a slurry of the activated Au in an aluminium counting tray.

A platinum source could be prepared and counted within two hours of the end of the irradiation. No iridium source was counted less than eight hours after the end of the irradiation.

Attempt to assign the 9.5 hr. activity unequivocally to a metastable state of Au^{196}.

The X-ray spectrum of freshly irradiated gold, freed from platinum and iridium activities, was examined using

a γ-scintillation spectrometer. The pulse height spectrum was plotted before and after the disappearance of the 9.5 hr. activity and the K X-ray peak shift was measured. The 5.6 day Au^{196} decays by electron capture with the emission of platinum X-rays, and the measured peak shift was consistent with the emission by the 9.5 hr. activity of gold X-rays, indicating that it decayed by isomeric transition to a gold ground state.

The decay of a metastable state by I.T. might be expected to leave the ground state in a different chemical form, which, if exchange did not occur, could be separated. Then, if the 5.6 day Au^{196} could be chemically separated from the 9.5 hr. gold activity, the latter could be unequivocally assigned to a metastable state of Au^{196}.

An examination of the literature revealed two references to the isolation of carrier-free Au^{198} from irradiated gold by the Szilard-Chalmers process.

Both methods were designed to ensure that isotopic exchange between free Au^{198} nuclei, recoiling from neutron capture reactions, and inactive gold could not occur.

In the first method, reported by Majer,[46] this condi-

tion is achieved by irradiating the gold as the aurate ion in alkaline solution. Free Au^{198} nuclei do not exchange with gold in the strongly complexed aurate and are collected on colloidal gold previously introduced into the solution. Under these conditions the colloidal gold gradually coagulates carrying the Au^{198} with a much higher specific activity than in the aurate.

Attempts to apply this method to the separation of Au^{196} from its 9.5 hr. proposed isomer were unsuccessful. Colloidal gold was introduced into a strongly alkaline solution of gold chloride prepared from freshly irradiated gold. The colloidal gold gradually coagulated and, after about ten hours, it was separated, washed and mounted for counting. It was found that only a small fraction of the total activity had been carried and this included 9.5 hr. as well as 5.6 day gold. Also, the ratio of the activities in the source did not differ significantly from their ratio in a source prepared from the aurate solution.

In the other method of isolating carrier-free Au^{198}, used by Herr,[47] the gold is irradiated in the form of an organic gold complex. The structure of the compound is not known, but its chemical formula is given

as $\left[(C_6H_5.CO.C(H):C(OH).C_6H_5)_3Si\right] AuCl_4$. It is very easily prepared by mixing the stoichiometric quantities of dibenzoylmethane, anhydrous gold chloride and silicon tetrachloride in chloroform. The compound recrystallises from acetonitrile as beautiful yellow crystals. The irradiated crystals are dissolved in benzonitrile and free Au^{198} nuclei, ejected from the complex molecules by (n, γ) reactions, are extracted into a dilute cyanide solution.

In preliminary experiments performed on this method, Herr's results could not be reproduced. Samples of the crystals were irradiated with thermal neutrons, but only about 15% of the induced Au^{198} activity could be extracted into the cyanide solution compared to the 95% claimed by Herr.

Nevertheless, the method was applied to the problem of separating Au^{196} from the proposed isomeric transition. Anhydrous gold chloride was prepared from irradiated gold by warming hydrogen gold chloride (obtained by evaporating a solution of the gold in HCl) at 220°C in a stream of chlorine. The organic compound was prepared, as described, and the cyanide extraction performed after leaving the crystals for a few hours to allow some of the 9.5 hr. activity to decay. The extracted activity was co-precipitated with bismuth

sulphide and a source was prepared. Again, the carried activity included the 9.5 hr. as well as the 5.6 day gold, and it was just a small fraction of the total activity in the gold organic compound.

It is apparent that the high stability claimed by Herr for the compound is not justified, as the activity that was extracted could not be attributed to a Szilard-Chalmers process. Also, it was later noticed that the yellow crystals turned black on standing in strong sunlight - not an indication of high stability.

The negative results of these experiments are not evidence of the mis-assignment of the 9.5 hr. activity to Au^{196m}, but rather of the unsuitability of the methods used. A more reliable method might well furnish positive results.

RESULTS AND DISCUSSION.

The results are presented in Tables 20, 21 and 22.

The present values of 2.60 mbs. $\pm$ 0.27 and 0.50 mb. $\pm$ 0.08 for the $Au^{197}(n,p)Pt^{197}$ and the $Au^{197}(n, \alpha)Ir^{194}$ cross sections closely agree with the recently reported values of Coleman et al[39] of 2.42 mbs. $\pm$ 0.24 and 0.43 $\pm$ 0.09 for the respective reactions. An earlier value of 20.5 mbs. $\pm$ 8 for the (n,p) cross section, reported

by Peck, is not consistent with the low cross sections for charged particle emission in this region of the Periodic Table. Peck investigated the proton spectrum resulting from the reaction by a nuclear emulsion technique and based his cross-section measurement on the proton yield. Some error in estimating the neutron flux or the total proton yield must have arisen.

Values of the cross sections for the independent production of the two nuclear isomers of Pt^{197} (Table 28) have not been previously reported. These values are interesting in comparison to the corresponding values for the production of Pt^{197} by the $Hg^{200}(n, \alpha)Pt^{197}$ reaction (Table 27). The ratio of the yields of the ground and metastable states of Pt^{197} appears to be slightly higher in the latter reaction, 1.38 ± 0.12 compared to 1.11 ± 0.14 in the $Au^{197}(n,p)Pt^{197}$ reaction.

There is still no definite evidence for the assignment of the 9.5 hr. activity to a metastable state of Au^{196}. A second metastable state of Au^{197} is another possibility.

IRRADN. NO.	SAMPLE REACTION: No. of target nuclei x N^{-1}	Chemical Yield %	self-absorption factor	A_o observed c.p.m.	A_o correct d.p.m.	REFERENCE REACTION: S	No of target nuclei x N^{-1}	A_o observed c.p.m.	A_o correct d.p.m.	S	MEASURED CROSS SECTION mbs.	MEAN
TABLE 20	RESULTS FOR THE $Au^{197}(n,p)Pt^{197}$ REACTION.											
43	6.31×10^{-3}	75.5	0.32	1.15×10^3	4.76×10^3	4.69	9.35×10^{-3}	2.04×10^5	2.28×10^6	3.79	2.37	2.60mbs. ± 0.27
44	6.53×10^{-3}	87.5	0.32	1.50×10^3	5.36×10^3	3.78	5.89×10^{-3}	1.11×10^5	1.25×10^6	2.95	2.86	
45	7.15×10^{-3}	64.6	0.33	1.11×10^3	5.23×10^3	4.23	4.49×10^{-3}	7.68×10^4	8.60×10^5	3.26	2.80	
46	1.32×10^{-2}	78.0	0.32	7.80×10^2	3.12×10^3	3.58	7.18×10^{-3}	5.10×10^4	5.71×10^5	2.99	2.36	

$t_{\frac{1}{2}} Pt^{197}$ = 19.7 hours.

TABLE 21	RESULTS FOR THE $Au^{197}(n,\alpha)Ir^{194}$ REACTION.											
43	"	33.9	0.33	9.4×10	8.43×10^2	"	"	"	"	"	0.41	0.50mbs. ± 0.08
44		26,7	0.33	8.2×10	9.26×10^2						0.49	
45		11.0	0.315	3.95×10	1.14×10^3						0.60	
46		15.2	0.325	3.3×10	6.70×10^2						0.50	

N is the Avogadro Number. $t_{\frac{1}{2}} Ir^{194}$ = 19.3 hours.

$\sigma_{Fe^{56}(n,p)Mn^{56}}$ = 124 mbs.

$c_{Mn^{56}}$ = 0.0893.

$t_{\frac{1}{2}} Mn^{56}$ = 2.58 hours.

TABLE 22 RESULTS FOR THE INDEPENDENT PRODUCTION OF Pt^{197m} AND Pt^{197g} (see equation 2) BY THE $Au^{197}(n,p)Pt^{197}$ REACTION.

IRRADN. NO.	No. of Pt^{197m} nuclei at t_o	No. of Pt^{197g} nuclei at t_o	$S_{Pt^{197m}}$	$S_{Pt^{197g}}$	$\frac{\sigma_{Au^{197}(n,p)Pt^{197g}}}{\sigma_{Au^{197}(n,p)Pt^{197m}}}$	Mean	$\sigma_{Au^{197}(n,p)Pt^{197m}}$ mbs.	$\sigma_{Au^{197}(n,p)Pt^{197g}}$ mbs.
45	1.44×10^6	3.77×10^6	2.63	4.23	1.18	1.11 ± 0.14	1.23 ± 0.15	1.37 ± 0.17
46	1.31×10^6	2.35×10^6	2.55	3.58	0.95			
47	1.54×10^6	4.04×10^6	1.74	2.80	1.21			

The counting efficiency of conversion electrons is taken as equal to that of β-particles with end point energies equal to twice the energy of the I.T.

The energy of the Pt^{197m}-Pt^{197g} I.T. = 0.337 MeV and it is highly converted.

The end point energy of the Pt^{197g} β-particles = 0.67 MeV

Then $c_{Pt^{197m}} = c_{Pt^{197g}}$

$\sigma_{Au^{197}(n,p)Pt^{197}}$ total = 2.60 mbs. (Table 18).

$t_{\frac{1}{2}}$ Pt^{197m} = 88 mins. $t_{\frac{1}{2}}Pt^{197g}$ = 19.7 hours.

h) IRRADIATION OF MERCURY.

Homogeneous mixtures of mercuric oxide and iron granules were irradiated.

Of the reactions induced in the mercury, those studied were:-

$Hg^{200}(n,p)Au^{200}$ ($t_{\frac{1}{2}}$ = 48 mins.)
$Hg^{201}(n,p)Au^{201}$ ($t_{\frac{1}{2}}$ = 26 mins.)
$Hg^{200}(n,\alpha)Pt^{197}$ ($t_{\frac{1}{2}}$ = 19.7 hrs.)
$Hg^{200}(n,\alpha)Pt^{197m}$ ($t_{\frac{1}{2}}$ = 88 mins.)
$Hg^{202}(n,\alpha)Pt^{199}$ ($t_{\frac{1}{2}}$ = 31 mins.)

The resultant species were chemically separated. Solid sources were prepared and counted under the end window counter.

Natural mercury contains seven stable isotopes and, even after chemical separations have been performed, the decay schemes of the different fractions remain quite complex. Also, the activities, induced by these reactions, were low making them even more difficult to resolve.

None of the half-lives, quoted above, were measured in this work. The 48 mins. of Au^{200} and 26 mins. of Au^{201} had to be assumed before the two activities could be resolved. Similarly it was necessary to assume the

literature value of 31 mins. for Pt^{199} and 88 mins. (measured in irradiation of gold) for Pt^{197m} before these activities could be resolved. The half-life of Pt^{197}, 19.7 hrs., was also taken as that measured in the irradiation of gold. The counting statistics of the Pt^{197} activity induced in mercury were not good enough to measure the half-life accurately.

Any 5.1 min. Hg^{205} activity, that may have been produced by the $Hg^{204}(n, \gamma)Hg^{205}$ reaction, was obscured by the much higher level of the 43.5 min. Hg^{199m} activity formed by both the $Hg^{199}(n,n')Hg^{199m}$ and $Hg^{200}(n,2n)Hg^{199m}$ reactions.

As values were obtained for the (n,p) cross sections of both Hg^{200} and Hg^{201}, it was thought that a value for the $Hg^{202}(n,p)Au^{202}$ reaction cross section would be useful, in that it would give an indication of any trend that might occur with increasing Neutron Number. Attempts were made to measure this cross section, but little more was achieved than a confirmation of the half-life of Au^{202} as about 25 secs.

EXPERIMENTAL DETAILS.

Preparation of gold and platinum carrier solutions.

Weighed amounts of gold foil and platinum wire were

dissolved in aqua regia. The solutions were diluted to a standard volume so as to contain about 10 mgs./ml. of gold and platinum respectively.

Isolation of gold fraction.

The mercuric oxide (ca. 1.5 gms.) was dissolved in 10 mls. conc. HCl with the minimum amount of conc. HNO_3 to ensure speedy dissolution. 2 mls. of the standard gold carrier solution and a little platinum carrier were added.

Step 1. The solution was diluted till it was 6N with respect to HCl and shaken in a separating funnel with an equal volume of ethyl acetate. Under these conditions only the gold is extracted into the organic phase. The aqueous phase was discarded.

Step 2. The organic phase was washed three times with equal volumes of 6N HCl.

Step 3. The organic layer was evaporated to dryness and the $HAuCl_4$ was taken up in 2N HCl.

Step 4. The gold was precipitated by reduction with SO_2 and coagulated by boiling. The precipitated gold was washed with water and collected on a glass fibre filter disc for counting under the end window counter. The source was dried at 110°C and weighed.

This procedure could be completed in twenty-five minutes.

The gold source comprised two fractions, 26 min. Au^{201} and 48 min. Au^{200}. The decay of this composite source was traced very closely right down to background and the decay curve was resolved, assuming the above values for the half-lives, by making use of the expression[48]

$$Ae^{\lambda_1 t} = A_1^{o} + A_2^{o} e^{\Delta\lambda t}$$

where, A was the total activity of the source at time, t.

A_1^{o} was the activity of 48 min. Au^{200} at time, t = 0.

A_2^{o} was the activity of 26 mins. Au^{201} at time, t = 0.

λ_1 is the decay constant of Au^{200}

and $\Delta\lambda = \lambda_2 - \lambda_1$, where λ_2 is the decay constant of Au^{200}.

Then plotting $Ae^{\lambda_1 t}$ against $e^{\Delta\lambda t}$, A_2^{o} was given by the slope of the curve and A_1^{o} by its intercept.

Attempt to measure the $Hg^{202}(n,p)Au^{202}$ cross section.

Au^{202} is reported as a Class E Isotope[49] (Element probable and mass number not established) with a half-life of about 25 secs. Irradiation of metallic mercury, which was counted in a liquid counter, certainly produced a 25 sec. activity. It had already been shown

by Mrs. E.B.M. Martin[50] that a 25 sec. activity was produced by the irradiation of thallium and there can be little doubt that this activity was indeed Au^{202}, induced in thallium by the $Tl^{205}(n, \alpha)Au^{202}$ reaction and in mercury by the $Hg^{202}(n,p)Au^{202}$ reaction. There was no indication in the literature as to the decay scheme or β^-particle energies of Au^{202} and all that could be ascertained from absorption measurements performed by Mrs. Martin was that the β's were exceptionally hard.

In the absence of information as to the energy of the Au^{202} β^-particles, it was not possible to determine the absolute disintegration rate of the activity in the standardised liquid counter, because the efficiency of the liquid counter varies linearly with β-energy. There was more hope counting the irradiated mercury under an end window counter, calibrated for thick sources.

Pilot irradiations were performed. Sealed capsules of metallic mercury and mercuric iodide were irradiated for 1 minute periods and transferred automatically from the target chamber to the counting room by means of the vacuum tube. (Irradiation of mercuric oxide was precluded in this case by the production, with a high

cross section, of 7.4 sec. N^{16} from the oxygen, which would obscure the 25 sec. Au^{202}).

It was possible to start counting 15 seconds after the end of the irradiation and the scaler, operated by the electronic timing device, counted for periods of 4.8 seconds with intervals of 1.2 seconds. The decay of the activities induced in the mercury could then be followed very closely. Even so, it was not possible to resolve the 25 sec. Au^{202} activity from the high level of 43.5 min. Hg^{199m}. A thin platinum absorber absorbed most of the 43.5 min. conversion electrons and X-rays and the 25 sec. activity became apparent, but it was at a low level and counting statistics were bad. Also, a correction would have to be introduced for absorption in the platinum foil, and, with the lack of knowledge of the decay scheme and β-energies of Au^{202}, it was felt that any value obtained for the $Hg^{202}(n,p)Au^{202}$ cross section would be insufficiently accurate to be valuable.

Isolation of platinum fraction.

The mercuric oxide (ca. 1.5 gms.) was dissolved in 10 mls. of aqua regia. 2 mls. of the standard platinum carrier solution and a little gold carrier were added. The platinum fraction was separated by the

procedure described by Meinke[51] with small modifications.

Step 1. Excess HCl was removed by evaporating to near dryness with the addition of conc. HNO_3. The completion of this step was signified by the precipitation of mercuric chloride.

Step 2. The mercuric chloride precipitate was dissolved by the addition of water and the solution was diluted to 15 mls.

Step 3. The solution was placed in a 100 mls. separating funnel and shaken with an equal volume of ethyl acetate. Under these conditions (absence of excess chloride ions) both gold and mercury were extracted into the organic layer, which was discarded.

Step 4. The extraction was repeated five times with the addition of gold and mercury carriers on the third extraction. The organic phase was discarded.

Step 5. The aqueous phase, containing the platinum fraction, was warmed and crystals of $NH_2OH.HCl$ were added to destroy excess HNO_3.

Step 6. The solution was made 6N with respect to HCl and ca. 15 mgs. of $SnCl_2$ crystals were added. These reduced Pt(IV) to Pt(II) with the formation of the familiar orange-red colouration.

Step 7. Excess $SnCl_2$ was removed by centrifugation and the red Pt(II) complex was extracted into an equal volume of ethyl acetate. The aqueous phase was discarded.

Step 8. The organic layer was washed several times with equal volumes of 6N HCl.

Step 9. The organic layer was evaporated to dryness and the residue was taken up in 2N HCl.

Step 10. Elemental Pt was precipitated by reduction with Grignard magnesium.

Step 11. The precipitated Pt was washed with water and a source for counting under the end window counter was prepared, dried at 110°C and weighed.

The procedure could not be completed in less than sixty-five minutes.

It was necessary to trace the decay of the platinum source very closely as it comprised several activities. After the subtraction of long-lived activities, the 31 min. Pt^{199} and 88 min Pt^{197m} activities were resolved graphically, again employing the expression[48]

$$Ae^{\lambda_1 t} = A_1^{o} + A_2^{o} . e^{-\Delta\lambda t}$$

and assuming the literature values of the half-lives.

The long-lived activity comprised 19.7 hr. Pt^{197}

and 3.16 day Au^{199}, the daughter of Pt^{199}, but the level of the latter activity was barely above background and was neglected.

RESULTS AND DISCUSSION.

The results are presented in Tables 23, 24, 25, 26 and 27.

Values of 3.36 mbs. ± 0.46 and 2.46 ± 0.26 have been obtained for the $Hg^{200}(n,p)Au^{200}$ and $Hg^{201}(n,p)Au^{201}$ cross sections. These are in good agreement with the values of 3.63 ± 0.36 and 2.12 ± 0.32 reported by Coleman et al[39] for the respective reactions.

The values obtained for the (n, α) cross sections differed sharply from Coleman's values. He reported 1.77 mbs. ± 0.35 and 1.01 mbs. ± 0.10 for the $Hg^{200}(n,\alpha)Pt^{197}$ and $Hg^{202}(n,\alpha)Pt^{199}$ cross sections. The values, obtained in the present work, are 0.44 mb. ± 0.05 and 0.31 mb. ± 0.03 for the respective reactions. This difference is hard to understand and no explanation is put forward, but the present values are more in line with the trend of low (n,α) cross sections, which is apparent in the high-Z region of the Periodic Table, e.g. $Au^{197}(n,\alpha)Ir^{194}$ = 0.50 mb. $Tl^{203}(n,\alpha)Au^{200}$ =

0.37 mb.[39] $Bi^{209}(n, \alpha)Tl^{206}$ = 0.46 mb.

The decreases in (n,p) and (n, α) cross sections with increasing Neutron Number are examples of the Levkovskii Trend. Levkovskii[52] observed that the (n,p) and (n, α) cross sections of isotopes decreased with increasing Neutron Number. In most of the examples he investigated the decreases were approximately by some multiple of two for each additional neutron in the nucleus. Levkovskii explained the Trend on the basis of the statistical theory of the compound nucleus. As the neutron/proton ratio in the nucleus increases, the emission of neutrons from the compound nucleus is favoured at the expense of charged particle emission. Examination of Paul and Clarke's values for (n,2n) cross sections[1] reveals that, in general, they increase with A at constant Z (at least, in the middle-Z region), confirming this hypothesis.

The measured decreases in Hg(n,p) and (n, α) cross sections are not as large as those measured by Levkovskii in the low and middle-Z regions of the Periodic Table. This might be explained by the predominance in the high-Z region of the direct mechanism for (n,p) and (n, α) reactions. Then, local neutron/proton ratios only must be considered and these are not going to be appreciably

affected by the addition of one neutron to a heavy nucleus.

It can be seen why a value for the $Hg^{202}(n,p)Au^{202}$ cross section would have been valuable. It might have provided further evidence of the Levkovskii Trend.

IRRADN. NO.	SAMPLE REACTION: No. of target nuclei x N-1	Chemical yield (%)	Self-absorption factor	A_o observed c.p.m.	A_o correct c.p.m.	S	REFERENCE REACTION: No. of target nuclei x N-1	A_o observed c.p.m.	A_o correct d.p.m.	S	MEASURED CROSS SECTION mbs.	MEAN
TABLE 23. RESULTS OF THE $Hg^{200}(n,p)Au^{200}$ REACTION.												
48	2.44×10^{-3}	70.6	0.32	4.45×10^{2}	1.97×10^{3}	2.60	1.09×10^{-2}	7.91×10^{3}	8.86×10^{4}	2.66	3.84	3.36mbs ± 0.46
49	1.90×10^{-3}	87.5	0.32	3.40×10^{2}	1.21×10^{3}	2.80	9.62×10^{-3}	6.66×10^{3}	7.46×10^{4}	2.93	3.32	
50	2.40×10^{-3}	77.5	0.32	8.30×10^{2}	3.34×10^{3}	4.15	8.80×10^{-3}	1.61×10^{4}	1.81×10^{5}	4.63	2.91	
TABLE 24. RESULTS FOR THE $Hg^{201}(n,p)Au^{201}$ REACTION.												
48	1.37×10^{-3}	70.6	0.32	3.14×10^{2}	1.39×10^{3}	2.53	"	"	"	"	2.74	2.46mbs ± 0.26
49	1.06×10^{-3}	87.5	0.32	2.40×10^{2}	8.56×10^{2}	2.64					2.40	
50	1.35×10^{-3}	77.5	0.32	5.85×10^{2}	2.36×10^{3}	3.66					2.24	

N is the Avogadro Number.

$\sigma_{Fe^{56}(n,p)Mn^{56}} = 124$ mbs.

$c_{Mn^{56}} = 0.0893$.

$t_{\frac{1}{2}} Mn^{56} = 2.58$ hours.

$t_{\frac{1}{2}} Au^{201} = 26$ mins.

IRRADN. NO.	SAMPLE REACTION: No. of target nuclei x N^{-1}	Chemical yield (%)	Self-absorption factor	A_o observed c.p.m.	A_o correct d.p.m.	S	REFERENCE REACTION: No. of target nuclei x N^{-1}	A_o observed c.p.m.	A_o correct d.p.m.	S	MEASURED CROSS SECTION mbs.	MEAN
TABLE 25. RESULTS FOR THE $Hg^{200}(n,\alpha)Pt^{197}$ REACTION.												
51	1.46×10^{-3}	89.3	0.32	8.5	2.97×10	1.76	3.24×10^{-3}	1.10×10^4	1.24×10^5	1.61	0.46	0.44mbs. ± 0.05.
52	1.57×10^{-3}	34.4	0.33	1.1×10	9.68×10	3.47	5.46×10^{-3}	7.00×10^4	7.83×10^5	3.26	0.38	
53	1.81×10^{-3}	54.8	0.325	1.73×10	9.70×10	2.84	5.85×10^{-3}	5.30×10^4	5.94×10^5	2.63	0.47	
$t_{\frac{1}{2}}$ Pt^{197} = 19.7 hours.												
TABLE 26. RESULTS FOR THE $Hg^{202}(n,\alpha)Pt^{199}$ REACTION.												
51	1.84×10^{-3}	89.3	0.32	1.80×10^2	6.30×10^2	1.10	"	"	"	"	0.32	0.31mbs. ± 0.03.
52	1.97×10^{-3}	34.4	0.33	3.40×10^2	3.00×10^3	2.53					0.34	
53	2.30×10^{-3}	54.8	0.325	3.28×10^2	1.84×10^3	1.85					0.28	

N is the Avogadro Number.

$t_{\frac{1}{2}}Mn^{56}$ = 2.58 hours.

$\sigma_{Fe^{56}(n,p)Mn^{56}}$ = 124 mbs.

$t_{\frac{1}{2}}Pt^{199}$ = 31 mins.

$c_{Mn^{56}}$ = 0.0893.

TABLE 27 RESULTS FOR THE INDEPENDENT PRODUCTION OF Pt^{197m} and Pt^{197g} BY THE $Hg^{200}(n, \alpha)Pt^{197}$ REACTION.

IRRADN. No.	No. of Pt^{197m} nuclei at t_o	No. of Pt^{197g} nuclei at t_o	$S_{Pt^{197m}}$	$S_{Pt^{197g}}$	$\frac{\sigma_{Hg^{200}(n, \alpha)Pt^{197g}}}{\sigma_{Hg^{200}(n, \alpha)Pt^{197m}}}$	Mean	$\sigma_{Hg^{200}(n, \alpha)Pt^{197m}}$ mb.	$\sigma_{Hg^{200}(n, \alpha)Pt^{197g}}$ mb.
51	1.15×10^4	2.40×10^4	1.44	1.76	1.51			
52	2.04×10^4	3.09×10^4	3.16	3.47	1.28	1.38 ± 0.12	0.18 ± 0.016	0.26 ± 0.023
53	2.80×10^4	4.83×10^4	2.45	2.84	1.34			

$c_{Pt^{197m}} = c_{Pt^{197g}}$ (see Table 20).

$\sigma_{Hg^{200}(n, \alpha)Pt^{197}}$ total = 0.44 mb. (Table 23).

$t_{\frac{1}{2}}Pt^{197m}$ = 88 mins. $t_{\frac{1}{2}}Pt^{197g}$ = 19.7 hrs.

i) IRRADIATION OF ARGON.

Liquid argon was irradiated in the vessel depicted in Fig. 19. The reactions observed were:-

$A^{40}(n,p)Cl^{40}$ ($t_{\frac{1}{2}}$ = 1.4 mins. ± 0.03)

$A^{40}(n,pn)Cl^{39}$ ($t_{\frac{1}{2}}$ = 55 mins. ± 0.8)

$A^{40}(n,\alpha)S^{37}$ ($t_{\frac{1}{2}}$ = 5 mins. ± 0.1)

The relative cross sections of these reactions were measured in a series of irradiations, and their absolute cross sections were determined by measuring the $A^{40}(n,\alpha)S^{37}$ cross section relative to that of the $Fe^{56}(n,p)Mn^{56}$ reaction: This was done by irradiating the liquid argon in the interstices of iron wool, which was packed into the irradiation vessel.

The measured half-lives of the induced activities are reported above.

EXPERIMENTAL DETAILS.

Irradiation procedure.

The irradiation vessel and associated apparatus are depicted in Fig. 19. The vessel was evacuated before being filled with argon from a cylinder. The argon was condensed by immersing the vessel in liquid air. The vessel, containing about 3 mls. of liquid argon when

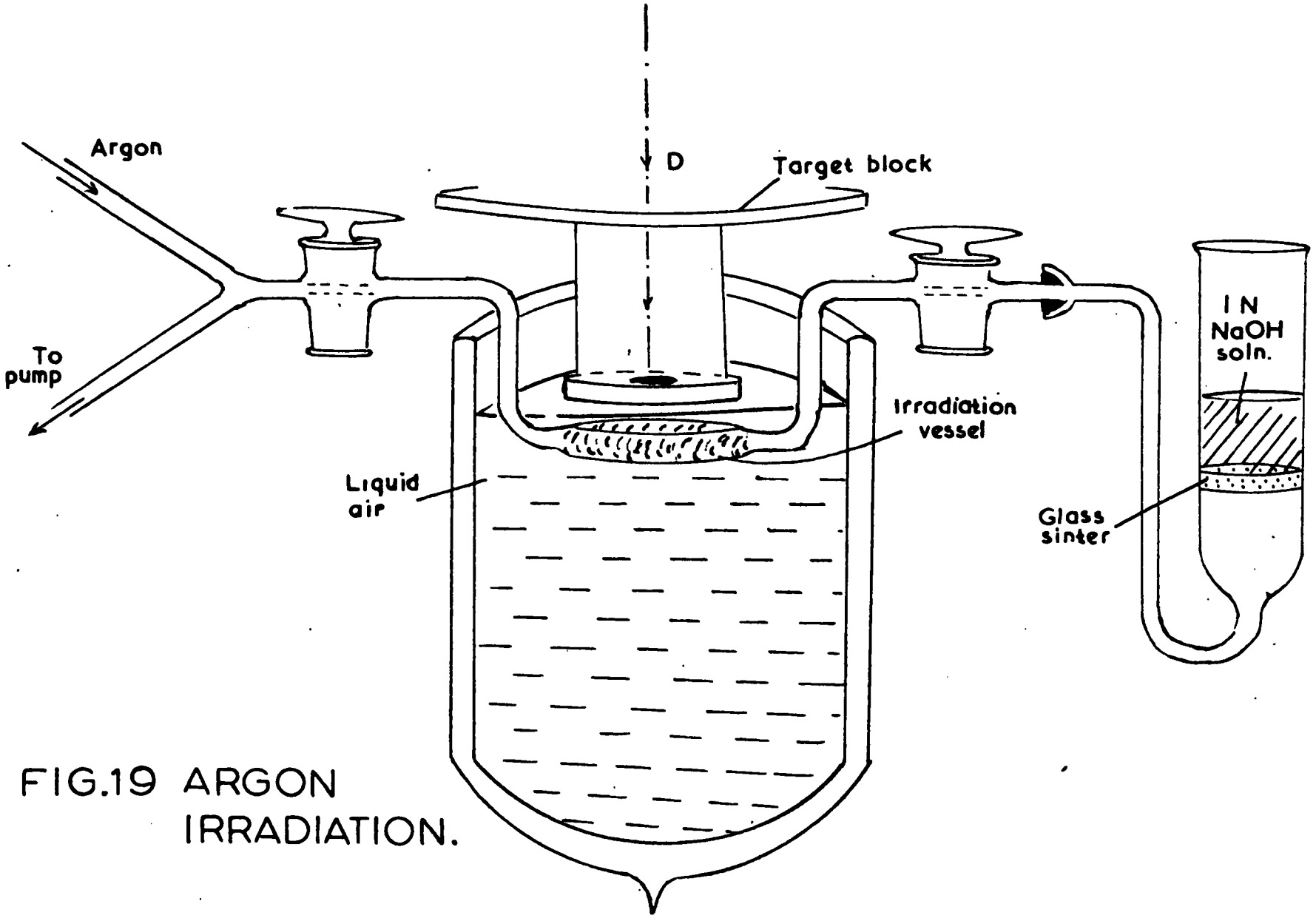

FIG.19 ARGON IRRADIATION.

full, was sealed and irradiated still immersed in liquid air.

After irradiation the argon was allowed to evaporate, bubbling through a 1N NaOH solution. This solution was then sucked back through the irradiation vessel to collect the activity sticking to the walls. (It had been shown in preliminary experiments that about 80% of the chlorine as well as the sulphur activity stuck to the walls of the irradiation vessel). The solution was made up to 10 mls. and counted in the standardised liquid counter. This procedure could be completed in about 6 mins. The 1.4 min. Cl^{40}, the 5 min. S^{37} and the 55 min. Cl^{39} activities were resolved graphically. A typical decay curve in reproduced in Fig. 20.

Estimation of the liquid counter efficiency for Cl^{40}.

The decay schemes of S^{37} and Cl^{39} are well established and their counting efficiencies were accurately interpolated from the liquid counter calibration curve. Cl^{40} has reported β's of 3.2 MeV and 7.5 MeV, but their proportions in the decay scheme are not known. But, whereas the liquid counter efficiency has been shown to

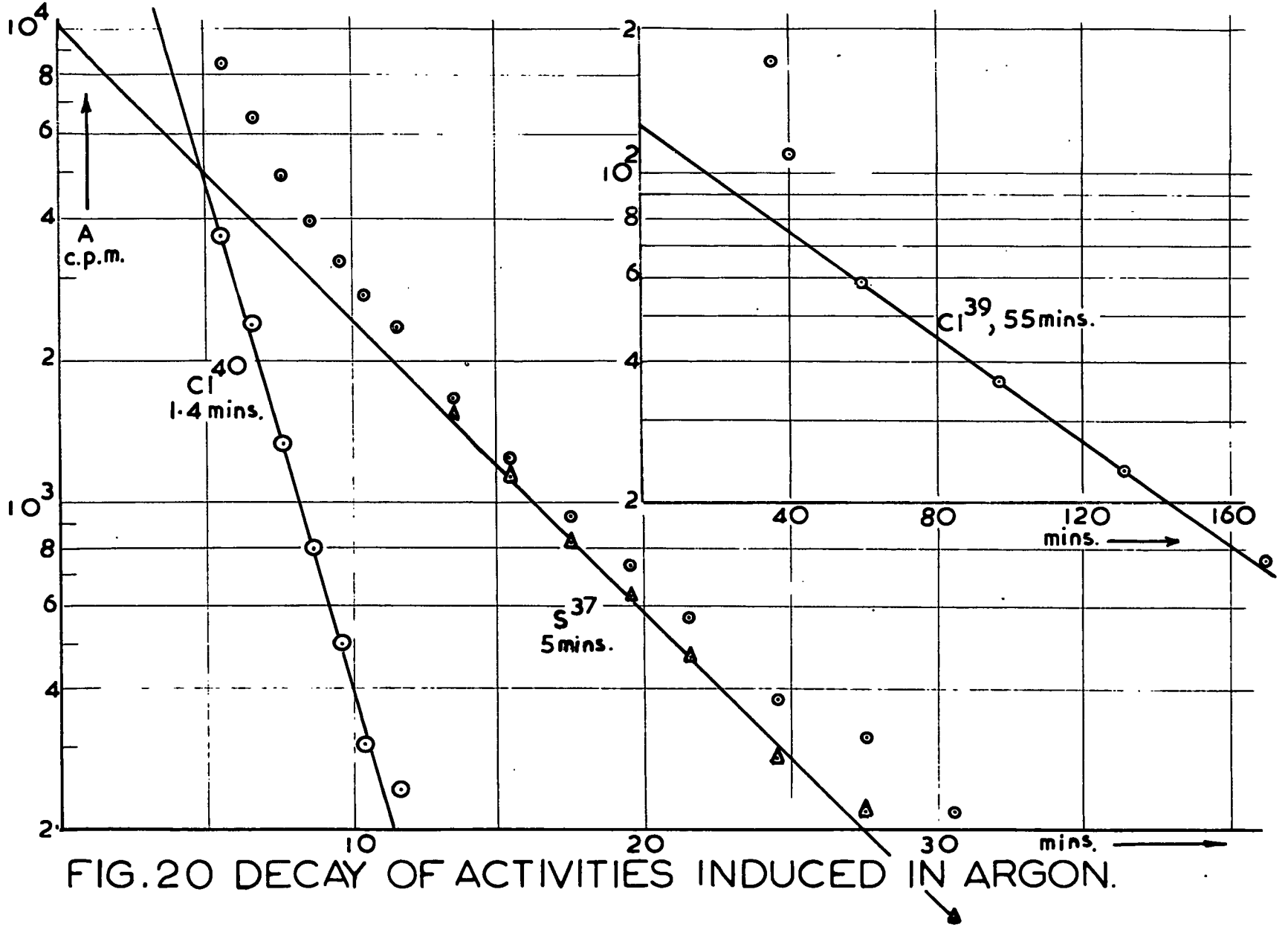

FIG. 20 DECAY OF ACTIVITIES INDUCED IN ARGON.

vary quite sharply with β^- energy, the variation in the end window counter efficiency is slight and, for energetic β's, efficiencies can be interpolated from the calibration curve with an error of only a few per cent. The counting efficiency of the liquid counter for Cl^{40} was measured relative to that of the end window counter for a Cl^{40} solid source.

A small volume (ca. 1 ml.) of liquid argon was irradiated for 2 mins. and the argon quickly boiled off. The irradiation vessel was washed with a standardised dil. HCl solution (ca. 1 mg./ml. of Cl^-) and the washings were made up to 20 mls. A 10 ml. aliquot part of this solution was counted in the liquid counter. A little conc. HNO_3 was added to the second half and AgCl was precipitated by the addition of excess 0.1N $AgNO_3$ solution. The AgCl ppt. was collected on a glass fibre filter disc and washed with dil. HNO_3, followed by alcohol and ether to dry. This source was prepared in about seven minutes from the end of the irradiation. It was uncontaminated by any S^{37} activity.

After correcting for the chemical yield of the procedure, the absolute disintegration rate of the source was determined by applying the correction factor

interpolated from the end window calibration curve. The observed Cl^{40} activity in the liquid counter was divided by the absolute disintegration rate, giving the liquid counter efficiency. The experiment was repeated in triplicate, yielding three results in close agreement.

Determination of the absolute cross sections.

For the determination of absolute cross sections, the liquid argon was irradiated in the interstices of iron wool, which was packed into the irradiation vessel. The cross section of the (n, α) reaction was measured relative to that of the iron reference and the two other argon cross sections followed from their values relative to the (n, α) cross section.

In this experiment, it was required to know accurately the volume of argon irradiated, and the NaOH washings had to be quantitatively collected. The iron wool was later recovered by breaking the irradiation vessel, and given the same treatment as the iron granules in other experiments. The Mn^{56} activity was traced in the liquid counter and decayed with the correct half-life.

RESULTS AND DISCUSSION.

The results of irradiations giving the relative values of the (n,p), (n,pn) and (n, α) cross sections are presented in Table 29 and the absolute value of the (n, α) cross section in Table 28.

It can be seen that the relative values of the three cross sections have been firmly established, but the two measurements of the absolute (n, α) cross section differ by a factor of two. This difference arises from the difficulty of measuring the volume of liquid argon in the iron-packed irradiation vessel, and it is likely that in the first measurement it has been overestimated. The value obtained from the second irradiation is more reliable, although further repetition of the experiment would seem desirable. The argon might be estimated by measuring the volume of the gas evaporating from the irradiation vessel.

These argon cross sections have not been previously measured.

The primary purpose of irradiating argon was to investigate evidence of the $A^{40}(n,pn)Cl^{39}$ reaction. This reaction has not been previously reported, but Colli et al[53] report (n,d) cross sections of the same order

of magnitude as (n,p) for P^{31}, S^{32} and Ca^{40}. Argon provides one of the few cases in which (n,pn) reactions can be studied by an activation technique. Most (n,pn) reactions result in stable products and, where activities are induced, the same activities are often induced by an (n,p) reaction on the A-1 neighbouring nuclide.

It is likely that the (n,pn) reaction proceeds, at least to some extent, by a direct mechanism of the pick-up type, where the proton is snatched from the nucleus by the incident neutron. The reaction is then an (n,d) rather than an (n,pn) reaction. This assumption is made on the basis of the results of Colli et al,[53] who present the deuteron spectra observed on irradiating P^{31} and S^{32}. These exhibit an intense deuteron line corresponding to the fundamental state of the residual nucleus. This type of spectrum, where the fundamental state is predominant, is indicative of a direct mechanism.

TABLE 28 RESULTS FOR THE $A^{40}(n,\alpha)S^{37}$ CROSS SECTION.

IRRADN. NO.	SAMPLE REACTION: No. of target nuclei x N^{-1}	A_o observed c.p.m.	A_o correct d.p.m.	S	No. of target nuclei x N^{-1}	REFERENCE REACTION: A_o observed c.p.m.	A_o correct d.p.m.	S	MEASURED CROSS SECTION mbs.	ACCEPTED VALUE
54	1.12×10^{-1}	2.16×10^4	2.40×10^5	0.42	8.75×10^{-3}	1.68×10^3	1.88×10^4	0.82	7.75	
55	7.70×10^{-2}	3.20×10^4	3.56×10^5	0.24	7.73×10^{-3}	1.58×10^3	1.77×10^4	0.45	15.0	15.0 mbs.

$\sigma_{Fe^{56}(n,p)Mn^{56}} = 124$ mbs. $C_{S^{37}} = 0.090$.

$t_{\frac{1}{2}}Mn^{56} = 2.58$ hours. $C_{Mn^{56}} = 0.0893$.

TABLE 29 THE RELATIVE VALUES OF THE $A^{40}(n,p)(n,pn)$ and (n,α) CROSS SECTIONS.

IRRADN. NO.	$A^{40}(n,p)Cl^{40}$: $A_o(Cl^{40})$ observed c.p.m.	$A_o(Cl^{40})$ correct d.p.m.	$S_{Cl^{40}}$	$A^{40}(n,pn)Cl^{39}$: $A_o(Cl^{39})$ observed c.p.m.	$A_o(Cl^{39})$ correct d.p.m.	$S_{Cl^{39}}$
56	5.8×10^4	2.21×10^5	0.277	1.28×10^2	1.31×10^3	0.44
57	4.6×10^4	1.75×10^5	0.278	6.2×10	6.33×10^2	0.47
58	4.8×10^4	1.83×10^5	0.217	7.8×10	7.95×10^2	0.35
59	3.6×10^4	1.37×10^5	0.197	±	-	-
60	-	-	-	9.6×10^2	9.80×10^3	3.22

$C_{Cl^{40}} = 0.262$ $t_{\frac{1}{2}}Bl^{40} = 1.4$ mins.

$C_{Cl^{39}} = 0.098$ $t_{\frac{1}{2}}Cl^{39} = 55$ mins.

$C_{S^{37}} = 0.090$ $t_{\frac{1}{2}}S^{37} = 5$ mins.

$A^{40}(n,\alpha)S^{37}$

$A_o(S^{37})$ observed c.p.m.	$A_o(S^{37})$ correct d.p.m.	$S_{S^{37}}$	$\frac{\sigma(n,p)}{\sigma(n,\alpha)}$	Mean	$\frac{\sigma(n,np)}{\sigma(n,\alpha)}$	Mean
1.00×10^4	1.11×10^5	0.383	0.775		0.113	
5.20×10^3	5.78×10^4	0.402	1.23		0.103	
6.50×10^3	7.22×10^4	0.295	0.965	1.00 ±	0.102	0.107 ±
4.80×10^3	5.33×10^4	0.283	1.04	0.19	±	0.006
2.60×10^4	2.89×10^5	0.963	±		0.112	

Then from Table 28 the absolute values of the n,p and the n,np cross sections respectively are 15.0 mbs. and 1.61 mbs.

j) IRRADIATION OF OSMIUM.

Examination of a current nuclide chart revealed that Re^{192} and W^{189}, the (n,p) and (n, α) products of Os^{192}, were unknown. Os^{192} is the most abundant isotope of osmium, and Re^{192} and W^{189} might reasonably be expected to decay with measurable half-lives. In an attempt to discover new activities, which might be assigned to Re^{192} and W^{189}, osmium was irradiated with 14 MeV neutrons.

EXPERIMENTAL DETAILS.

Pure osmium metal was irradiated for 15 mins. and quickly transferred to the counting room by means of the "rabbit". The activated osmium was counted through a 48 mg./cm.^{2} gold absorber to eliminate the X-rays and conversion electrons from the activities induced in lighter osmium isotopes. At first the scaler was operated by a timing device, counting for periods of 10.8 secs. with 1.2 sec. intervals. The decay of the activities induced in the osmium was followed for 20 hrs. The gross decay curve is reproduced in Fig. 21.

RESULTS AND DISCUSSION.

After the subtraction of long-lived activity (17 hr.

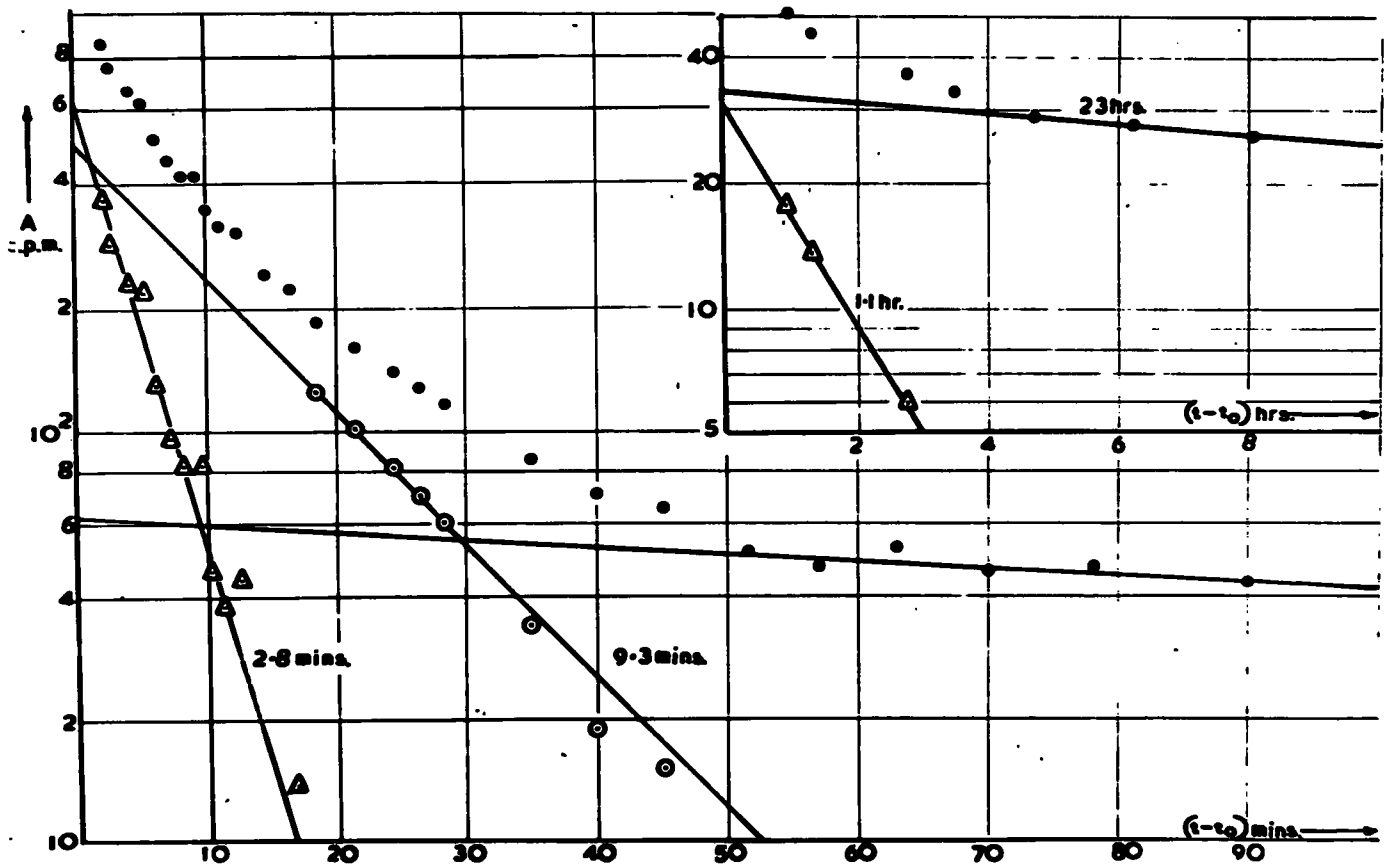

FIG.21 ACTIVITIES INDUCED IN OSMIUM.

Re^{188} and 24 hr. W^{187}), the gross β-decay curve resolved into 2.8 min., 9.3 min. and 1.1 hr. activities.

All of these activities have previously been reported, although the 9.3 min. half-life is slightly lower than the literature value (9.8 mins.).

Aten and Feyfer[54] observed the 2.8 min. activity in good yield from both the fast neutron and 26 MeV deuteron irradiations of osmium. They performed radiochemical separations and the 2.8 min. activity followed the rhenium fraction. It was then fairly unequivocally assigned to Re^{190}, formed by the $Os^{190}(n,p)Re^{190}$ and $Os^{192}(d,\alpha)Re^{190}$ reactions.

This assignment has been confirmed in the present work by cross-bombardment. A 2.3 min. activity was induced in pure iridium metal by 14 MeV neutrons. This could only be Re^{190}, produced by the $Ir^{193}(n,\alpha)Re^{190}$ reaction. The lower half-life (2.3 mins. instead of 2.8 mins.) was probably due to contamination by the β's from 1.4 min. Ir^{192m}. These constitute only about 0.1% of the total Ir^{192m} decay scheme, but the cross section for the production of the latter will be three orders of magnitude greater than that for the production of Re^{190}. The Ir^{192m} conversion electrons were cut out by an absorber.

Aten and Feyfer[54,55] also observed a 9.8 min. activity which followed rhenium chemistry, but only from the fast neutron irradiation of osmium. It was not produced by irradiation with 26 MeV deuterons. Assignment of this activity to Re^{189}, Re^{191} or Re^{192} is consistent with its lack of production by an Os(d, α) reaction. Of these, the current issue of Nuclear Data favours the assignment to Re^{191} on the basis of its reported β^--energy (1.8 MeV). β^--decay-energy systematics indicate Q values of 1,2 and 4 MeV respectively for Re^{189}, Re^{191} and Re^{192}.

But, from an examination of Fig. 21, it can be seen that the 9.8 min. activity is produced with roughly the same cross section as the 2.8 min. Re^{190}. This is credible only if it is produced by an (n,p) reaction, because Os(n,pn) cross sections at 14 MeV can be assumed, on the basis of a recent paper by Barry et al,[56] to be an order of magnitude smaller than the (n,p) cross sections. Re^{191} can only be formed by an (n,pn) reaction, and, for that reason,it seems unlikely to be the correct assignment for the 9.8 min. activity.

Assignment to Re^{189} also seems unlikely, as a $\sim$200 day activity has already been assigned to it.

It is concluded that the 9.8 min. activity is correctly assigned to Re^{192}.

The 1.1 hr. activity observed has been tentatively assigned by Halder and Wiig[57] to Re^{186m}.

k) IRRADIATION OF YTTERBIUM

Examination of a current nuclide chart revealed that the (n,p) and (n, α) products of Yb^{176} and the (n,p) product of Yb^{173} were unknown. Several irradiations of natural ytterbium oxide were performed and two new activities with half-lives of 2 $\pm$ 0.5 mins. and 9 $\pm$ 1 mins. were observed.

These activities might be assigned to Tm^{173}, Tm^{176} or Er^{173}.

Wille and Fink[41] recently reported the results of irradiations of enriched isotopes of ytterbium. They observed the 2 min. activity from Yb^{176}, but, with the impossibility of performing a radiochemical separation in the short time available, they were unable to assign it to either Tm^{176} or Er^{173}.

They also observed a 7.5 $\pm$ 1 min. activity (probably the same as the 9 min. activity observed here) from Yb^{173}, but not from Yb^{176}. This could be Tm^{173}, but, according to Wille and Fink, it was not produced in a high enough yield.

1) EXAMINATION OF POSSIBLE (n,He^3) REACTIONS

In a recent paper Kumabe et al[58] have reported (n,He^3) reactions for Mn^{55}, Co^{59}, As^{75} and Rh^{103} with 14.8 MeV neutrons. They report cross sections for these reactions of the order of millibarns. As, in a previous survey carried out in this laboratory, no 2 min. activity corresponding to the (n,He^3) product of Mn^{55} had been detected, an attempt was made to reproduce the results of Kumabe and his co-workers. All four of the nuclides, listed above, were irradiated and their decay curves analysed in a search for the products of possible (n,He^3) reactions, but their existence could not be verified. It is certain that these reactions do not occur with the cross sections reported by Kumabe. Upper limits of the cross sections, calculated from the results obtained in the present work, are an order of magnitude smaller than Kumabe's values.

EXPERIMENT DETAILS.

Irradiation of cobalt.

"Spec-pure" cobalt metal was irradiated for 2 mins. and quickly transferred to the counting room by means of the "rabbit". The activated cobalt was placed under the end window counter and counted for periods

of 10.8 secs. with 1.2 sec. intervals, the scaler being operated by an electronic timing device. The decay of the activity induced in the cobalt was followed for five hours. On resolving the decay curve, a small amount of a 1.8 min. activity, possibly Mn^{57}, the (n,He^3) product of Co^{59}, was detected in the presence of the high yield of 2.58 hr. Mn^{56} from the (n, α) reaction. Repetition of the experiment produced the same result, but, in each case, the 1.8 min. activity was so low as to barely exceed the limits of errors arising from counting statistics. An upper limit of the (n,He^3) cross section was calculated relative to the predetermined value (35 mbs.) of the (n, α) cross section.

Irradiation of arsenic.

Two homogeneous mixtures of iron and arsenious oxide were irradiated. The iron was removed from the mixtures and treated as described elsewhere. The gallium activity induced in the arsenic was chemically separated from the target material and counted under the end window counter. The decay of this source was followed for four half-lives of the 14.1 hr. (n, α) product, Ga^{72}. Evidence of the presence of Ga^{73}, the 5 hr. product of an (n,He^3)

reaction, was slight and ambiguous, but an upper limit of the (n,He^3) cross section was calculated. This experiment also furnished a value for the $As^{75}(n, \alpha)Ga^{72}$ cross section (Table 30).

Isolation of gallium.

The irradiated As_2O_3 (ca. 1.5 gms.) was dissolved in 20 mls. of conc. HCl with a few milligrammes of GeO_2. 1 ml. of a standardised gallium carrier solution (ca. 5 mgs./ml.) was added.

Step 1. The solution was evaporated to dryness, the germanium and arsenic distilling off with the HCl as $GeCl_4$ and $AsCl_3$.

Step 2. The gallium residue was taken up in 5 mls. of conc. HCl and Step 1 was repeated to remove the last traces of Ge and As.

Step 3. The gallium residue was taken up in 10 mls. of 6N HCl and, when cool, was extracted twice with equal volumes of ethyl ether. The two ether layers were combined.

Step 4. The combined ether layer was washed four times with one-third volumes of 6N HCl.

Step 5. The gallium was back-extracted into 5 mls. of water. This was repeated and the two aqueous

layers were combined.

Step 6. Crystals of Rochelle salt were dissolved in the aqueous solution, which was rendered just alkaline by the addition of dilute ammonia, and the gallium was precipitated by adding an excess of a 5% solution of 8-hydroxy-quinoline in 2N acetic acid.

Step 7. The Ga "oxinate" ppt. was collected on a glass fibre filter disc, dried at 110°C. and weighed.

These gallium sources could be prepared and counted within one hour of the end of the irradiation. The gallium carrier solution was standardised gravimetrically, weighing as the "tri-oxinate". This was precipitated under the conditions recommended by Schoeller and Powell.[59]

RESULTS AND DISCUSSION.

In Table 31 the results obtained for the upper limits of (n,He^3) cross sections in Mn^{55}, Co^{59}, As^{75} and Rh^{103} are compared with the values reported by Kumabe et al. The results quoted for Mn^{55} and Rh^{103} were obtained by Mrs. E.B.M. Martin.

It is impossible to reconcile Kumabe's results with the present work. It was at first felt that the cross sections quoted in millibarns were, in fact,

TABLE 31. THE ESTIMATED UPPER LIMITS OF CROSS SECTIONS OF THE (n,He^3) REACTION IN VARIOUS TARGET NUCLIDES COMPARED WITH THE VALUES REPORTED BY KUMABE ET AL.[58]

Target nuclide	(n,He^3) cross section		Q value (MeV)
	Present work (mbs.)	Kumabe et al. (mbs.)	
Mn^{55}	0.1	2 - 6	- 12.65
Co^{59}	0.1	1.0 - 3.0	- 12.41
As^{75}	0.3	3 - 7	- 9.82
Rh^{103}	0.1	1.5 - 3.5	- 8.46

supposed to be in microbarns, but then the activities could not be resolved from the gross decay curves. It is difficult enough to see how the 2 min. V^{53}, produced with a cross section of 2-6 mbs. by the $Mn^{55}(n,He^3)V^{53}$ reaction, was resolved from the 3.5 min. (n,p) and (n,α) products of Mn^{55}, which are produced with a cross section of 150 mbs. Decay curves were not published. In the present work it was difficult enough to detect the 2 min. Mn^{57} (from Co^{59}) in the presence of 2.58 hr. Mn^{56}, which is formed with a cross section of only 35 mbs.

The isolation of the gallium activity from irradiated arsenic was an improvement on Kumabe's

experiment where no chemistry was performed. The latter analysed the gross decay curve which, besides the reported 5 hr. (n,He^3) product, included 82 min. Ge^{75} and 14.1 hr. Ga^{72}. According to Kumabe, the 5 hr. Ga^{73} was produced with a cross section of the same order as the (n, α) cross section, but gallium sources, prepared in the present work, decayed almost exactly with the literature value of the half-life of the $Ga^{72}(n,\alpha)$ product, i.e. 14.1 hrs. There was only the slightest evidence of a shorter activity at the beginning of the decay curves.

The only conclusion that can be drawn from the present work is that Kumabe et al were mistaken.

IRRADN. NO.	SAMPLE REACTION				REFERENCE REACTION					MEASURED CROSS SECTION mbs.	MEAN
	No. of target nuclei x N^{-1}	Chemical yield (%)	Self-absorption factor	A_o observed c.p.m.	A_o correct d.p.m.	S	No. of target nuclei x N^{-1}	A_o observed c.p.m.	A_o correct d.p.m.	S		

TABLE 30. RESULTS FOR THE $As^{75}(n,\alpha)Ga^{72}$ REACTION.

61	1.81×10^{-2}	39.1	0.30	2.15×10^{3}	1.73×10^{4}	3.49	8.85×10^{-3}	6.57×10^{4}	7.36×10^{5}	3.12	7.5	8.4 mbs. $\pm$ 1.1
62	1.82×10^{-2}	82.5	0.30	3.30×10^{3}	1.33×10^{4}	3.49	6.93×10^{-3}	3.00×10^{4}	3.36×10^{5}	3.12	9.3	

$t_{\frac{1}{2}}Ga^{72}$ = 14.1 hours.

$t_{\frac{1}{2}}Mn^{56}$ = 2.58 hours. $c_{Mn^{56}}$ = 0.0893.

CHAPTER 5

COLLECTED RESULTS AND DISCUSSION

Summary of results

All cross sections are quoted relative to an assumed value of 124 mbs. for the $Fe^{56}(n,p)Mn^{56}$ cross section.

TABLE 32. (n,p) CROSS SECTIONS.

Target nuclide	Product nuclide	Half-life	Cross section (mbs.)
Mg^{24}	Na^{24}	15.0 hrs. ± 0.1	178 ± 12
Al^{27}	Mg^{27}	9.5 mins.	73.5
A^{40}	Cl^{40}	1.4 mins. ± 0.03	15.1
I^{127}	Te^{127}	9.2 hrs. ± 0.1*	3.17 ± 0.27
Ba^{138}	Cs^{138}	33.1 mins. ± 0.6	1.56 ± 0.26
Au^{197}	Pt^{197}	19.7 hrs. ± 0.4	2.60 ± 0.27
Hg^{200}	Au^{200}	48 mins.	3.36 ± 0.46
Hg^{201}	Au^{201}	26 mins.	2.46 ± 0.26
Bi^{209}	Pb^{209}	3.17 mins. ± 0.04	0.97 ± 0.08

* Lower limit since only one isomer observed.

TABLE 33. (n,pn) CROSS SECTION.

A^{40}	Cl^{39}	55.0 mins. ± 0.8	1.61

Target nuclide	Product nuclide	Half-life	Cross section (mbs.)
TABLE 34.	(n, α) CROSS SECTIONS.		
Al^{27}	Na^{24}	15.0 hrs. $\pm$ 0.1	117 $\pm$ 5
A^{40}	S^{37}	5.0 mins. $\pm$ 0.1	15.0
Co^{59}	Mn^{56}	2.58 hrs.	34.8 $\pm$ 1.3
As^{75}	Ga^{72}	14.1 hrs. $\pm$ 0.2	8.4 $\pm$ 1.0
Au^{197}	Ir^{194}	19.4 hrs. $\pm$ 0.6	0.50 $\pm$ 0.08
Hg^{200}	Pt^{197}	19.7 hrs. $\pm$ 0.4	0.44 $\pm$ 0.05
Hg^{202}	Pt^{199}	31 mins.	0.31 $\pm$ 0.03
Bi^{209}	Tl^{206}	4.18 mins. $\pm$ 0.02	0.46 $\pm$ 0.06
TABLE 35.	(n, γ) CROSS SECTIONS.		
Mn^{55}	Mn^{56}	2.58 hrs.	1.29 $\pm$ 0.23
I^{127}	I^{128}	25.0 mins. $\pm$ 0.1	6.5 $\pm$ 0.8
Ba^{138}	Ba^{139}	84.0 mins $\pm$ 0.6	1.70 $\pm$ 0.15
Bi^{209}	Bi^{210}	5 days.	0.67 $\pm$ 0.04
TABLE 36.	(n,2n) CROSS SECTION.		
I^{127}	I^{126}	13 days	1600 $\pm$ 60

The standard deviations quoted simply record the spread of experimental results and do not include an allowance for systematic errors. They are due to the counting statistics of induced activities and to small uncertainties in chemical yield and neutron flux determinations. The general lowness of standard deviations is a measure of the success of the homogeneous mixture technique for monitoring the neutron flux.

The attention paid to counter calibration has reduced systematic errors, arising from the estimation of counting efficiencies, to a minimum. Measured counting efficiencies were thought to be accurate to within one or two per cent. Where it was not possible to measure counting efficiencies directly, they could be interpolated from the calibration curves with an estimated error of plus or minus three per cent.

Greater accuracy in the determination of absolute disintegration rates is considered the biggest improvement on the results of previous workers. This includes the more recent work of Fink et al,[34,41] who, in otherwise painstaking experiments, estimated their counting efficiencies by the unreliable semi-empirical method described in Chapter 2. Only Coleman et al,[39] who measured induced activities by a 4π technique could claim equal accuracy.

The present work has corrected one or two inaccuracies in Paul and Clarke's original paper,[1] but confirms the trend, observed by them and now generally accepted, of the failure with increasing Z of the evaporation theory of the compound nucleus to give an adequate account of (n,p) and (n, α) reactions. In the high-Z region, measured (n,p) and (n, α) cross sections are as much as four orders of magnitude higher than their values calculated on the basis of the statistical treatment of Blatt and Weisskopf.[2]

To acoount for this trend Paul and Clarke proposed an alternative mechanism by which (n,p) and (n, α) reactions might proceed. They proposed a direct interaction process in which the incident neutron interacts strongly with only one proton or α-particle in the target nucleus, which escapes before much energy sharing takes place. This process becomes more important with increasing Z, as the emission of charged particles from the compound nucleus is supressed by the increasing height of the Coulomb barrier.

Further evidence of direct interactions competing with the evaporation process in nuclear reactions was provided by experiments examining the energy distributions and differential cross sections of reactions emitting

charged particles. Fulmer and Cohen[60] studied (p, α) reactions with 23 MeV protons. For low-Z targets (Al,Ni,Cu), all but the highest energy α-particles were emitted isotropically, consistent with the statistical nature of the evaporation process from a compound nucleus. The high energy α's showed forward peaking characteristic of a process proceeding without the prior formation of a compound nucleus. For Pd (middle-Z), the forward peaked α's included all those from 12 MeV upwards. Lower energy α's were isotropic. For Pt(high-Z), all α-particles showed forward peaking and no sign of statistical processes was left. These results are supported by the work of Gugelot,[61] who observed the same trends in (p,p') reactions for 18 MeV protons, and Eisborg and Igo[62] found strongly forward peaked differential cross sections for 31 MeV protons in (p,p') reactions on Pb, Au, Ta and Sn for all energies of p'.

Several workers have demonstrated anisotropic proton distributions from (n,p) reactions induced by 14 MeV neutrons. The results of these experiments are reviewed in a recent paper by Colli et al,[63] who discuss possible mechanisms of the direct interaction process.

The general picture presented is of the direct interaction process competing with the evaporation process

over the whole range of Z, but becoming predominant in the high-Z region, where the evaporation process is suppressed by the Coulomb barrier.

Brown and Muirhead[3] have proposed a nuclear model for (n,p) reactions which takes account of a direct interaction process. This model is based on the extreme assumption that the target nucleus can be represented by an assembly of non-interacting nucleons and that a nuclear reaction proceeds in three stages, (i) an initial collision between the incident nucleon and one of those contained in the target nucleus followed by (ii) the formation of an excited nucleus which subsequently decays (iii). The emission of nucleons can occur in stages (i) and (iii). The emission of nucleons in stage (i) occurs in a period of about 10^{-22} sec. (the time taken for a fast neutron to traverse a heavy nucleus) and in stage (iii) in a period many orders of magnitude longer (the estimated lifetime of a compound nucleus is about 10^{-13} secs.). Brown and Muirhead calculated the separate contributions of stages (i) and (iii), i.e. the separate contributions of the direct interaction and compound nucleus processes, to the total (n,p) cross sections of a number of reactions for 14 MeV neutrons. The effective contribution of the compound nucleus

process to (n,p) reactions in the high-Z region is zero on the basis of this model.

In Table 37 (n,p) cross sections measured in the present work are compared with values calculated by Brown and Muirhead[3] or by Coleman et al[39] using Brown and Muirhead's model.

TABLE 37. COMPARISON OF MEASURED (n,p) CROSS SECTIONS WITH VALUES CALCULATED ON THE BASIS OF BROWN AND MUIRHEAD'S MODEL.

Target nuclide	Observed cross section mbs.	Calculated cross section mbs.	ratio $\frac{\sigma \text{ obs.}}{\sigma \text{ calc.}}$
Mg^{24}	178	205/	0.87
Al^{27}	75.5	64/	1.13
I^{127}	3.17*	18.5x	0.17*
Ba^{138}	1.56	3.0x	0.52
Au^{197}	2.60	6.4x	0.41
Hg^{200}	3.36	3.0x	1.12
Hg^{201}	2.46	3.9x	0.63
Bi^{209}	0.97	7.2x	0.14

* Lower limit since only one isomer observed.

/ Brown and Muirhead.[3]

x Coleman et al.[39]

With the exception of Bi^{209} and the possible exception of I^{127}, the observed and calculated cross sections agree within a factor of two. In addition, there does not seem to be any systematic change in the agreement with increasing Z. These facts can be considered as good evidence for the type of direct mechanism envisaged by Brown and Muirhead, although the authors themselves point out that the model is a gross oversimplification, ignoring the detailed properties of individual nuclei.

The actual mechanism of direct interactions remains in doubt. The success of Brown and Muirhead's model suggests that they proceed by direct nucleon-nucleon collisions throughout the nuclear volume, although the possibility of the enhanced production of protons at the nuclear surface was not overlooked. Nucleons emitted by this process leave the nucleus instantaneously before any energy sharing has taken place at all. An alternative mechanism, which is supported by the emission of α-particles, as well as protons and neutrons, by direct interaction, assumes that energy sharing occurs in a small localised part of the nucleus, involving only a fraction of the nucleons, before emission takes place. The nuclear temperature in the "heated" locality is much greater than

if complete equilibrium had been reached in the formation of a compound nucleus. Sufficient energy can then be concentrated on one nucleon to enable it to negotiate the Coulomb barrier.

After considering the systematics of 14 MeV neutron reactions, Rosen[64] favours the latter mechanism. Colli[63] has concluded that both types of mechanism occur and that both seem to be connected with the nuclear surface.

The measurement of (n, γ) cross sections is restricted to those elements in which the activity is not obscured by activities induced by (n,n') and (n,2n) reactions, which have, at these energies, much higher cross sections.

Capture cross sections for 14 MeV neutrons would have been expected from the results of Hughes et al[14] for 1 MeV neutrons, to be vanishingly small. In fact, for heavy nuclides, they are equally favoured with (n,p) and (n, α) reactions. The possibility of these unexpectedly high (n, γ) cross sections being due to the capture of degraded neutrons or D+D neutrons has been eliminated experimentally.

Lane and Lynn[65] have presented a theoretical interpretation of this observation. They have shown that, whereas the statistical treatment of the compound nucleus adequately predicts Hughes' results, predictions for 14 MeV neutrons underestimate observed values by from two

to four orders of magnitude. They have proposed a direct capture process to account for (n, γ) reactions at high energies. Here the captured neutron radiates and makes a transition to a lower orbit within the nucleus before losing its identity in the compound nucleus. Calculations of capture cross sections at 14 MeV made on the basis of this model are still an order of magnitude lower than observed values, but adequately predict their dependence on mass number.

An examination of the γ-spectra radiated by capture reactions at high energies might throw some light on to the nature of this direct process.

REFERENCES

1. Paul, E.B. and Clarke, R.L. Can. J. Phys., 31, 267 (1953).
2. Blatt, J.M. and Weisskopf, V.F. Theoretical Nuclear Physics. Chap. VIII. (John Wiley and Sons, Inc., New York, 1952).
3. Brown, G. and Muirhead, H. Phil. Mag., 2, 16, 473 (1957).
4. Blosser, H.G., Goodman, C.D., Handley, T.H. and Randolph, M.L. Phys. Rev., 100, 429 (1955).
5. Blosser, H.G., Handley, T.H. and Goodman, C.D. Bull. Am. Phys. Soc., 1, 224 (1956).
6. Blosser, H.G., Goodman, C.D. and Handley, T.H. Phys. Rev., 110, 531 (1958).
7. Forbes, S.G. Phys. Rev., 88, 1309 (1952).
8. Yasumi, S.J. Phys. Soc. (Japan), 12, 443 (1957).
9. Martin, H.G. Phys. Rev., 93, 498 (1954).
10. Battat, M.E. and Ribe, F.L. Phys. Rev., 89, 80 (1953).
11. Peck, R.A. Phys. Rev., 106, 965 (1957).
12. Hughes, D.J., Spatz, W.D.B. and Goldstein, N. Phys. Rev., 75, 1781 (1949).
13. Hughes, D.J. and Sherman, D. Phys. Rev., 78, 632 (1950).

14. Hughes, D.J., Garth, R.C. and Levin, J.S. Phys. Rev., 91, 1423 (1953).

15. Cohen, A.V., Hyder, S.B. and White, P.H. Nucl. Phys., 1, 278 (1956).

16. Allan, D.L. Nucl. Phys., 6, 464 (1958).

17. Paneth, F.A. Endeavour, 12, 5 (1953).

18. Terrell, H. and Holm, D.M. Phys. Rev., 109, 2031 (1958).

19. Gleason, T.H., Taylor, M.N. and Tabern, P. Nucleonics, 8, No. 5, 12 (1951).

20. Burt, B.P. Nucleonics, 5, No. 2, 28 (1949).

21. Nervik, W.E. and Stevenson, P.C. Nucleonics, 10, No. 3, 18 (1952).

22. Cuninghame, J.G., Sizeland, M.L. and Willis, H.H. A.E.R.E. C/R 2054 (1957).

23. Pate, B.D. and Yaffe, L. Can. J. Chem., 33, 15 (1955); 610 (1955); 1656 (1955).
ibid., 34, 265 (1956)

24. Hawkings, R.C., Merritt, W.F. and Craven, H.H. Proceedings of Symposium, Maintenance of Standards, Nat. Phys. Lab. (H.M. Stationery Office, London, 1952).

25. Martin, E.B.M. Unpublished handbook, Londonderry Laboratory for Radiochemistry, Durham University.

26. Graves, E.R., Rodrigues, A.A., Goldblatt, M. and Meyer, D.I. Rev. Sci. Inst., 20, 579 (1949).

27. Fowler, J.L. and Brolley, J.E., Jr. Rev. Mod. Phys., 28, 103 (1956).

28. Kraus, K.A. and Nelson, G.E. J. Am. Chem. Soc., 75, 1460 (1953).

29. Dalton, J.C. and Welch, G.A. Handbook of XVth Congress, International Union of Pure and Applied Chemistry, V-7, 147 (1956).

30. Haissinsky, M. Electrochimie. (Hermann and Cle., Paris, 1946).

31. Bagnall, K.W. Chemistry of the Rare Radioelements. (Butterworths Sci. Pub., London, 1957).

32. Schwarzenbach, G. Complexometric Titrations (Methuen & Co. Ltd., London, 1956).

33. Kern, B.D., Thompson, W.E. and Ferguson, J.M. Nucl. Phys., 10, 226 (1959).

34. Poularikas, A. and Fink, R.W. Phys. Rev., 115, 989 (1959).

35. Khurana, C.S. and Hans, H.S. Nucl. Phys., 13, 88 (1959).

36. Haling, H., Peck, R.A. and Eubank, E.M. Phys. Rev., 106, 971 (1957).

37. Vogel, A.I. Quantitative Inorganic Analysis (Longmans, 1953).

38. Perkin, J.L., O'Connor, L.P. and Coleman, R.F. Proc. Phys. Soc., 72, 505 (1958).

39. Coleman, R.F., Hawker, B.E., O'Connor, L.P. and Perkin, J.L. Proc. Phys. Soc., 73, 215 (1959).

40. Cheng, K.L. Anal. Chem., 26, 1977 (1954).

41. Wille, R.G. and Fink, R.W. Phys. Rev., 118, 242 (1960).

42. Van Lieshout, R., Girgis, R.K., Ricci, R.A., Wapstra, A.H. and Ythier, C. Physica, 25, 703 (1959).

43. Bresesti, M. and Roy, J.C. Can. J. Chem. 38, 194 (1960).

44. Stevenson, P.C., Franke, A.A., Borg, R. and Nervik, W. J. Am. Chem. Soc., 75, 4876 (1953).

45. Busch, D.D., Prospero, J.M. and Naumann, R.A. Anal. Chem., 31, 884 (1959).

46. Majer, V. Naturwiss. 25, 252 (1937).

47. Herr, W. Z. Naturforsch, 3a, 645 (1948).

48. Freiling, E.C. and Burney, L.R. Nucleonics, 13, No. 9, 112 (1956).

49. Stromiger, D., Hollander, J.M. and Seaborg, G.T. Rev. Mod. Phys., 30, 585 (1958).

50. Martin, E.B.M. Private communication.

51. Meinke, W. A.E.C.D.-2738 (1949).

52. Levkovskii, V.N. Sov. Phys. J.E.T.P. 4, 291 (1957). ibid., 6, 1174 (1958).

53. Colli, L., Cvelbar, F., Micheletti, S. and Pignanelli, M. Nuovo Cimento, 13, 868 (1959).

54. Aten, A.W.H . and Feyfer, G.O. Physica, 21, 543 (1955).

55. Aten, A.W.H. and Feyfer, G.O. Physica, 19, 1143 (1953).

56. Barry, J.F., Coleman, R.F., Hawker, B.E. and Perkin, J.L. Proc. Phys. Soc., 74, 632 (1959).

57. Halder, B.C. and Wiig, F.O. Phys. Rev., 105, 1285 (1957).

58. Kumabe, I., Poularikas, A.D., Rreiss, I.L. Gardner, D.G. and Fink, R.W. Phys. Rev. 118, 242 (1960).

59. Schoeller, W.R. and Powell, A.R. The Analysis of Minerals and Ores of the Rarer Elements. (Charles Griffin & Co. Ltd., London, 1955).

60. Fulmer, C.B. and Cohen, B.L. Phys. Rev., 112, 1672 (1958).

61. Gugelot, P.C. Phys. Rev., 93, 425 (1954).

62. Eisborg, R.M. and Igo, G. Phys. Rev., 93, 1039 (1954).

63. Colli, L., Facchini, U, Iori, I., Marcazzan, M.G. and Sona, A.M. Nuovo Cimento, 13, 730 (1959).

64. Rosen, L. Private communication to Levinson, C.A. Nuclear Spectroscopy Part B (Academic Press, London, 1960).

65. Lane, A.M. and Lynn, J.E. Proceedings of the Second International Conference on Peaceful Uses of Atomic Energy, Geneva, 1958) 15, 38.

ACKNOWLEDGEMENTS

I wish to record my sincere thanks to the following:

Mr. G.R. Martin, Reader in Radiochemistry in the University of Durham, under whose supervision this work was carried out, for his sound advice and the benefit, in many discussions, of his wide knowledge of radiochemistry.

Mrs. E.B.M. Martin for her keen interest in this work and for permission to make use of several of her results.

The Department of Scientific and Industrial Research for the award of a Research Studentship, during the tenure of which this work was undertaken.

J.H. Davies.